

**ANALYSIS OF TNT, DNA METHYLATION, AND HAIR
PIGMENTATION VIA GAS CHROMATOGRAPHY-MASS
SPECTROMETRY AND SPECTROSCOPIC TECHNIQUES**

by

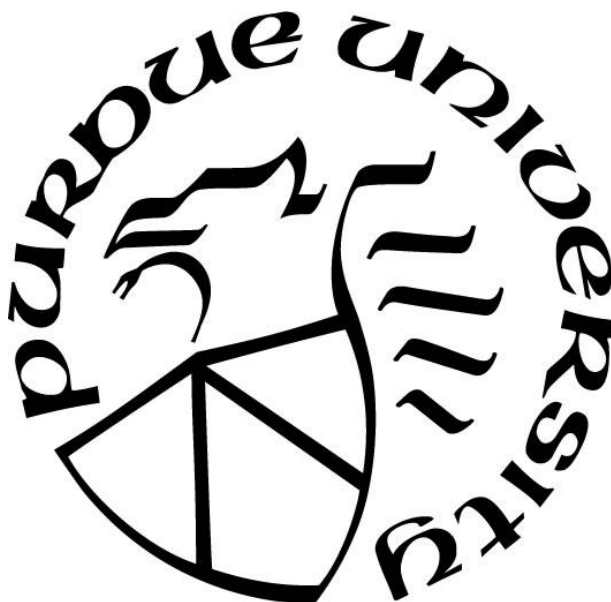
Jacqueline Ruchti

A Thesis

Submitted to the Faculty of Purdue University

In Partial Fulfillment of the Requirements for the degree of

Master of Science



Department of Chemistry

Indianapolis, Indiana

August 2019

THE PURDUE UNIVERSITY GRADUATE SCHOOL
STATEMENT OF COMMITTEE APPROVAL

Dr. John Goodpaster, Chair

Department of Chemistry & Chemical Biology

Dr. Nicholas Manicke

Department of Chemistry & Chemical Biology

Dr. Christine Picard

Department of Biology

Approved by:

Dr. John Goodpaster

Head of the Graduate Program

For my family, friends, and mentors, who have always supported me and encouraged me to always push past any obstacles I encounter.

ACKNOWLEDGMENTS

I would like to thank my advisor, Dr. John Goodpaster, for his guidance, mentorship, and patience throughout the journey toward my master's degree. I also want to thank my colleagues Zackery Roberson, Ashur Rael, Courtney Cruse, Kymeri Davis, and Logan Hickey for their help along the way. Lastly, I would like to thank Logan Hickey for mentoring me in the laboratory and for his research, which laid the foundation for Chapter 1 of my thesis.

TABLE OF CONTENTS

LIST OF TABLES	6
LIST OF FIGURES	7
LIST OF ABBREVIATIONS.....	11
ABSTRACT.....	13
CHAPTER 1. M-VAC COLLECTION EFFICIENCY OF TNT	1
1.1 Introduction.....	1
1.2 Experimental.....	4
1.3 Results and Discussion	6
1.4 Conclusion	18
CHAPTER 2. ANALYSIS OF DNA METHYLATION IN BLOWFLIES	20
2.1 Introduction.....	20
2.2 Experimental.....	24
2.3 Results and Discussion	25
2.4 Conclusion	44
CHAPTER 3. ANALYSIS OF HAIR PIGMENTATION.....	46
3.1 Introduction.....	46
3.2 Experimental.....	51
3.3 Results and Discussion	55
3.4 Conclusion	66
CHAPTER 4. FUTURE DIRECTIONS	68
4.1 M-Vac Collection Efficiency of TNT Project	68
4.2 Analysis of DNA Methylation in Blowflies	71
4.3 Analysis of Hair Pigmentation.....	73
REFERENCES	77
VITA.....	81

LIST OF TABLES

Table 1-1. Experimental Partition Coefficients and their Respective Log P Values.....	12
Table 1-2. TNT Mass Recovery from T-Shirt Samples Collected via M-Vac	15
Table 2-1. Nucleobases, Nucleosides, and Nucleotides of key DNA methylation compounds analyzed in this work	22
Table 2-2. Other major Nucleobases, Nucleosides, and Nucleotides found in DNA and/or RNA	23
Table 2-3. Nucleosides in the Nucleoside Test Mix and their Respective Nucleobases	35
Table 4-1. Parameters of Blowfly DNA Aging Study	73

LIST OF FIGURES

Figure 1-1. M-Vac System.....	3
Figure 1-2. Diagram of M-Vac's Simultaneous Spray and Vacuum ¹¹	3
Figure 1-3. Total Ion Chromatogram (TIC) of 300 ppb DNT (6.6 min) and 300 ppb TNT (7.6 min) in Chloroform.....	7
Figure 1-4. Structure and significant fragmentation of TNT overlaid on its mass spectrum	7
Figure 1-5. Structure and significant fragmentation of DNT overlaid on its mass spectrum	8
Figure 1-6. Extracted Ion Chromatograms for m/z 210 from PCIA Liquid-liquid Extractions of TNT, using 50 μ L of a 20 ppm Chloroform Solution of TNT with a 2-minute solvent delay (orange) and 500 μ L of a 20 ppm Chloroform Solution of TNT with a 4-minute solvent delay (grey).....	9
Figure 1-7. Calibration Curve from Total Ion Chromatograms of Chloroform Solutions of TNT run via liquid injection and in sequence with partition coefficient study samples for water, lysis buffer, and lysis buffer with proteinase K and incubation.....	11
Figure 1-8. Calibration Curve from Total Ion Chromatograms of Chloroform Solutions of TNT which were run in sequence with the Butterfield's Buffer partitioned samples and T-shirt samples via liquid injection	12
Figure 1-9. Calibration Curve of Water Solutions of TNT via Immersion SPME	13
Figure 1-10. Calibration curve for TNT in Butterfield's Buffer performed via Immersion SPME and in sequence with post-blast backpack debris samples.....	14
Figure 1-11. Overlaid Total Ion Chromatograms of samples prepared with solutions of 10 ppm and 50 ppm TNT in Chloroform applied to T-shirts and Extracted	15
Figure 1-12. Overlaid Total Ion Chromatograms of a 1 ppm TNT in Chloroform Solution (blue) and Post-Blast Backpack Debris Samples prepared via the Charcoal Strip Extraction method (orange) and the Chloroform Extraction method (grey) and analyzed via Liquid Injection	16
Figure 1-13. Extracted Ion Chromatograms of m/z 210 for the Direct Chloroform Extraction of TNT from Backpack Pieces of two different surfaces.....	17
Figure 1-14. Overlaid Total Ion Chromatograms of 300 ppb TNT in Butterfield's Buffer Calibrant Solution (blue) and Backpack Sample taken via the Filtration method (orange) and analyzed via Immersion SPME.....	18
Figure 2-1. Total Ion Chromatogram (SIM mode) of a 25 ppm Acetonitrile solution of MTBSTFA derivatized 5-methyl Cytosine	26
Figure 2-2. Structure and Significant Fragmentation of MTBSTFA derivatized 5-methyl Cytosine nucleobase overlaid on its Mass Spectrum	26

Figure 2-3. Stacked Total Ion Chromatograms of 6 Nucleobase calibrants in acetonitrile (100 ppm) derivatized with BSTFA	27
Figure 2-4. Structure and Significant Fragmentation of BSTFA derivatized Uracil nucleobase overlaid on its Mass Spectrum.....	28
Figure 2-5. Structure and Significant Fragmentation of BSTFA derivatized Thymine nucleobase overlaid on its Mass Spectrum.....	28
Figure 2-6. Structure and Significant Fragmentation of BSTFA derivatized Cytosine nucleobase overlaid on its Mass Spectrum.....	29
Figure 2-7. Structure and Significant Fragmentation of BSTFA derivatized 5-methyl Cytosine nucleobase overlaid on its Mass Spectrum	29
Figure 2-8. Structure and Significant Fragmentation of BSTFA derivatized Adenine nucleobase overlaid on its Mass Spectrum.....	30
Figure 2-9. Structure and Significant Fragmentation of BSTFA derivatized Guanine nucleobase overlaid on its Mass Spectrum.....	30
Figure 2-10. Calibration curve of Acetonitrile solutions of Cytosine from 2 ppm to 10 ppm	31
Figure 2-11. Calibration curve of Acetonitrile solutions of 5-methyl Cytosine from 2 ppm to 10 ppm	32
Figure 2-12. Calibration curve of Acetonitrile solutions of Cytosine to 5-methyl Cytosine from 2 ppm to 10 ppm	32
Figure 2-13. Calibration curve of Acetonitrile solutions of Cytosine from 1 ppm to 4 ppm, using the ion m/z 240.....	33
Figure 2-14. Calibration curve of Acetonitrile solutions of 5-methyl Cytosine from 1 ppm to 4 ppm, using the ion m/z 269.....	33
Figure 2-15. Calibration curve of Acetonitrile solutions of Cytosine to 5-methyl Cytosine from 1 ppm to 4 ppm, using the ions m/z 240 and m/z 269, respectively.....	34
Figure 2-16. Uracil Extracted Ion Chromatograms of an Acetonitrile solution of BSTFA Derivatized Nucleoside Test Mix, containing Pseudouridine (25 ppm), Cytidine (50 ppm), Uridine (25 ppm), 3-methyl Cytidine Methosulfate (100 ppm), 2-thio Cytidine (10 ppm), 1-methyl Adenosine (25.5 ppm), 2'-0-methyl Cytidine (20 ppm), 7- methyl Guanosine (25 ppm), Inosine (25 ppm), Guanosine (25 ppm), Ribothymidine (50 ppm), and 5-methyl Cytidine (100 ppm) ...	36
Figure 2-17. Thymine Extracted Ion Chromatograms of an Acetonitrile solution of BSTFA Derivatized Nucleoside Test Mix, containing Pseudouridine (25 ppm), Cytidine (50 ppm), Uridine (25 ppm), 3-methyl Cytidine Methosulfate (100 ppm), 2-thio Cytidine (10 ppm), 1-methyl Adenosine (25.5 ppm), 2'-0-methyl Cytidine (20 ppm), 7- methyl Guanosine (25 ppm), Inosine (25 ppm), Guanosine (25 ppm), Ribothymidine (50 ppm), and 5-methyl Cytidine (100 ppm) ...	37
Figure 2-18. Cytosine and 5-methyl Cytosine Extracted Ion Chromatograms of an Acetonitrile solution of BSTFA Derivatized Nucleoside Test Mix, containing Pseudouridine (25 ppm), Cytidine (50 ppm), Uridine (25 ppm), 3-methyl Cytidine Methosulfate (100 ppm), 2-thio Cytidine	

(10 ppm), 1-methyl Adenosine (25.5 ppm), 2'-0-methyl Cytidine (20 ppm), 7- methyl Guanosine (25 ppm), Inosine (25 ppm), Guanosine (25 ppm), Ribothymidine (50 ppm), and 5-methyl Cytidine (100 ppm)..... 38

Figure 2-19. Adenine Extracted Ion Chromatograms of an Acetonitrile solution of BSTFA Derivatized Nucleoside Test Mix, containing Pseudouridine (25 ppm), Cytidine (50 ppm), Uridine (25 ppm), 3-methyl Cytidine Methosulfate (100 ppm), 2-thio Cytidine (10 ppm), 1-methyl Adenosine (25.5 ppm), 2'-0-methyl Cytidine (20 ppm), 7- methyl Guanosine (25 ppm), Inosine (25 ppm), Guanosine (25 ppm), Ribothymidine (50 ppm), and 5-methyl Cytidine (100 ppm) ... 39

Figure 2-20. Guanine Extracted Ion Chromatograms of an Acetonitrile solution of BSTFA Derivatized Nucleoside Test Mix, containing Pseudouridine (25 ppm), Cytidine (50 ppm), Uridine (25 ppm), 3-methyl Cytidine Methosulfate (100 ppm), 2-thio Cytidine (10 ppm), 1-methyl Adenosine (25.5 ppm), 2'-0-methyl Cytidine (20 ppm), 7- methyl Guanosine (25 ppm), Inosine (25 ppm), Guanosine (25 ppm), Ribothymidine (50 ppm), and 5-methyl Cytidine (100 ppm) ... 40

Figure 2-21. Total ion chromatograms (SIM mode) of an Acetonitrile solution of BSTFA Derivatized Nucleoside Test Mix, containing Pseudouridine (25 ppm), Cytidine (50 ppm), Uridine (25 ppm), 3-methyl Cytidine Methosulfate (100 ppm), 2-thio Cytidine (10 ppm), 1-methyl Adenosine (25.5 ppm), 2'-0-methyl Cytidine (20 ppm), 7- methyl Guanosine (25 ppm), Inosine (25 ppm), Guanosine (25 ppm), Ribothymidine (50 ppm), and 5-methyl Cytidine (100 ppm) ... 41

Figure 2-22. Total Ion Chromatogram (Scan) of an Acetonitrile solution of Fly DNA (2.25 ppm) Derivatized with BSTFA 42

Figure 2-23. Uracil Extracted Ion Chromatograms of Fly DNA (2.25 ppm) Derivatized with BSTFA 43

Figure 2-24. Thymine Extracted Ion Chromatograms of Fly DNA (2.25 ppm) Derivatized with BSTFA 44

Figure 3-1. Structure of Hair³⁶ 47

Figure 3-2. Structure of Eumelanin Monomer..... 48

Figure 3-3. Structure of Pheomelanin Monomer 48

Figure 3-4. Production of 2,3,5-PTCA (bottom left) and 2,3-PDCA (bottom right) from Eumelanin Monomer (top) via Hydrogen Peroxide Oxidation..... 49

Figure 3-5. Production of 4-AT (bottom left) and 3-AT (bottom right) from Pheomelanin Monomer (top) via Hydroiodic Acid Hydrolysis 50

Figure 3-6. Total ion chromatograms of an Acetonitrile solution of DMF-DMA derivatized 3-AT over 3 days 55

Figure 3-7. Structure and Significant Fragmentation of DMF-DMA derivatized 3-AT, Kinetic Product 56

Figure 3-8. Structure and Significant Fragmentation of DMF-DMA derivatized 3-AT, Thermodynamic Product..... 56

Figure 3-9. Total ion chromatograms of Acetonitrile solutions of BSTFA derivatized 3-AT (200 ppm) (blue) and 2,3,5-PTCA (7500 ppm) (orange).....	57
Figure 3-10. Structure and Significant Fragmentation of BSTFA derivatized 3-AT overlaid on its Mass Spectrum.....	58
Figure 3-11. Structure and Significant Fragmentation of BSTFA derivatized 2,3,5-PTCA overlaid on its Mass Spectrum.....	58
Figure 3-12. Total Ion Chromatograms of an Acetonitrile solution of 200 ppm 3-AT, 2 TMS via SIM mode (blue) and scan mode (orange).....	59
Figure 3-13. Calibration curve for Acetonitrile solutions of BSTFA derivatized 3-AT via Liquid Injection	59
Figure 3-14. Stacked FTIR ATR Spectra of blonde (top) and brown (bottom) hair	61
Figure 3-15. Stacked FTIR ATR Spectra of brown hair with varying resolution at 16 scans.....	62
Figure 3-16. Stacked FTIR ATR Spectra of brown hair with varying number of scans at a resolution of 4 cm ⁻¹	63
Figure 3-17. Stacked MSP Spectra of blonde hair (blue), brown hair (orange), and black hair (grey)	64
Figure 3-18. Stacked Raman Spectra of the Melanin Degradation Products 2,3,5-PTCA and 3-AT	65
Figure 3-19. Stacked Raman Spectra for Analysis of Eumelanin: 2,3,5-PTCA (blue), <i>Sepia Officinalis</i> Melanin (orange), and Black Hair (grey).....	66
Figure 4-1. A Smiths Detection Guardion portable GC-MS ⁵²	69
Figure 4-2. Diagram of a Torion T-9 portable GC-MS ⁵⁵	70
Figure 4-3. Top view diagram of a Torion T-9 portable GC-MS ⁵⁵	70
Figure 4-4. Normalized Combined FTIR and MSP Spectra of Blonde Hair, Brown Hair, and Black Hair	74
Figure 4-5 Normalized and Mean Centered, Combined FTIR and MSP Spectra of Blonde Hair, Brown Hair, and Black Hair	75
Figure 4-6. Normalized, Mean Centered, and Autoscaled, Combined FTIR and MSP Spectra of Blonde Hair, Brown Hair, and Black Hair.....	75

LIST OF ABBREVIATIONS

2,3-PDCA	Pyrrole-2,3-Dicarboxylic Acid
2,3,5-PTCA	Pyrrole-2,3,5-Tricarboxylic Acid
3-AT	L-3-Aminotyrosine
AAAF	N-Acetoxy-2-Acetylaminofluorene
AAF	2-Acetylaminofluorene
AHC	Agglomerative Hierarchical Clustering
ATR	Attenuated Total Reflectance
BSTFA	N,O-bis-(trimethylsilyl)trifluoroacetamide
CID	Collision Induced Dissociation
DA	Discriminant Analysis
DEFFI-MS	Desorption Electro-Flow Focusing Ionization-Mass Spectrometry
DMF-DMA	N,N-Dimethylformamide Dimethyl Acetal
DNA	Deoxyribonucleic Acid
DNT	2,4-Dinitrotoluene
FTIR	Fourier-Transform Infrared Spectroscopy
GC	Gas Chromatograph
GC-FID	Gas Chromatography-Flame Ionization Detector
GC-MS	Gas Chromatography-Mass Spectrometry
HCl	Hydrochloric Acid
HPLC-FLD	High Performance Liquid Chromatography with Spectrofluorimetric Detection
IBCF	Isobutyl chloroformate
IED	Improvised Explosive Device
IR	Infrared Spectroscopy
ISIL	Islamic State of Iraq and the Levant
IUPUI	Indiana University-Purdue University Indianapolis
LC-MS	Liquid Chromatography-Mass Spectrometry
MS	Mass Spectrometer
MS-AFLP	Methylation-Sensitive Amplified Fragment Length Polymorphisms

MSD	Mass Selective Detector
MSP	Microspectrophotometry
M-Vac	Microbial-Vac System
MTBSTFA	N-Methyl-N-tert-butyldimethylsilyltrifluoroacetamide
P _{CW}	The partition coefficient of a solute in a chloroform/water system
P _{CL}	The partition coefficient of a solute in a chloroform/lysis buffer system
P _{CLP}	The partition coefficient of a solute in a chloroform/lysis buffer with proteinase K (incubated) system
P _{CB}	The partition coefficient of a solute in a chloroform/Butterfield's buffer system
P _{OW}	The partition coefficient of a solute in an octanol/water system
PCA	Principal Component Analysis
PCIA	Phenol Chloroform Isoamyl Alcohol
PDMS/DVB	Polydimethylsiloxane/Divinylbenzene
RNA	Ribonucleic Acid
SPME	Solid Phase Microextraction
SERS	surface-enhanced Raman spectroscopy
t-BDMCS	tert-Butylchlorodimethylsilane
TMCS	Trimethylchlorosilane
TMS	Trimethylsilyl
TNT	2,4,6-Trinitrotoluene
XBO	xenon short arc

ABSTRACT

Author: Ruchti, Jacqueline, S. MS

Institution: Purdue University

Degree Received: August 2019

Title: Analysis of TNT, DNA Methylation, and Hair Pigmentation via Gas Chromatography-Mass Spectrometry and Spectroscopic Techniques

Committee Chair: Dr. John Goodpaster

Gas chromatography-mass spectrometry (GC-MS) is a commonly used analytical technique that efficiently separates and identifies various volatile organic compounds. Here GC-MS was used with new methodologies for detecting 2,4,6-trinitrotoluene (TNT), deoxyribonucleic acid (DNA) methylation, and hair melanins. Spectroscopic techniques including Fourier-Transform Infrared Spectroscopy (FTIR), Microspectrophotometry (MSP), and Raman Spectroscopy were also used for detecting hair melanins. These methodologies would determine the following: 1) if TNT could be simultaneously collected and extracted with DNA; 2) if DNA methylation could determine the aging of DNA in blowflies; and 3) if an objective metric for hair pigmentation can be established.

For the first study, it was hypothesized that simultaneous analysis of post-blast debris for DNA and explosive compounds could improve explosives investigations. Hence, DNA and explosive residues would need to be separated via an extraction method. In preliminary work, GC-MS analysis via immersion solid phase microextraction (SPME) was optimized to directly analyze Microbial-Vac System (M-Vac) buffer extracts for explosives.

In this work, the PCIA extraction method was then applied to liquid samples rather than the traditional swab samplings. To maintain good layer partitioning and TNT peak resolution, the volume ratio of PCIA to Lysis Buffer to chloroform solution of TNT was set to 1:1:1. However, PCIA extraction was later deemed unnecessary for the chemical extraction of TNT. Instead, simpler methods of liquid-liquid extraction, charcoal strip extraction, and filtration were devised for extracting TNT prior to traditional DNA extraction methods. The partitioning of TNT, a common military explosive, was studied for the following four aqueous/organic solutions: water/chloroform, Lysis Buffer/chloroform, Lysis Buffer with proteinase K (incubated)/chloroform, and Butterfield's Buffer/chloroform. A liquid injection method was developed for the chloroform layer. An immersion SPME method was developed for the aqueous

layer. Since the Log P value for TNT in an octanol/water solution is 1.6, TNT was expected to partition by approximately 40:1 between octanol and water. However, the partitioning of TNT between Chloroform and Water was inconclusive. TNT partitioned by approximately 3:5 between Chloroform and Lysis Buffer, 1:2 between Chloroform and Lysis Buffer with proteinase K (incubated), and 35:2 between Chloroform and Butterfield's Buffer.

Due to the ability of the M-Vac to collect DNA from rough and porous surfaces, the device was tested for its effectiveness in also collecting TNT. Evidence collected via the M-Vac device was analyzed by GC-MS after extraction. Samples prepared via the chloroform partition method or charcoal strip extraction method were run via liquid injection while samples prepared via the filtration method were run via liquid immersion SPME. Following the application of a 50 ppm chloroform solution of TNT to pieces of a white t-shirt, TNT was successfully detected via the chloroform partition method. To simulate samples from an explosives investigation, a backpack containing a pipe bomb filled with TNT was detonated in a secured field. However, TNT was not successfully detected in any post-blast backpack debris samples prepared via the three extraction methods. Upon performing a direct liquid extraction with other post-blast backpack debris samples, it was determined that the amount of TNT on the post-blast backpack debris was too low. Hence, the M-Vac's efficiency for collecting TNT from post-blast debris is inconclusive. Therefore, other M-Vac buffer solutions, concealment materials, and explosive compounds should be explored.

For the second study, analyzing DNA methylation may determine the age of blowflies and thus improve the estimate of a post-mortem interval. A method for quantitatively analyzing the nucleobases (Cytosine, Thymine, Adenine, Guanine, and Uracil) was developed. DNA methylation most often occurs on the cytosine bases. Therefore, 5-methyl cytosine was also analyzed. Each nucleobase and 5-methyl Cytosine was derivatized with N,O-bis-(trimethylsilyl)trifluoroacetamide + 1% trimethylchlorosilane (BSTFA + 1% TMCS) and analyzed via a GC-MS liquid injection method. All five nucleobases and 5-methyl Cytosine were successfully derivatized with this reagent and heat, resulting in three trimethylsilyl (TMS) groups in the derivatized Guanine and two TMS groups in the derivatized Thymine, Cytosine, 5-methyl Cytosine, Adenine, and Uracil. DNA extracted from a common blowfly (*Phormia Regina*) was also analyzed by these GC-MS application methods. However, the concentrations fell below the limit of detection. Therefore, other derivatization methods and quantitative techniques should be explored prior to performing the blowfly DNA aging study.

For the third study, it was hypothesized that analyzing the chemical composition of hair can provide quantitative identification for human hair pigmentation. Determining the population distribution for human hair phenotypes could improve forensic investigations. Hence, eumelanin and pheomelanin would need to be simultaneously analyzed and quantitated. In this work, a method for quantitatively analyzing the two types of human hair melanin (eumelanin and pheomelanin) was developed. As major degradation products of eumelanin and pheomelanin, pyrrole-2,3,5-tricarboxylic Acid (2,3,5-PTCA) and L-3-aminotyrosine (3-AT), respectively, were studied. 2,3,5-PTCA and 3-AT were derivatized with N,O-bis-(trimethylsilyl)trifluoroacetamide + 1% trimethylchlorosilane (BSTFA + 1% TMCS) and analyzed via a GC-MS liquid injection method. 2,3,5-PTCA and 3-AT were successfully derivatized with this reagent and heat. Then liquid extraction methods were applied to *Sepia Officinalis* melanin to produce the melanin degradation products. However, liquid extractions were later deemed unnecessary for the chemical analysis of melanin degradation products. Instead, spectroscopic methods of FTIR, MSP, and Raman were explored for analyzing hair structure, pigmentation, and melanin degradation products.

Due to the abilities of FTIR to identify trace compounds and MSP to identify the color of a compound, these spectroscopic techniques were tested for their effectiveness to analyze hair. Hair samples analyzed by FTIR required the use of attenuated total reflectance (ATR) to reduce saturated absorption. The same samples analyzed by MSP required preparation with glycerin solution and quartz slides to broaden the wavelength range for detecting spectral features in the UV range. Hair structure and pigmentation were successfully detected by FTIR and MSP. However, Raman spectroscopy would be better suited for quantitatively determining the chemical composition of hair. Upon analyzing hair samples via Raman spectroscopy, weak signals from melanin were detected. Hence, the Raman's efficiency for detecting melanin would be better determined with a longer laser excitation wavelength and greater power.

CHAPTER 1. M-VAC COLLECTION EFFICIENCY OF TNT

1.1 Introduction

Improvised explosive devices (IEDs) have become common tools for criminals and terrorists at both the national and international levels. IEDs have been used in suicide bombings, embassy bombings, and automobile bombings. They are commonly contained in items such as pipes, bags, and bottles. These devices and associated tactics have been dynamic and dangerous, and more strategic analyses must be developed for both. Though many terrorist organizations have origins in the Middle East, Africa, and Asia, they have spread themselves globally and have begun receiving greater assistance from lone-wolf terrorists.¹ As their reach spreads and grows stronger, our countermeasures and analyses must as well.

In 2017, there were 687 explosive incidents in the United States. Of those incidents, 113 were caused by IEDs.² This includes an incident in late 2017 where a lone-wolf terrorist associated with the Islamic State of Iraq and the Levant (ISIL) planned an attack with “a foot-long pipe that contained black powder, a battery, wiring, nails and screws.”³ A few months later, another individual potentially associated with ISIL brought a homemade IED concealed in his backpack to his high school. The backpack contained “a metal soup can filled with shot gun shells containing BB pellets” as well as gasoline, an empty matchbox, black gun powder, an improvised fuse, and additional shrapnel.⁴ Outside the United States, bombing incidents are not uncommon. Globally there were 3,825 explosive incidents in 2017.⁵ This included a truck bomb which used “several hundred kilograms of military-grade and homemade explosives” to attack the center of Mogadishu.⁶ Two years earlier in another attempt for jihad, the Erawen Shrine in Bangkok was attacked by individuals using a pipe bomb filled with approximately three kilograms of TNT.⁷

While some devices are detected prior to detonation, many are not and require post-blast investigation. Explosives incidents require forensic scientists to perform multiple analyses, particularly DNA analysis and explosives analysis. Extraction and analysis of DNA from explosive device fragments can be used to identify any individual(s) who have been in contact with the device, such as the IED assemblers, handlers, and victims. Analysis of the chemical composition of the explosive(s) utilized can identify the source of the explosive device. Several GC-MS methods for detecting 2,4-DNT and TNT have been previously reported.⁸ However, there are no current

methods for simultaneously collecting both types of evidence. Furthermore, the method would need to maintain or improve the extraction efficiency of both the DNA and explosive from a given item of evidence.

Explosive compounds are generally classified as inorganic or organic in terms of their chemical composition and high or low in terms of their explosive power. Here we focus on TNT, which is classified as an organic high explosive. As a high explosive, TNT detonates rather than deflagrates. Due to its conversion into gaseous products, only trace amounts of the explosive residue are generally obtained post-blast. Furthermore, this explosive residue is spread amongst the IED fragments, soil, and any witness material. To detect these trace amounts, sensitive methods such as GC-MS are needed.

Work previously completed by Jordan Ash and Logan Hickey included the optimization of GC-MS parameters for explosives analysis and the analysis of TNT after collection via swabbing, respectively. These analyses involved sample collections via swabbing or taking a cutting. However, these two methods greatly limit the surface area being examined. They rely on collecting samples from areas which may or may not contain the targeted material. Additionally, efficient swabbing is more difficult with porous surfaces. These limitations result in low recoveries of targeted materials.⁹⁻¹⁰

Here we evaluated the efficiency of a relatively new collection technique, particularly pertaining to sampling explosives evidence. If efficient, this technique would improve the productivity in a post-blast investigation. Since DNA and explosives analyses are generally isolated from one another and analyzed in series, investigations can suffer from extensive examination time. Furthermore, explosives analyses generally involve extractions that are incompatible with DNA analyses and may involve excessive handling that can decrease the potential recovery of DNA.

With the ability to collect evidence from porous surfaces, the M-Vac is tested here as a potential solution. An M-Vac system installed at IUPUI (Figure 1-1) has proven effective for collecting DNA but had yet to be applied to explosive residues. The M-Vac is a wet-vacuum sampling device, which uses a pressurized stream of Butterfield's Buffer (Potassium Dihydrogen Phosphate diluted in demineralized water) to dislodge particles present on a porous surface while simultaneously vacuuming the particles into its collection bottle (Figure 1-2). This system allows the collection of a larger surface area than was previously possible via other sampling techniques.¹¹



Figure 1-1. M-Vac System

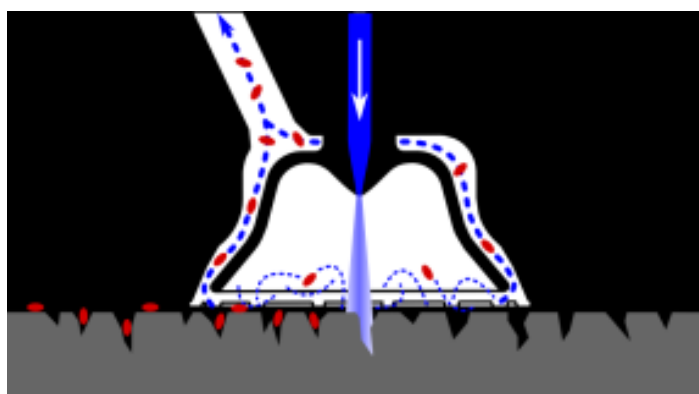


Figure 1-2. Diagram of M-Vac's Simultaneous Spray and Vacuum¹¹

Prior to applying the M-Vac to explosive residue samples, methods for analyzing explosives in the M-Vac's buffer solution needed to be developed for detection and characterization. To further understand the original concentrations of explosives present, the partition coefficient of the explosive must be determined. Thus, methods for analyzing TNT in aqueous and organic solvents were developed using GC-MS. This method is sensitive, relatively selective, and specific.

1.2 Experimental

Materials

2,4,6-Trinitrotoluene was purchased from Omni Distribution, Inc. 2,4-Dinitrotoluene (DNT) was purchased from Spectrum Chemical MFG Corp. Chloroform (HPLC grade) and polydimethylsiloxane/divinylbenzene (PDMS/DVB) SPME fibers were purchased from Sigma-Aldrich. Acetone (GC Resolv), Phenol Chloroform Isoamyl Alcohol (PCIA) (Biotech Grade), Methanol (HPLC grade), liquid injection caps and vials, 0.45 μm Nylon filters, Finnpiettes, Touch Mixer Model 232 vortex, and an accuSpin Micro 17 centrifuge were purchased from Fisher Scientific. Butterfield's Buffer was purchased from Microbial-Vac Systems, Inc. SPME vials and caps were purchased from Restek. Pierce IP Lysis Buffer, 1 mL plastic syringes, and a 500 μL eVol dispensing syringe were purchased from Thermo Scientific. Proteinase K Solution (20 mg/mL) was purchased from Promega Corporation. Milli-Q Water was obtained via a Thermo Scientific Thermo E-Pure Water Purification System. 1.5 mL polypropylene micro centrifuge tubes and a Hanes ComfortSoft white cotton t-shirt were commercially purchased. Galvanized steel pipes (1 in. x 8 in.) were purchased from Southland. A polyester/polypropylene blend backpack was commercially manufactured and obtained at a scientific conference. Activated charcoal strips were purchased from Albrayco Technologies, Inc. A Reacti-Therm Heating/Stirring Module was purchased from Pierce Chemical Company. An M-Vac system was purchased from Microbial-Vac Systems, Inc. A 6890N GC and a 5975 inert MSD were purchased from Agilent Technologies.

Methods

Adjusted DNA Extraction

A 500 μL sample of TNT in Chloroform was added to a centrifuge tube. Then similar to a general liquid-liquid extraction for DNA,¹² 500 μL of Lysis Buffer and 50 μL of proteinase K were added to the tube. The centrifuge tube was incubated at approximately 85 $^{\circ}\text{C}$ for 4 hours. Following incubation, the tube was centrifuged for a few seconds. Then the top layer was discarded, and 500 μL of PCIA was added to the tube. The tube was centrifuged again for 1 minute at 13,000 rpm. Finally, the new top layer was discarded as well, and the chloroform layer was extracted for analysis via liquid injection on the GC-MS.

Partition Coefficient/M-Vac Extraction Methods

Chloroform Partition

To determine partition coefficients, 2 mL of a chloroform solution of TNT and 2 mL of either buffer or water were placed into a test tube. To determine the M-Vac's collection efficiency, 2 mL of a Butterfield's Buffer extract collected with the M-Vac was placed into a test tube with 2 mL of chloroform. In both scenarios, the sealed test tube was then vortexed for approximately 1 minute, allowed to rest for approximately 2 minutes, and then repeated. The chloroform layer was extracted and run on the GC-MS via liquid injection.

Charcoal Strip Extraction

TNT was extracted with Butterfield's Buffer via M-Vac collection. Then a charcoal strip was placed in a vial with approximately 15 mL of the collected solution for approximately 3 hours. The charcoal strip was removed, and 2 mL of chloroform was used to extract any TNT present on the charcoal strip.

Filtration

TNT was extracted with Butterfield's Buffer via M-Vac collection. Then between 15 and 20 mL of the collected solution was filtered through a 0.45 μm Nylon filter. DNA would be expected to form a film on the Nylon filter while the TNT would be expected to remain in solution and pass through the Nylon filter.

Liquid Injection Volumetric Internal Standard

A 1.5 mL aliquot was placed in a vial. A 600 ppb DNT internal standard solution was placed in a wash bottle. The liquid syringe collected 1 μL of the sample and 1 μL of the internal standard, resulting in halved concentrations.

Liquid Immersion Solid-Phase Microextraction (SPME)

In liquid immersion SPME, a 15 mL aliquot was placed in a vial, agitated, and heated. Meanwhile a fiber was introduced to the vial such that the sample will be adsorbed onto the fiber coating. This method has generally shown increased sensitivity over traditional liquid injection.¹⁰ The sample was filtered through a 0.45 μm Nylon filter prior to analysis.

Instrumental

M-Vac System (M-Vac)

An M-Vac was used as a collection technique prior to GC-MS analysis. Butterfield's buffer was sprayed onto the surface of the sample while being vacuumed into the collection bottle simultaneously. This was performed in rotation with solely using the vacuum. The spray was used as necessary to collect approximately 50 mL of solution.

GC-MS

An Agilent 6890N Network GC coupled to an Agilent 5975 Inert MSD was used for all analyses, along with a Gerstel MultiPurpose Sampler. Utilizing the incubation station for the autosampler, samples were heated to 60°C for 1 minute prior to the introduction of the polydimethylsiloxane (PDMS) fiber for 30 minutes. The column used was a DB5-MS with dimensions of 30 m x 0.25 mm x 0.25µm. Hydrogen carrier gas was utilized at a flow rate of 2.0 mL/min. The oven temperature program started at 60°C for 1 minute and was then ramped at 20°C/min to 210°C and held there for 1 minute. The mass transfer line into the MS was set to 280°C and the source temperature was set to 230°C. The MS was in negative ionization mode. Selected ion monitoring was used at m/z 89 ([DNT – 2NO₂]⁺ or [TNT – 3NO₂]⁺), m/z 165 ([DNT – OH]⁺), and m/z 210 ([TNT – OH]⁺) for detection of DNT and TNT.^{8, 13} The total scan time was 9.5 minutes, scanning from 40 amu to 550 amu.

1.3 Results and Discussion

GC-MS Detection of TNS and DNT

Due to the variety of explosives used, a separation technique prior to detection using an MS is needed. GC-MS sufficiently separates and identifies TNT from DNT, our explosives of interest (Figures 1-3, 1-4, and 1-5).

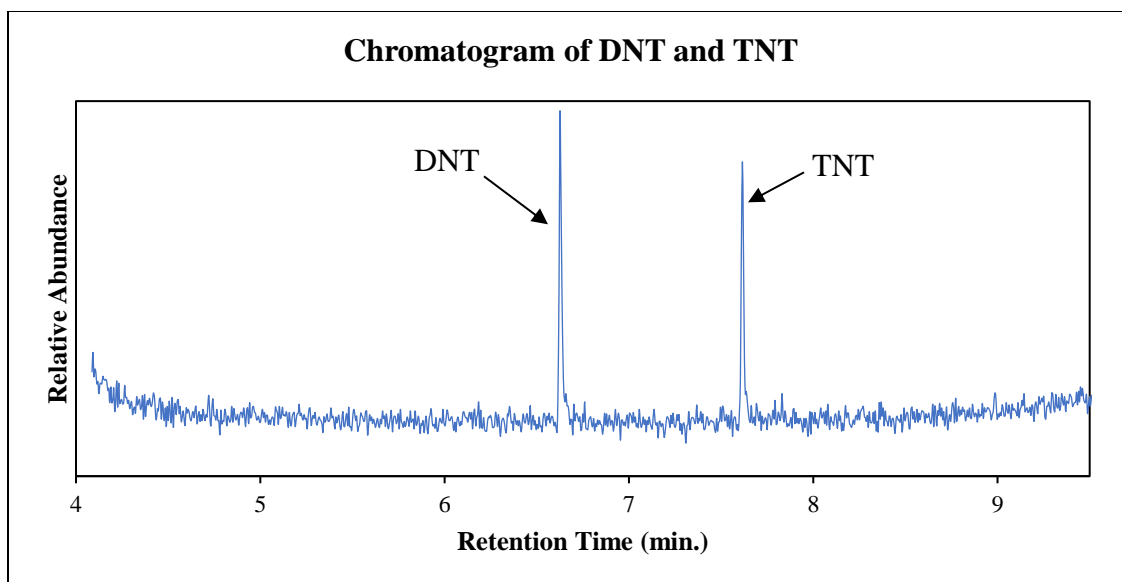


Figure 1-3. Total Ion Chromatogram (TIC) of 300 ppb DNT (6.6 min) and 300 ppb TNT (7.6 min) in Chloroform

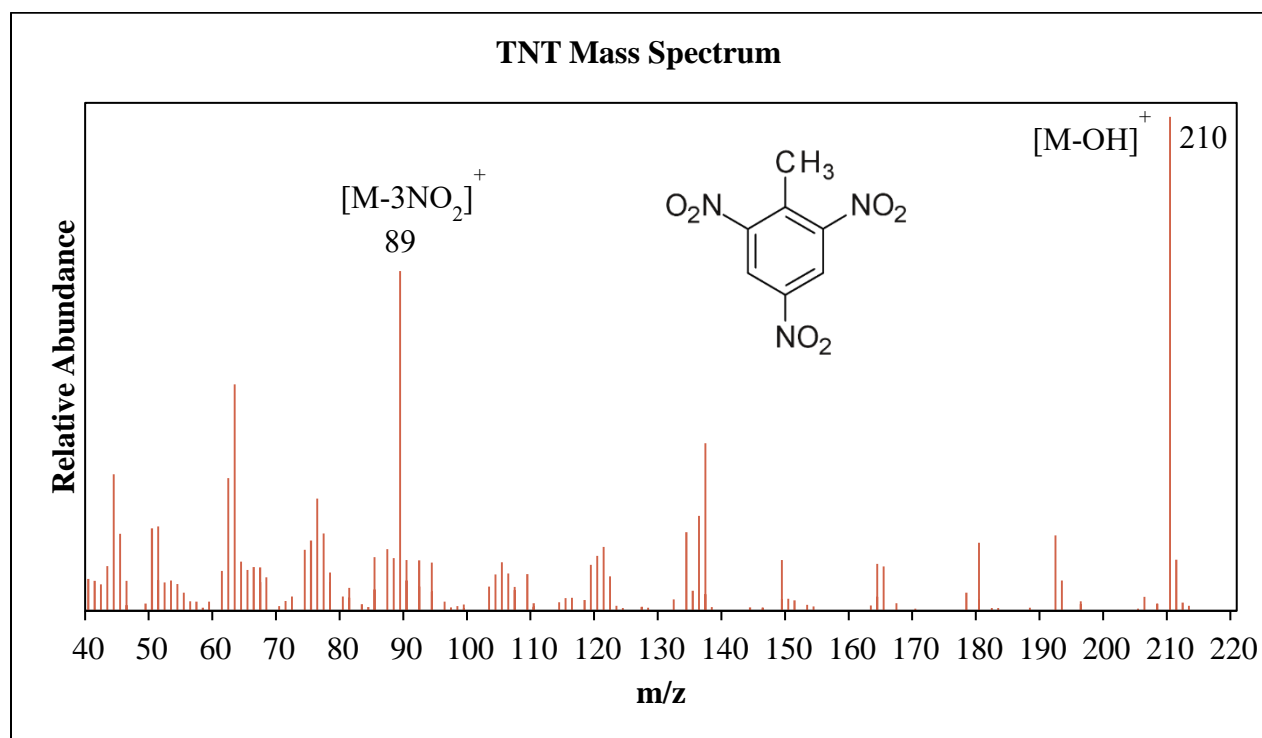


Figure 1-4. Structure and significant fragmentation of TNT overlaid on its mass spectrum

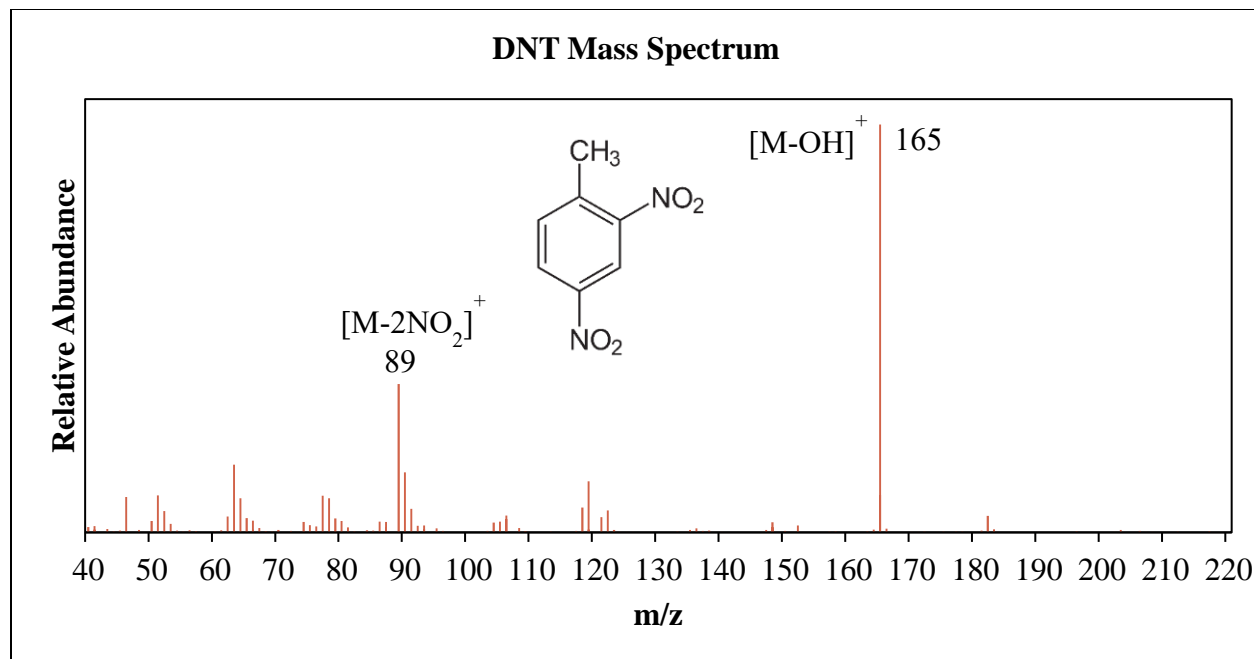


Figure 1-5. Structure and significant fragmentation of DNT overlaid on its mass spectrum

Optimization of a General DNA PCIA Extraction

As preparation for samples collected via M-Vac, liquid solutions of TNT were used rather than using the traditional swabbing method. A general Phenol Chloroform Isoamyl Alcohol (PCIA) extraction for DNA was performed initially to optimize the parameters for the extraction and GC-MS analysis. A large phenol peak area was observed despite the 2-minute solvent delay. Therefore, the solvent delay was adjusted to 4 minutes to avoid further hindrance from the phenol peak. The ratio of PCIA to Lysis Buffer was set at 1:1 to provide good layer separation. However, the poor resolution of the small TNT peak required an adjustment to the extraction method. Rather than reducing the volume of PCIA, the volume of the chloroform solutions of TNT was increased to concentrate the TNT and thus to improve its peak resolution (Figure 1-6).

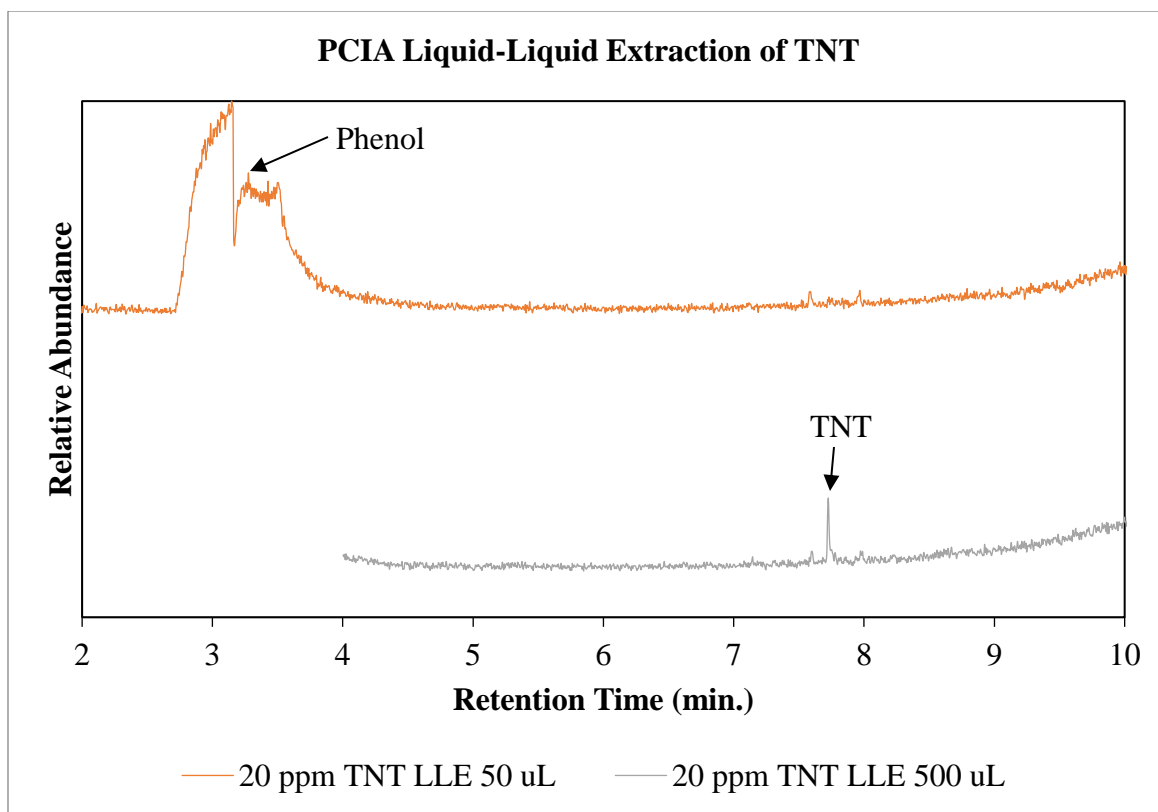


Figure 1-6. Extracted Ion Chromatograms for m/z 210 from PCIA Liquid-liquid Extractions of TNT, using 50 μL of a 20 ppm Chloroform Solution of TNT with a 2-minute solvent delay (orange) and 500 μL of a 20 ppm Chloroform Solution of TNT with a 4-minute solvent delay (grey)

Upon further consideration, PCIA extraction was deemed unnecessary for the chemical extraction of TNT. One alternative method would be to filter out the DNA from the solution collected via M-Vac. Meanwhile the TNT would likely remain in solution and pass through the filter. A second alternative method would include the partitioning of the collected solution into an aqueous layer and an organic layer. In this partitioning method, TNT would be expected to gather in the organic layer while DNA gathered in the aqueous layer. A third alternative method would include extracting the TNT from the collected solution with a charcoal strip.

Partition Coefficient Study

Determination of partition coefficients (P) for TNT in the examined aqueous/organic mixtures (i.e. P_{CW} , P_{CL} , P_{CLP} , and P_{CB}) was desired for estimating the potential recovery of TNT utilizing the M-Vac and a liquid-liquid extraction. The partition coefficient for each mixture was

calculated by using Equation 1-1. Determining the Log P values as well provides a better indication of the hydrophilicity/lipophilicity of the compound. A negative value indicates that the compound is hydrophilic, whereas a positive value indicates that the compound is lipophilic. A zero value indicates neutrality such that the compound has an equivalent affinity for both the aqueous and organic layers. The Log P value for each mixture was calculated by taking the logarithm of the partition coefficient or by using the equivalent,¹⁴ Equation 1-2.

$$P = \frac{[TNT]_{\text{organic layer}}}{[TNT]_{\text{aqueous layer}}} \quad (1-1)$$

$$\text{Log } P = \text{Log} \frac{[TNT]_{\text{organic layer}}}{[TNT]_{\text{aqueous layer}}} \quad (1-2)$$

Since the literature value of Log P for TNT is 1.6, TNT is expected to partition by approximately 40:1 between octanol and water, respectively (Equation 1-3). This partition coefficient was used to predict the partitioning of TNT between chloroform and water via Equations 1-4 and 1-5. Then this partition coefficient for TNT in chloroform and water would form a basis for the partition coefficients for TNT in chloroform and each extraction buffer.¹⁴

$$P_{OW} = 10^{\text{Log } P_{OW}} = 10^{1.6} \approx 40 \quad (1-3)$$

$$\text{Log } P_{CW} = (1.13) * \text{Log } P_{OW} - 1.34 \approx 0.46 \quad (1-4)^{15}$$

$$P_{CW} = 10^{\text{Log } P_{CW}} = 10^{0.468} \approx 2.94 \quad (1-5)$$

Liquid Injection

A liquid injection method was developed for detecting 2,4-DNT and TNT in chloroform. Using this method, quantitative analysis was performed. 2,4-DNT was held at a constant concentration of 300 ppb. TNT concentrations ranged between 50 ppb and 1 ppm to create calibration curves. Upon analysis, good linearities ($R^2 = 0.99$) were achieved for TNT concentrations between 50 ppb and 1 ppm (Figures 1-7 and 1-8).

Using the linear regression equation $y = 15.413x - 778.73$, the amount of TNT remaining in the chloroform layer after partitioning with the aqueous layer (i.e. water, Lysis Buffer, or Lysis Buffer with Proteinase K and incubation) was calculated. Since each extract was run in triplicate, the concentrations of TNT were averaged for each aqueous layer. The averaged concentrations were then used to calculate the three partition coefficients (Table 1-1), using Equation 1-1. The solution of Chloroform and Butterfield's Buffer produced the only partition coefficient in favor of the organic layer.

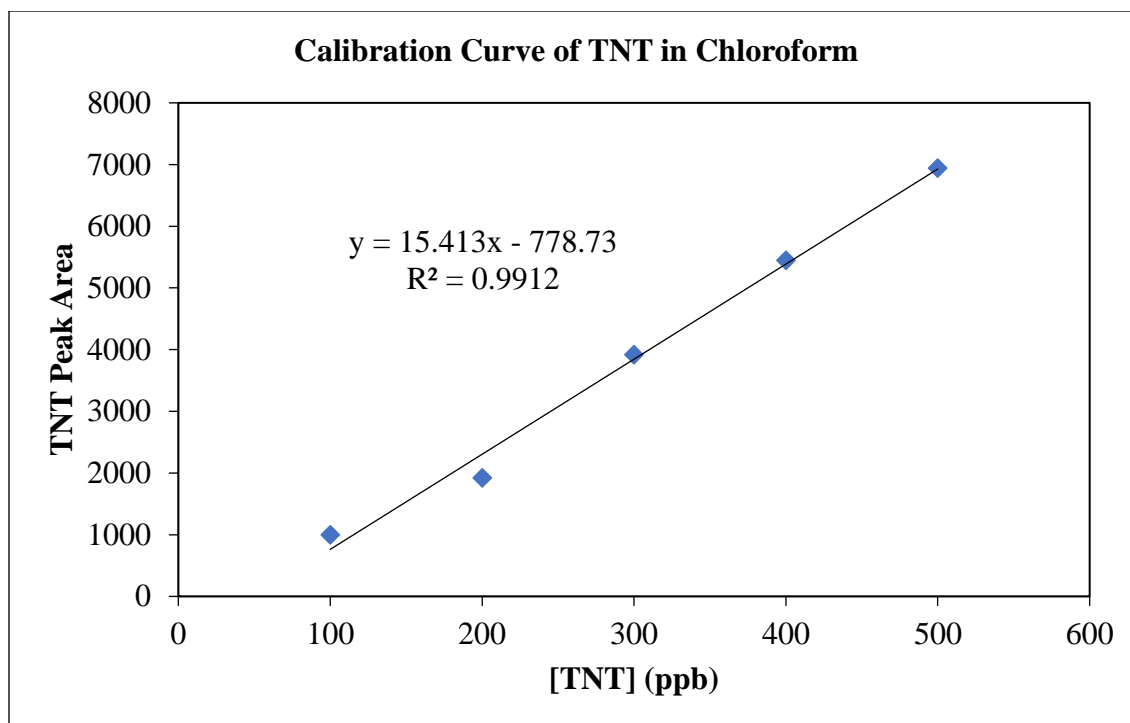


Figure 1-7. Calibration Curve from Total Ion Chromatograms of Chloroform Solutions of TNT run via liquid injection and in sequence with partition coefficient study samples for water, lysis buffer, and lysis buffer with proteinase K and incubation

$$[TNT] = \frac{(TNT\ Peak\ Area) + 778.73}{15.413} \quad (1-6)$$

This was repeated for the partition coefficient for TNT in chloroform and Butterfield's Buffer. Since this was performed later, new calibrants were prepared and run in sequence with the extracted samples. Therefore, the linear regression equation, $y = 0.0019x - 0.0931$, was used for the calculations (Figure 1-8).

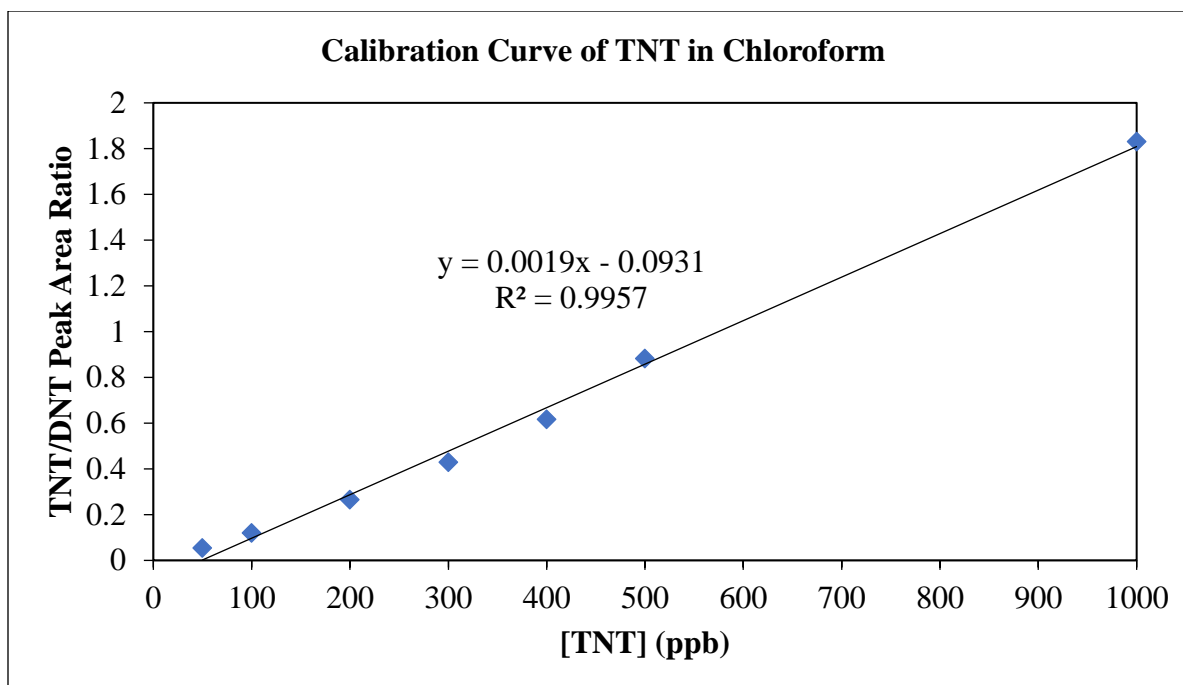


Figure 1-8. Calibration Curve from Total Ion Chromatograms of Chloroform Solutions of TNT which were run in sequence with the Butterfield's Buffer partitioned samples and T-shirt samples via liquid injection

$$[TNT] = \frac{\left(\frac{TNT}{DNT} \text{ Peak Area Ratio}\right) + 0.0931}{0.0019} \quad (1-7)$$

Table 1-1. Experimental Partition Coefficients and their Respective Log P Values

TNT in Chloroform Partitioned with...	Average P	Standard Deviation of P	Average Log P	Standard Deviation of Log P
Water	< 0	N/A	N/A	N/A
Lysis Buffer	0.636	0.186	-0.209	0.126
Lysis Buffer + Proteinase K + Incubation	0.524	0.089	-0.284	0.071
Butterfield's Buffer	9.07-15.4*	4.53	0.958-1.190*	1.074

*Due to an outlier, only two values were averaged for the Butterfield's Buffer partitioning with chloroform. Therefore, the range is shown instead of the average value.

Liquid Immersion SPME

A liquid immersion SPME method was developed for detecting TNT in aqueous solutions. Using this method, quantitative analysis was performed. 2,4-DNT was held at a constant concentration of 600 ppb for the water solutions. TNT concentrations ranged between 50 ppb and 1 ppm to create calibration curves. Upon analysis, good linearities ($R^2 = 0.95$ and $R^2 = 0.98$) were detected for TNT concentrations between 200 ppb and 1 ppm in Water (Figure 1-9) and TNT concentrations between 50 ppb and 1 ppm in Butterfield's Buffer (Figure 1-10), respectively. Analyzing TNT in water via liquid immersion SPME provided a basis for analyzing TNT in Butterfield's Buffer, which would require minimal sample preparation when extracting the TNT with the M-Vac.

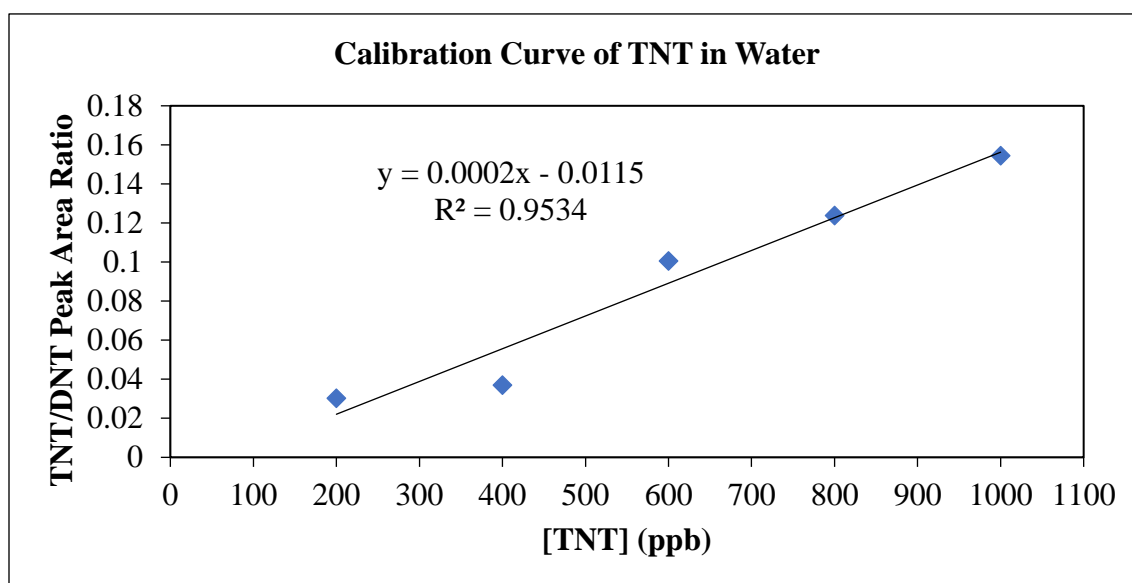


Figure 1-9. Calibration Curve of Water Solutions of TNT via Immersion SPME

$$[TNT] = \frac{\left(\frac{TNT}{DNT} \text{ Peak Area Ratio} \right) + 0.0115}{0.0002} \quad (1-8)$$

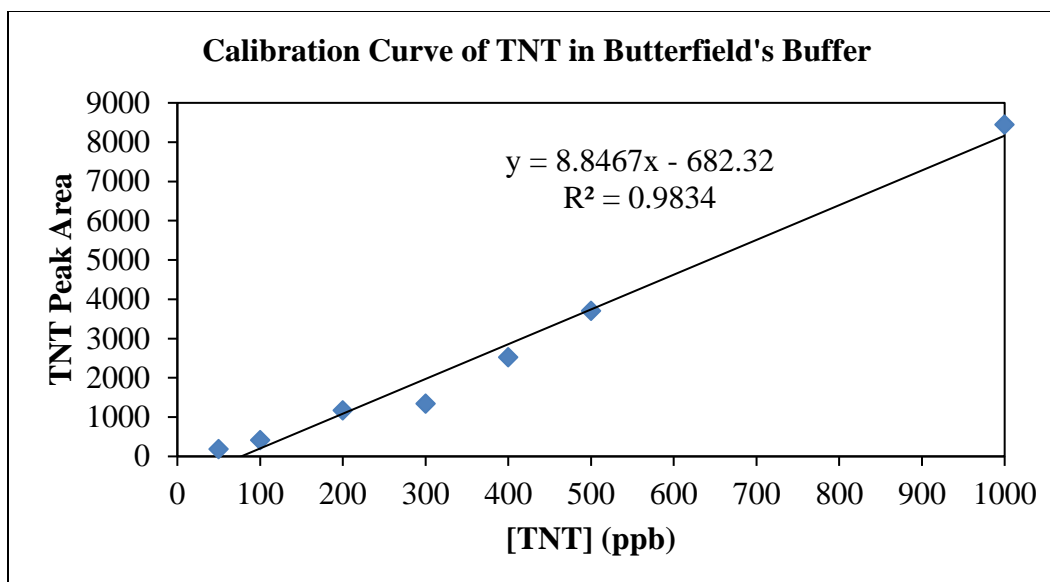


Figure 1-10. Calibration curve for TNT in Butterfield's Buffer performed via Immersion SPME and in sequence with post-blast backpack debris samples

$$[TNT] = \frac{(TNT \text{ Peak Area}) + 682.32}{8.8467} \quad (1-9)$$

M-Vac Collection Efficiency

Due to the ability of the M-Vac to collect DNA from rough and porous surfaces, the device was used to test its effectiveness in collecting TNT. Evidence collected via the M-Vac device was analyzed by GC-MS via the liquid injection method or liquid immersion SPME method after liquid-liquid extraction or filtration, respectively.

Liquid Injection

Using the liquid injection method for detecting 2,4-DNT and TNT in chloroform, quantitative analysis was performed. 2,4-DNT was held at a constant concentration of 300 ppb. A 500 μ L aliquot of a 10 ppm solution of TNT in chloroform was applied to the center of three individual 3 in. x 3 in. T-shirt pieces. This was repeated for a 50 ppm solution of TNT in chloroform with three new T-shirt pieces. After allowing these T-shirt pieces to sit overnight, the M-Vac used Butterfield's Buffer to extract TNT from the T-shirt pieces. Approximately 25 mL of

solution was collected for each piece and placed in separate vials. The chloroform partition method was performed. Then the samples were run in sequence with the calibrants from Figure 1-15.

Using the linear regression equation $y = 0.0019x - 0.0931$, the amount of TNT in the chloroform layer after partitioning with the Butterfield's Buffer extract was calculated. Since each solution was run in triplicate, the mass of TNT was averaged for both the 10 ppm aliquots and 50 ppm aliquots (Figure 1-11). The instrument's sensitivity for the 10 ppm aliquot samples was insufficient for this method. Therefore, only the averaged mass for the 50 ppm aliquot samples was used to determine the percentage of mass recovered (Table 1-2), using Equation 1-10.

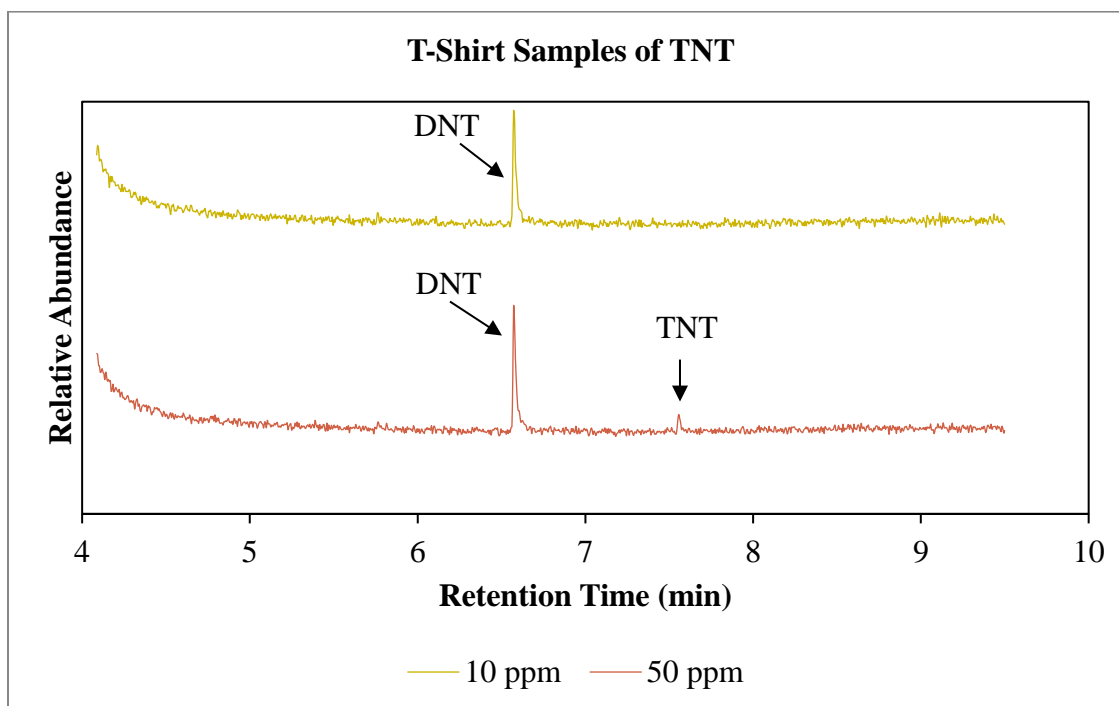


Figure 1-11. Overlaid Total Ion Chromatograms of samples prepared with solutions of 10 ppm and 50 ppm TNT in Chloroform applied to T-shirts and Extracted

Table 1-2. TNT Mass Recovery from T-Shirt Samples Collected via M-Vac

		Standard Deviation
Mass (μg) applied to T-shirt	25.0	-
Mass (μg) recovered	0.285	0.0251
% Mass Recovered	1.14	0.100

$$\% \text{ Mass Recovered} = \frac{\text{Mass (mg) recovered}}{\text{Mass (mg) applied to T-shirt}} * 100 \quad (1-10)$$

TNT powder and a 0.2 lb. TNT booster were packed into a galvanized pipe, which was then placed into a backpack and under a wood board/steel cage apparatus. After the explosive device was detonated, the remaining backpack pieces were placed in a metal paint can with an airtight seal. After three larger pieces of the backpack were removed from the can, the M-Vac used Butterfield's Buffer to extract TNT from them. Approximately 50 mL of solution was collected for each sample piece. For each sample, the solution was evenly divided into 3 separate vials for 3 different methods (i.e. chloroform partition method, charcoal strip extraction method, and filtration method). Then the samples from the chloroform partition method and charcoal strip extraction method were run via liquid injection. However, no TNT peaks were apparent for the backpack samples (Figure 1-12).

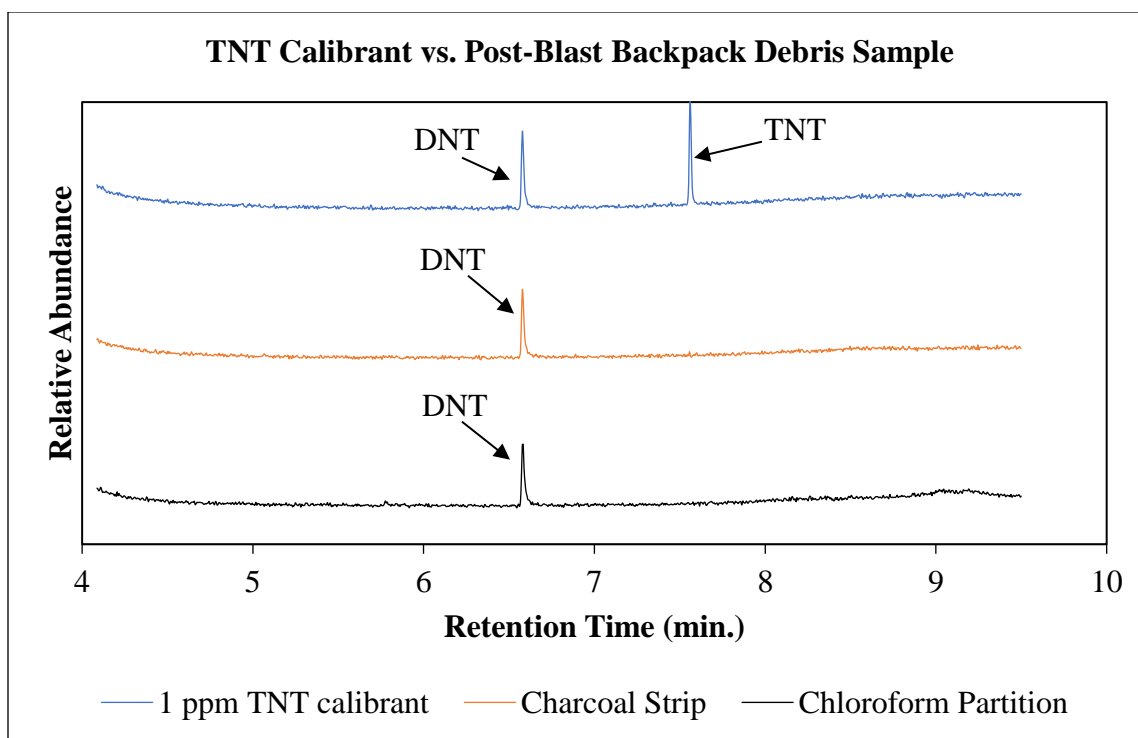


Figure 1-12. Overlaid Total Ion Chromatograms of a 1 ppm TNT in Chloroform Solution (blue) and Post-Blast Backpack Debris Samples prepared via the Charcoal Strip Extraction method (orange) and the Chloroform Extraction method (grey) and analyzed via Liquid Injection

Furthermore, no TNT peaks were present in the m/z 210 extracted ion chromatograms for these samples. To determine the cause of these absent TNT peaks, a direct liquid extraction was performed. Chloroform was used to extract any TNT present on new post-blast backpack debris

pieces removed from the sealed metal paint can. The chloroform extract was run on the GC-MS via liquid injection. Again, no TNT was detected (Figure 1-13).

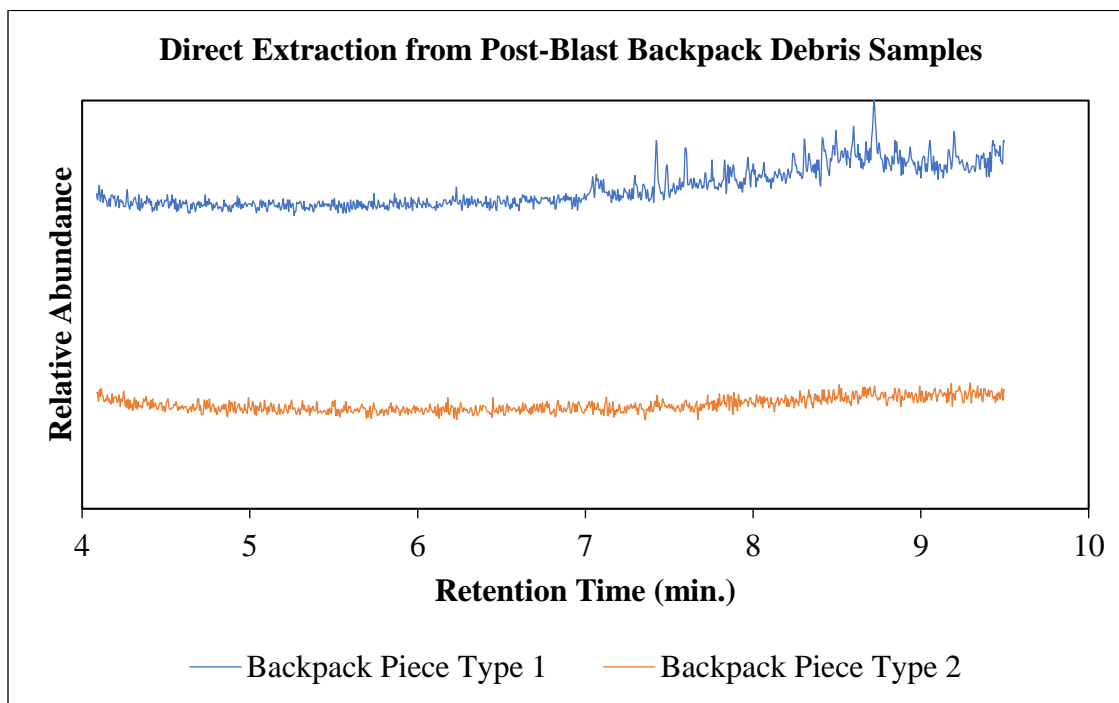


Figure 1-13. Extracted Ion Chromatograms of m/z 210 for the Direct Chloroform Extraction of TNT from Backpack Pieces of two different surfaces

Liquid Immersion SPME

The samples collected via the filtration method were run on the GC-MS via liquid immersion SPME. This method reduced the sample preparation and utilized greater sensitivity compared to traditional liquid injection. Although this method detected Butterfield Buffer solutions of TNT between 50 ppb and 1 ppm, no TNT peaks were detected in the total ion chromatograms or extracted ion chromatograms for the post-blast backpack debris samples tested (Figure 1-14). Therefore, either no TNT was present on the samples prior to collection or the sensitivity was insufficient for this method.

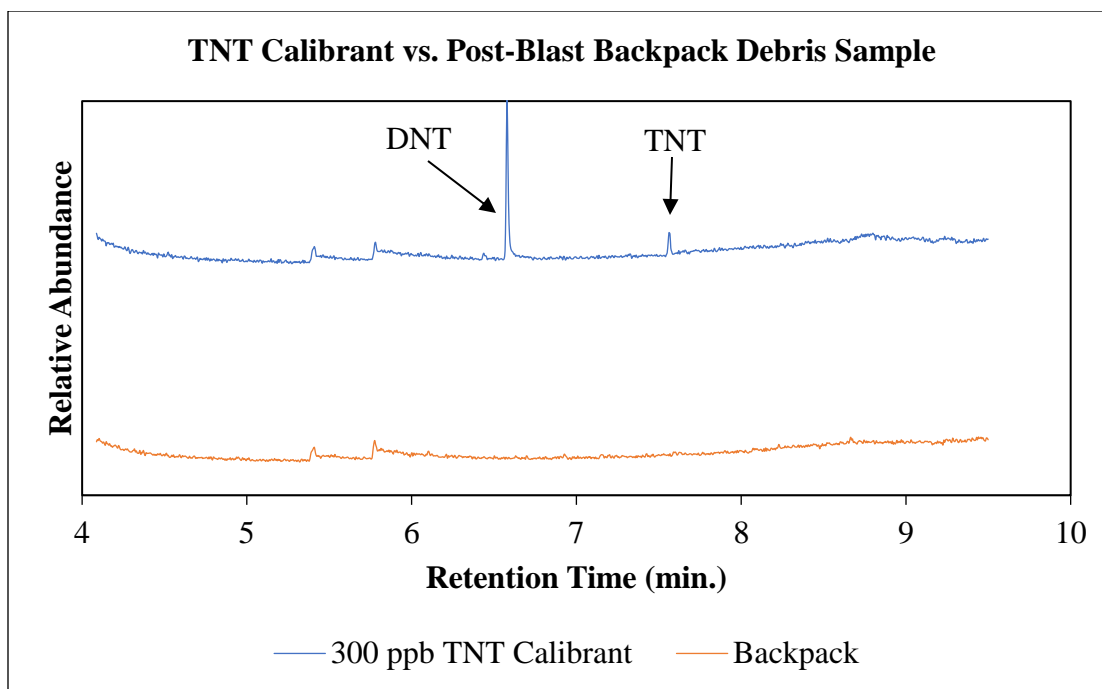


Figure 1-14. Overlaid Total Ion Chromatograms of 300 ppb TNT in Butterfield's Buffer Calibrant Solution (blue) and Backpack Sample taken via the Filtration method (orange) and analyzed via Immersion SPME

1.4 Conclusion

Two methods for analyzing the partitioning of TNT between aqueous and organic layers were explored. Samples of TNT in chloroform and given aqueous layers were analyzed by each method to provide a basis for analyzing samples collected by the M-Vac. Three new partition coefficients were successfully determined for TNT between chloroform and given aqueous solutions (Table 1-1). Overall, TNT greatly favored the chloroform layer over the aqueous layer. Hence, TNT was better analyzed via liquid injection after an organic extraction or via immersion SPME after filtration only. However, determining a partition coefficient for TNT between chloroform and water was unsuccessful. The interactions within this solution resulted in uncertain increases in TNT concentration.

Prior to collecting potential TNT residue from post-blast backpack debris, known samples were collected from t-shirt pieces via M-Vac. There was little TNT recovery from the t-shirt pieces with the M-Vac (Table 1-2). When post-blast backpack debris samples were collected via M-Vac, there was no indication that TNT was extracted with the Butterfield's Buffer since the chromatograms showed no peaks for TNT (Figures 1-12, 1-13, and 1-14). Hence, the M-Vac

proved to be an ineffective new collection method for TNT residue on post-blast debris. If the M-Vac is to be used for the collection of explosive residue, optimization must be performed with various extraction buffers, explosive materials, and debris materials to determine the M-Vac's potential for recovery of explosive material. These possibilities will be discussed further in "Chapter 4: Future Work."

CHAPTER 2. ANALYSIS OF DNA METHYLATION IN BLOWFLIES

2.1 Introduction

Determining the age of an adult blowfly can aid in determining the postmortem interval (PMI) of a cadaver. An estimate of the minimum time the individual was deceased could be determined by the age of the oldest fly. Therefore, the adult flies must be distinguished as ones that recently completed their development on that cadaver or ones that made their way into the scene. However, the aging of DNA in each blowfly species is unknown. Currently an estimation of the age of an adult fly can be determined by methods including analyzing the amount of pyrimidine in the eye and the degree of wear and tear on the wings.¹⁶⁻¹⁷ However, these methods have been impractical and sometimes inaccurate.

Since DNA methylation has been shown to control some aspects of gene expression, obtaining DNA samples from blowflies can be important for forensic analysis. Hence, analysis of the DNA methylation may provide quantitative identification for the age of a given blowfly and thus a postmortem interval for a cadaver. DNA methylation occurs primarily at the carbon 5 of the cytosine nucleobase to produce 5-methyl cytosine (Table 2-1).¹⁸ Cytosine methylation has been studied via methods including GC-MS, LC-MS, and MS-AFLP, or whole genome sequencing following bisulfite conversion of the cytosines.¹⁹⁻²¹ Both chemical and genetic methods can determine the relative degree of methylated cytosines vs. unmethylated cytosines. However, only pyrosequencing can currently determine where the methylation changes occur in a given DNA sample. Unfortunately, this method is the most expensive and requires a completely sequenced genome.²²

With the ability to separate and identify trace levels of organic compounds, GC-MS could be the solution. Through the quantitative analysis of DNA methylation via GC-MS, an X-Y plot could be formed to further determine a blowfly's age based on its ratio of methylated DNA to unmethylated DNA. DNA is made up of two strands of nucleotides bonded to one another. Hence, nucleotides are structural subunits of nucleic acids. They consist of a 5-carbon sugar, a phosphate group, and a nitrogenous base. They can be further broken down into nucleosides and nucleobases. Nucleosides consist of the 5-carbon sugar and a nitrogenous base. Nucleobases solely consist of the nitrogenous base. Primarily comprised of Carbon, Nitrogen, and Hydrogen atoms, the

nitrogenous base can be either a pyrimidine or a purine. While pyrimidines are single ring structures, purines are two-ringed structures. The purines found in DNA include Adenine and Guanine. The pyrimidines found in DNA include thymine and cytosine. Additionally, Thymine is replaced by the pyrimidine Uracil in RNA.²³ These structures are further elucidated in Tables 2-1 and 2-2.

Since DNA methylation occurs most often on the nucleobase Cytosine, Cytosine and 5-methyl Cytosine will be analyzed to determine peak area ratios against known ages of blowflies tested. Prior to analyzing blowfly DNA samples via GC-MS, a method for quantitatively analyzing the four DNA nucleobases (Adenine, Cytosine, Guanine, and Thymine), 5-methyl Cytosine, Uracil, and their respective nucleosides was developed (Tables 2-1 and 2-2). Thus, a method for analyzing derivatized nucleobases and nucleosides in acetonitrile was developed. To better detect these compounds via gas chromatography, they were derivatized to increase volatility and more readily vaporize. Derivatization reagents are used to attach functional groups to the compounds to decrease polarity and increase volatility, thermal stability, and selectivity.²⁴

For detection purposes, the concentration of each nucleobase must also be considered, especially when presented in a DNA sample. Due to Chargaff's base pairing rules, there should be an equivalent number of Adenines and Thymines and an equivalent number of Cytosines and Guanines.²⁵ For example, if a given DNA sample is 36% Guanine and Cytosine and 64% Adenine and Thymine, then Cytosine comprises only 18% of the DNA nucleobases. The Cytosine nucleobase comprises 45.68% of the Cytosine nucleoside molecular weight or 34.38% of the Cytosine nucleotide molecular weight. Hence, if the original DNA solution is a nucleotide mix, then the Cytosine nucleobase only comprises 6.19% of the sample. On the other hand, if the original DNA solution is a nucleoside mix, then the Cytosine nucleobase only comprises 8.22% of the sample. As methylation occurs, the number of Cytosines should decrease while the number of 5-methyl Cytosines should increase.

Table 2-1. Nucleobases, Nucleosides, and Nucleotides of key DNA methylation compounds analyzed in this work

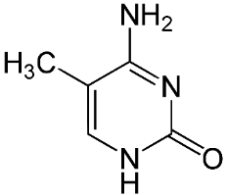
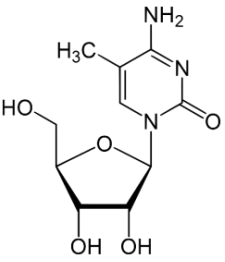
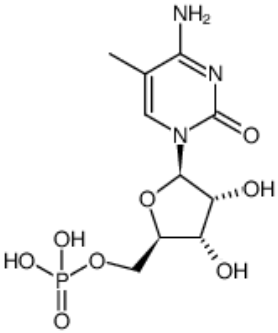
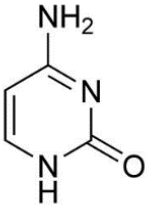
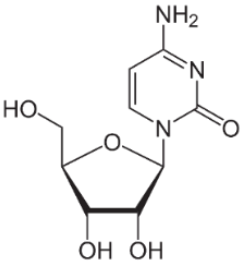
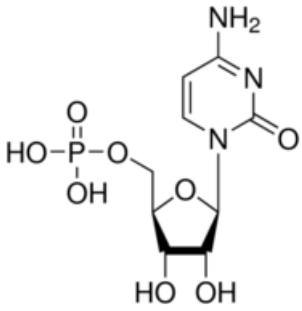
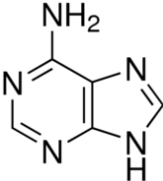
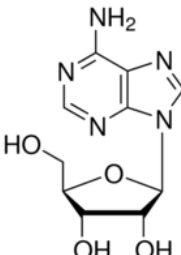
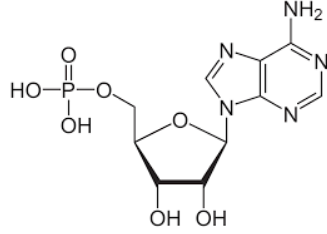
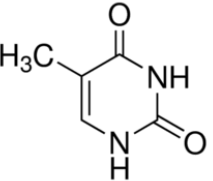
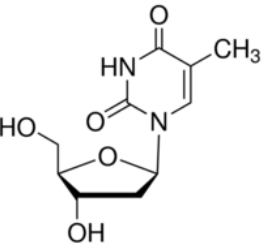
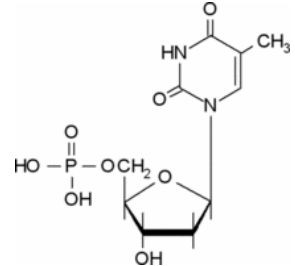
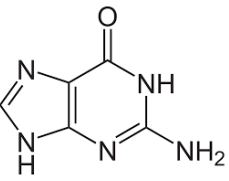
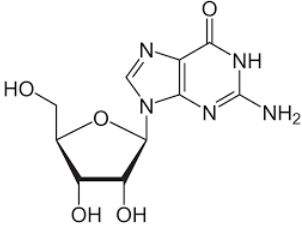
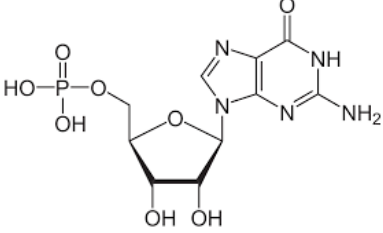
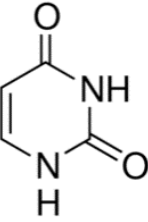
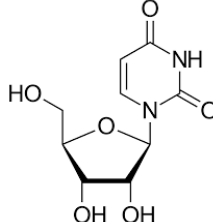
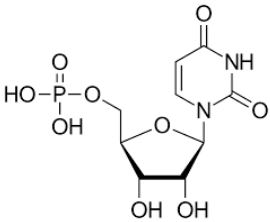
Letter Abbreviations	Nucleobases	Nucleosides	Nucleotides
5mC	 <p>5-methyl cytosine</p>	 <p>5-methyl cytidine</p>	 <p>5-methyl cytidine monophosphate</p>
c	 <p>Cytosine</p>	 <p>Cytidine</p>	 <p>Cytidine monophosphate</p>

Table 2-2. Other major Nucleobases, Nucleosides, and Nucleotides found in DNA and/or RNA

Letter Abbreviations	Nucleobases	Nucleosides	Nucleotides
A	 <p>Adenine</p>	 <p>Adenosine</p>	 <p>Adenosine monophosphate</p>
T	 <p>Thymine</p>	 <p>Thymidine</p>	 <p>Thymidine monophosphate</p>
G	 <p>Guanine</p>	 <p>Guanosine</p>	 <p>Guanosine monophosphate</p>
U	 <p>Uracil</p>	 <p>Uridine</p>	 <p>Uridine monophosphate</p>

2.2 Experimental

Materials

A Nucleosides Test Mix (1x1mL, Varied Conc.) was purchased from Sigma-Aldrich. Adenine (99%), Thymine (99%), Guanine (99+%), Cytosine (98+%), 5-methyl Cytosine (97%), and Formic acid (88+%) were purchased from Thermo Fisher Scientific Chemicals, Inc. Uracil (99+%) was purchased from Acros Organics. BSTFA with 1% TMCS and MTBSTFA with 1% t-BDMCS were purchased from CovaChem. Acetonitrile (HPLC Grade), liquid injection caps and vials, Finnpiettes, and a Touch Mixer Model 232 vortex were purchased from Fisher Scientific. A 500 μ L eVol dispensing syringe was purchased from Thermo Scientific. Milli-Q Water was obtained via a Thermo Scientific Thermo E-Pure Water Purification System. A Reacti-Therm Heating/Stirring Module was purchased from Pierce Chemical Company. DNA Degradase Plus was purchased from Zymo Research Corp. A 6890N GC and a 5975 inert MSD were purchased from Agilent Technologies. *Phormia Regina* fly samples were collected.

Methods

Fly DNA Extraction

Phormia Regina flies were killed at -80°C and their heads crushed with a mortar and pestle. The samples were preserved in 95% ethanol prior to being run through a Qiagen DNeasy Kit. Degradase Plus was added to further degrade the samples. Then the samples were incubated at 37°C overnight.²⁶

Keto-enol Tautomerization

To prepare the nucleobases for derivatization, the nucleobases needed to be converted into their enol form. Solutions of nucleobases were hydrolyzed in 88% formic acid were heated at maximum temperature on a ReactiTherm for approximately 90 minutes.²⁰

MTBSTFA Derivatization

The tautomerized nucleobase solutions were evaporated to dryness under Nitrogen. MTBSTFA + 1% t-BDMCS was added to solutions of nucleobases in acetonitrile, such that Acetonitrile:MTBSTFA was 1:1. Then the solutions were heated at 60°C for 15-30 minutes.²⁰

BSTFA Derivatization

The tautomerized nucleobase solutions were evaporated to dryness under Nitrogen. BSTFA + 1% TMCS was added to solutions of nucleobases in acetonitrile, such that Acetonitrile:BSTFA was 1:1. Then the solutions were heated at 60 °C for 15-30 minutes.²⁰

Liquid Injection

The derivatized solutions of the 5 nucleobases were analyzed using a 30 m Agilent technologies DB-5MS column with a 250 µm inner diameter and a 0.25 µm film thickness.

Instrumental

GC-MS

An Agilent 6890N Network GC coupled to an Agilent 5975 Inert MSD was used for all analyses, along with a Gerstel MultiPurpose Sampler. The column used was a DB5-MS with dimensions of 30 m x 0.25 mm x 0.25µm. Hydrogen carrier gas was utilized at a flow rate of 2.0 mL/min. The oven temperature program started at 50°C for 2 minutes and was then ramped at 5°C/min to 210°C and held there for 2 minutes. The mass transfer line into the MS was set to 250°C and the source temperature was set to 230°C. The MS was in negative ionization mode. Selected ion monitoring was used and set at m/z 255 [Thymine, 2 TMS – CH₃]⁺, m/z 270 [Thymine, 2 TMS – H]⁺, m/z 254 ([5-methyl Cytosine, 2 TMS – CH₃]⁺ or [Cytosine, 2 TMS – CH₃]⁺), m/z 240 [Cytosine, 2 TMS – H]⁺, m/z 269 [5-methyl Cytosine, 2 TMS – H]⁺, m/z 279 [Adenine, 2 TMS – H]⁺, m/z 264 [Adenine, 2 TMS – CH₃]⁺, m/z 367 [Guanine, 2 TMS – H]⁺, and m/z 352 [Guanine, 2 TMS – CH₃]⁺ for detection of the five nucleobases derivatized with BSTFA. Selected ion monitoring was used and set at m/z 296 [5-methyl Cytosine, 2 TBDMS – C₄H₉]⁺ and m/z 282 [5-methyl Cytosine, 2 TBDMS – C₅H₁₂]⁺ for detection of the 5-methyl Cytosine derivatized with MTBSTFA. The total scan time was 36 minutes, scanning from 40 amu to 550 amu.

2.3 Results and Discussion

Derivatization

MTBSFTA + 1% t-BDMCS

N-Methyl-N-tert-butyltrimethylsilyltrifluoroacetamide + 1% tert-Butylchlorodimethylsilane (MTBSTFA + 1% t-BDMCS) was chosen for its moderate reactivity

with hindered hydroxyl and amine functional groups since these are found in the targeted compounds.²⁴ To quickly determine whether MTBSTFA would improve the detection of the nucleobases, 5-methyl cytosine was derivatized and run using a ramp of 20°C/min.

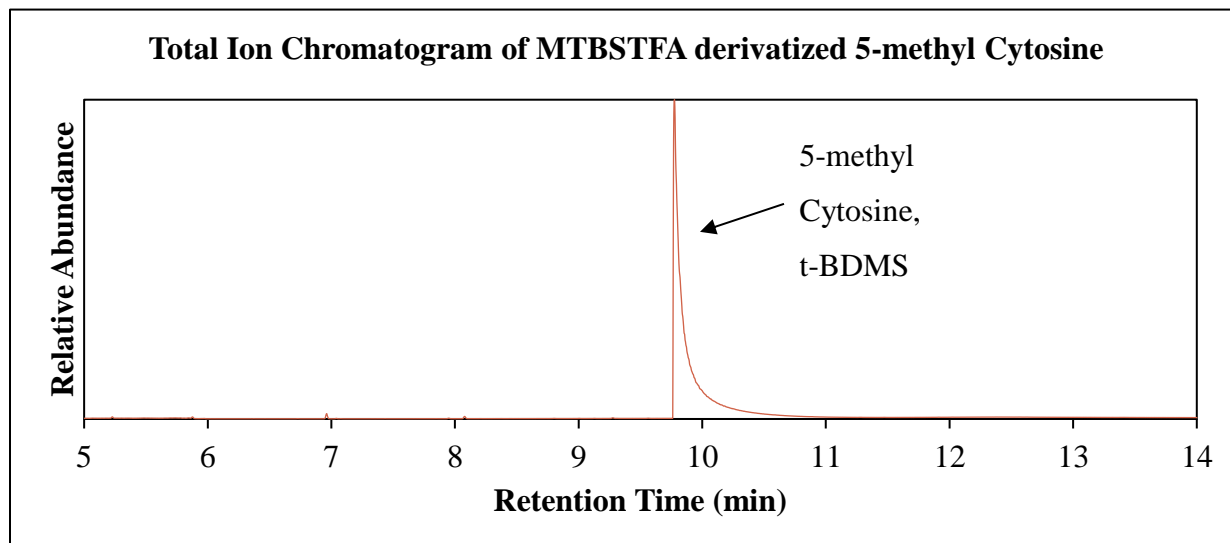


Figure 2-1. Total Ion Chromatogram (SIM mode) of a 25 ppm Acetonitrile solution of MTBSTFA derivatized 5-methyl Cytosine

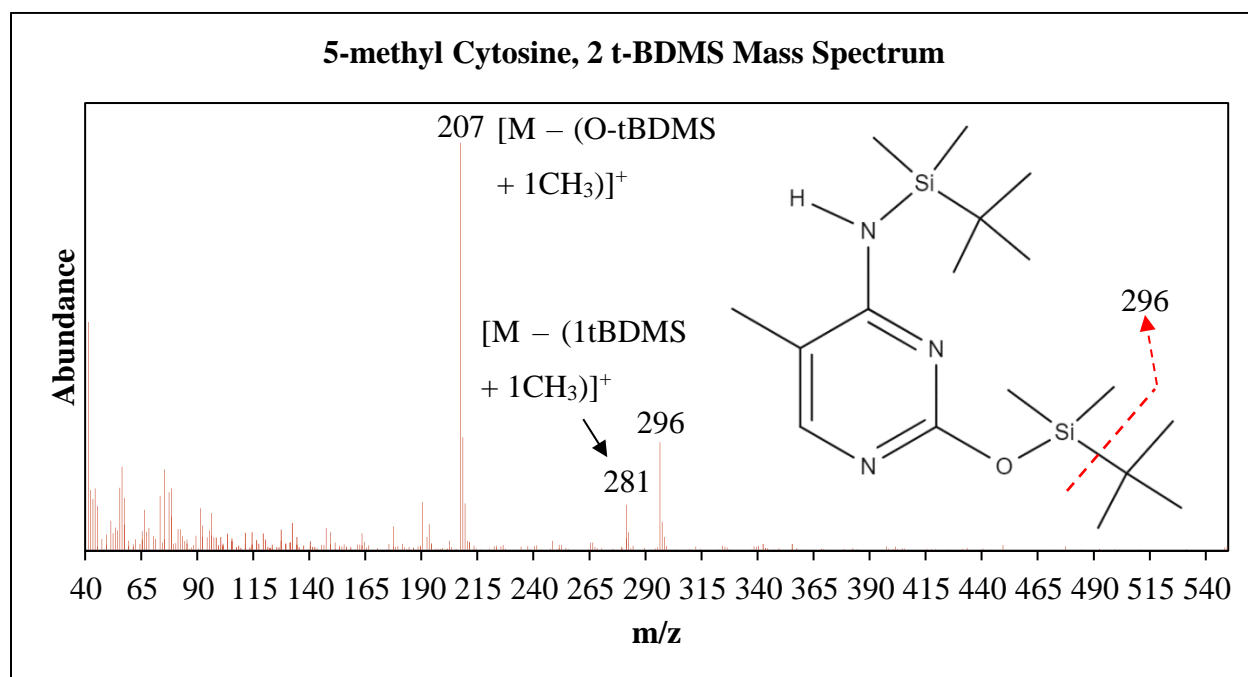


Figure 2-2. Structure and Significant Fragmentation of MTBSTFA derivatized 5-methyl Cytosine nucleobase overlaid on its Mass Spectrum

BSTFA + 1% TMCS

N,O-bis(trimethylsilyl)trifluoroacetamide + 1% Trimethylchlorosilane (BSTFA + 1% TMCS) was chosen for its high reactivity with hindered hydroxyl functional groups and moderate reactivity with hindered amine functional groups since these are found in the targeted compounds.²⁴ All 6 nucleobases were able to be fully derivatized by BSTFA. GC-MS sufficiently separated (Figure 2-3) and identified (Figures 2-4, 2-5, 2-6, 2-7, 2-8, and 2-9) the BSTFA-derivatized nucleobases. Whereas three trimethylsilyl groups attached to Guanine, only two trimethylsilyl groups attached to the other nucleobases analyzed (Figures 2-4, 2-5, 2-6, 2-7, 2-8, and 2-9).

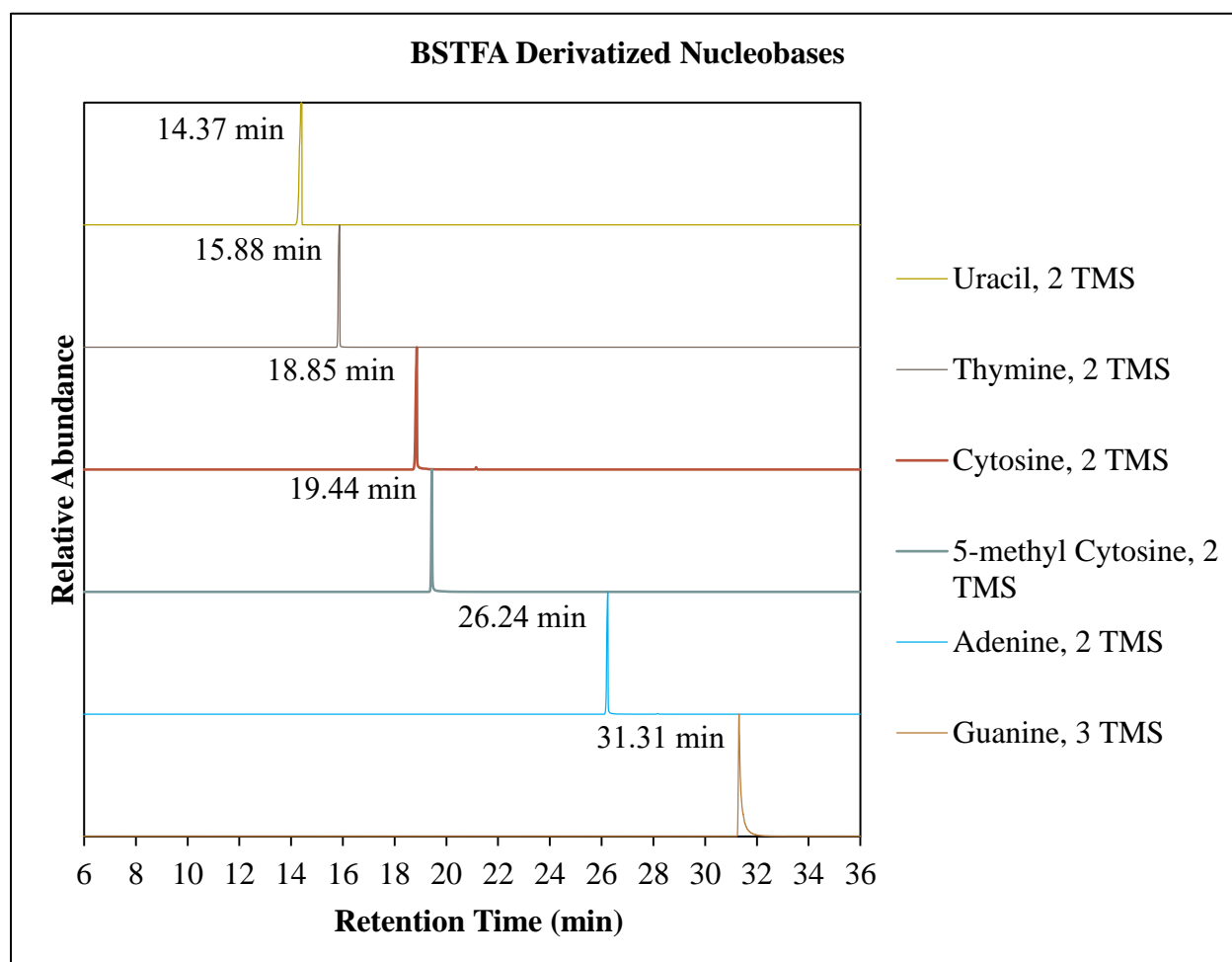


Figure 2-3. Stacked Total Ion Chromatograms of 6 Nucleobase calibrants in acetonitrile (100 ppm) derivatized with BSTFA

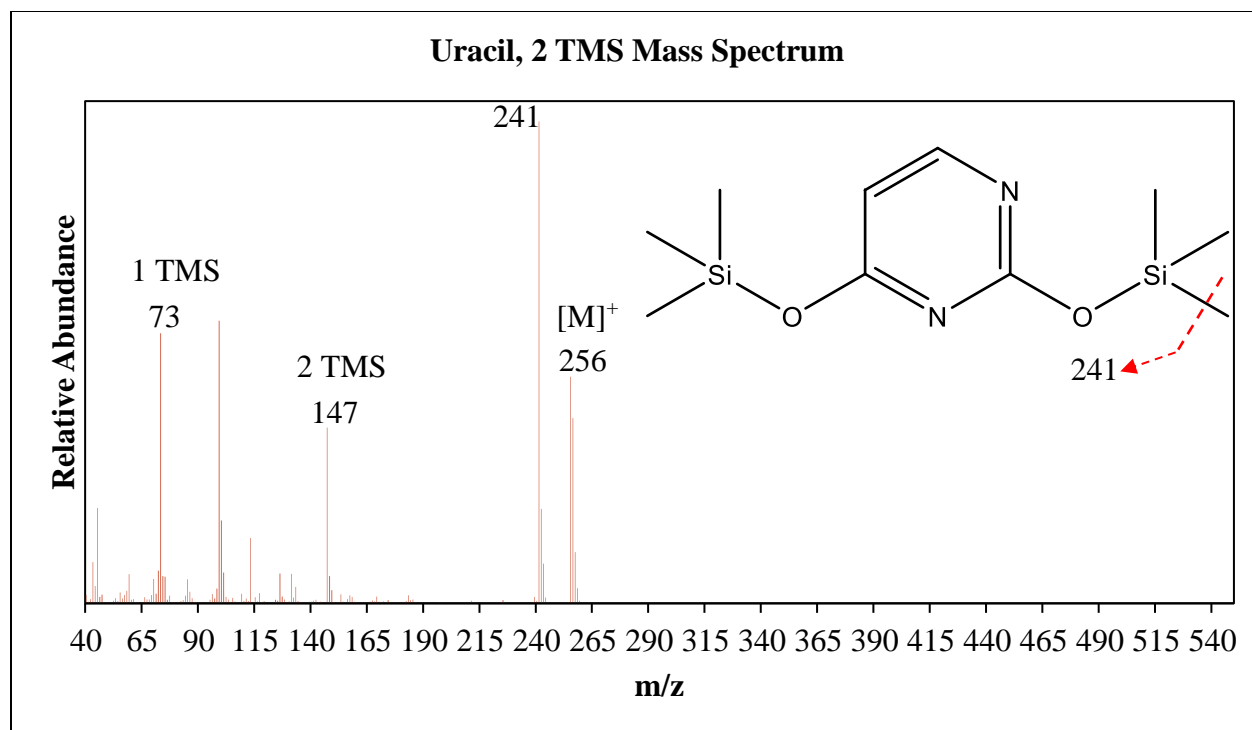


Figure 2-4. Structure and Significant Fragmentation of BSTFA derivatized Uracil nucleobase overlaid on its Mass Spectrum

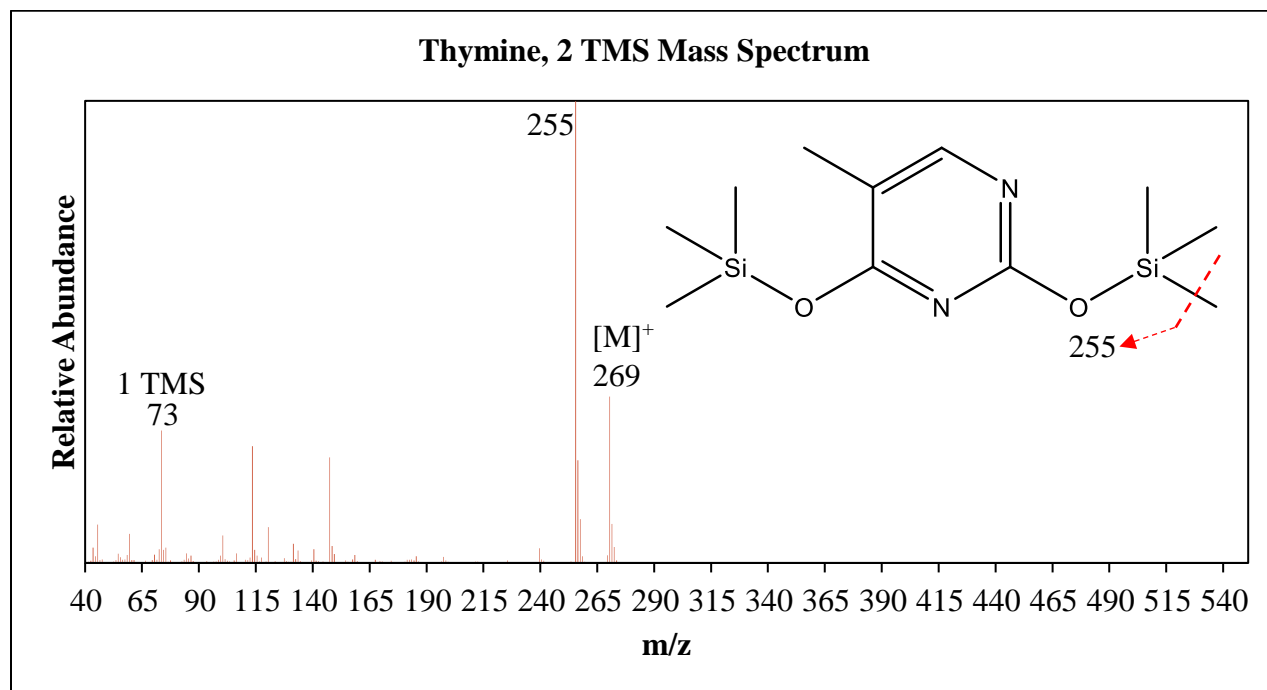


Figure 2-5. Structure and Significant Fragmentation of BSTFA derivatized Thymine nucleobase overlaid on its Mass Spectrum

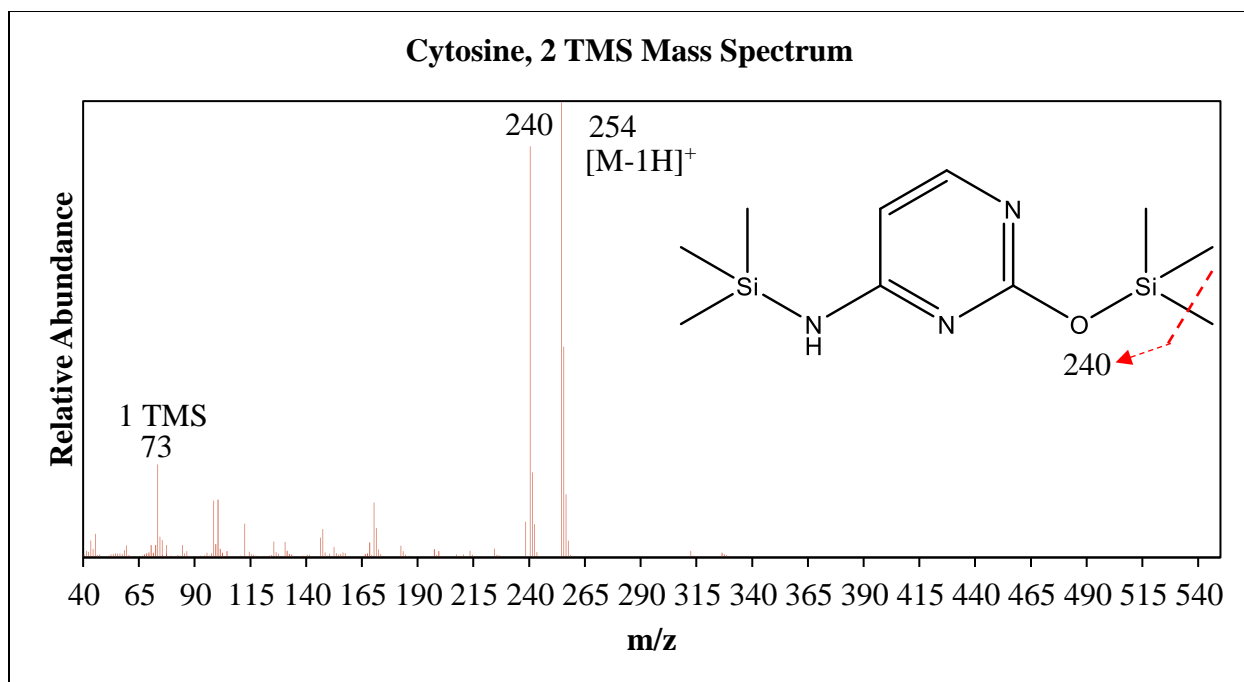


Figure 2-6. Structure and Significant Fragmentation of BSTFA derivatized Cytosine nucleobase overlaid on its Mass Spectrum

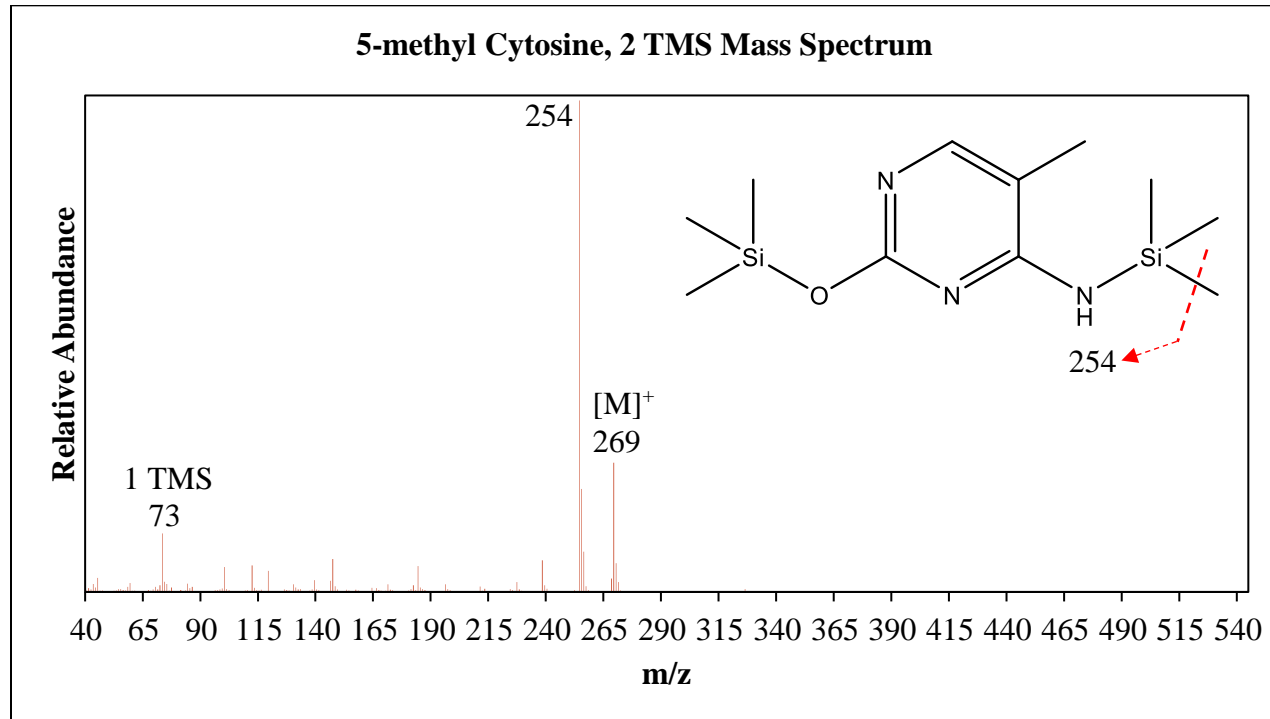


Figure 2-7. Structure and Significant Fragmentation of BSTFA derivatized 5-methyl Cytosine nucleobase overlaid on its Mass Spectrum

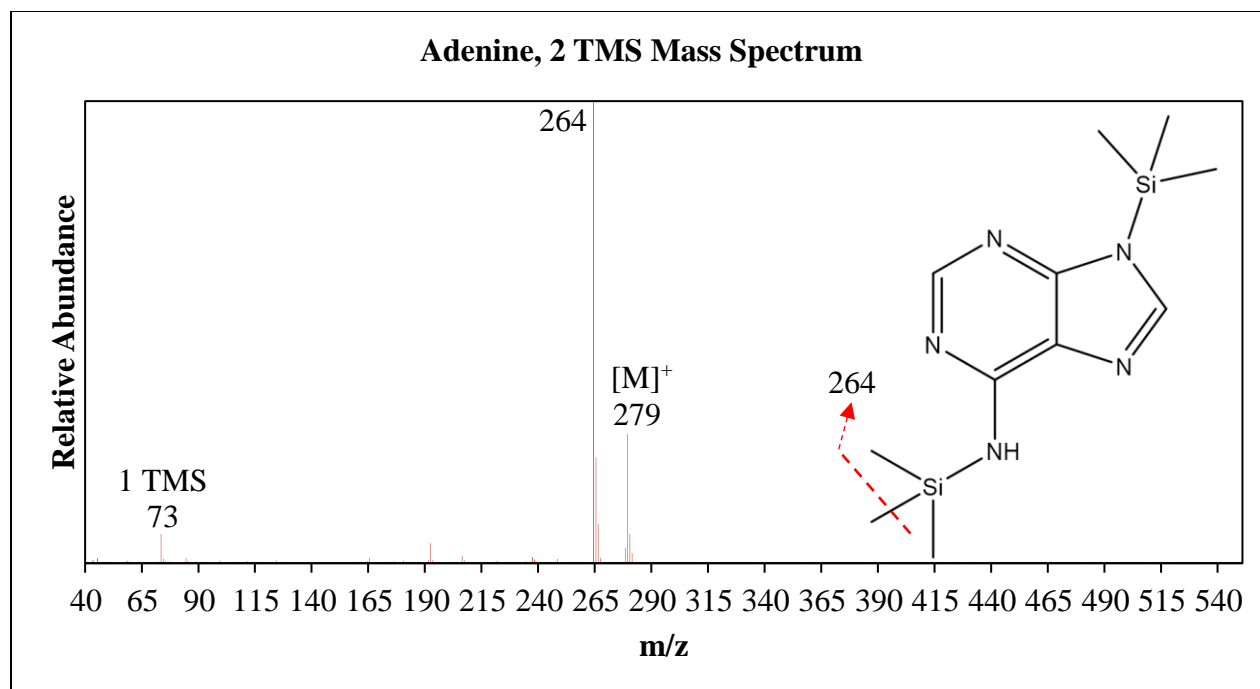


Figure 2-8. Structure and Significant Fragmentation of BSTFA derivatized Adenine nucleobase overlaid on its Mass Spectrum

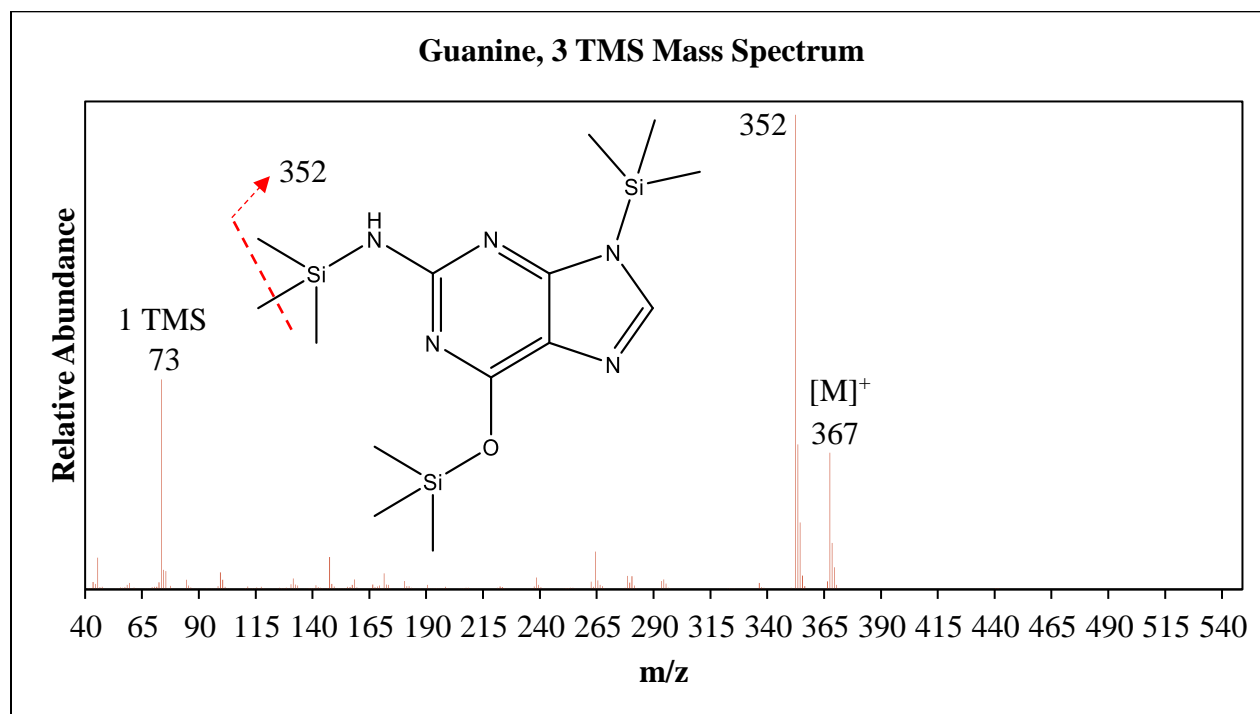


Figure 2-9. Structure and Significant Fragmentation of BSTFA derivatized Guanine nucleobase overlaid on its Mass Spectrum

Calibration Curves

The linearity between 2 ppm and 10 ppm is poor for both Cytosine and 5-methyl Cytosine (Figure 2-10 and 2-11, respectively). Although there is relatively good linearity for the ratio of Cytosine to 5-methyl Cytosine between these concentrations, this was expected since it should have a horizontal slope (Figure 2-12). With a 1 ppm limit of detection, the next concentration range explored was 1 ppm to 4 ppm. With this range and the use of quantitative ions, the linearity for both Cytosine and 5-methyl Cytosine significantly improved (Figures 2-10, 2-11, 2-13, and 2-14). Meanwhile, the linearity for the ratio of Cytosine to 5-methyl Cytosine significantly decreased, resulting in a defined curvature (Figures 2-12 and 2-15).

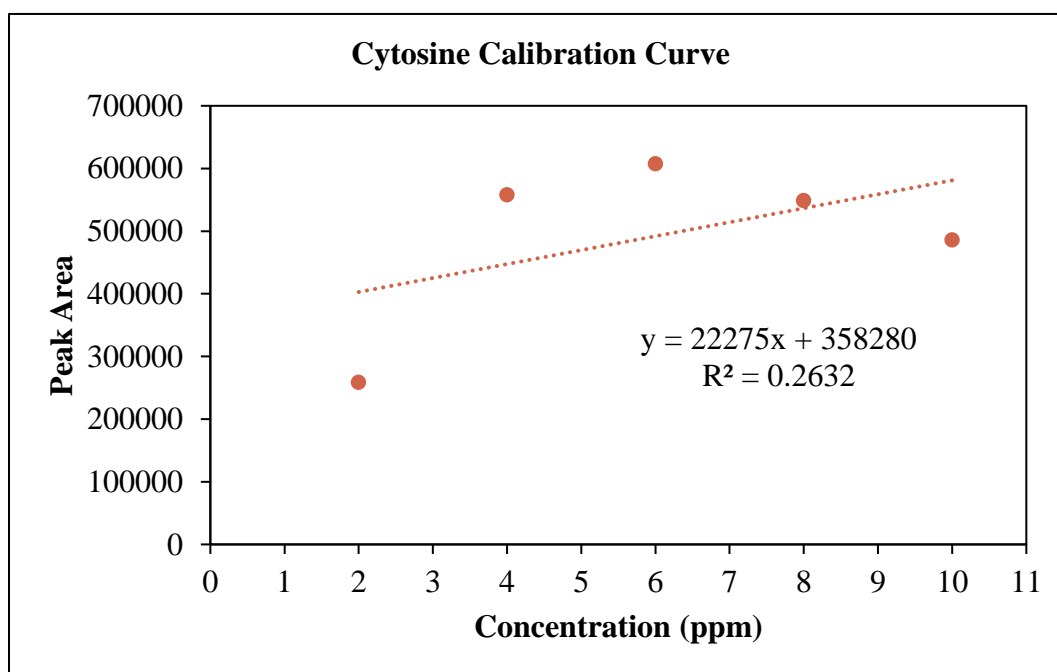


Figure 2-10. Calibration curve of Acetonitrile solutions of Cytosine from 2 ppm to 10 ppm

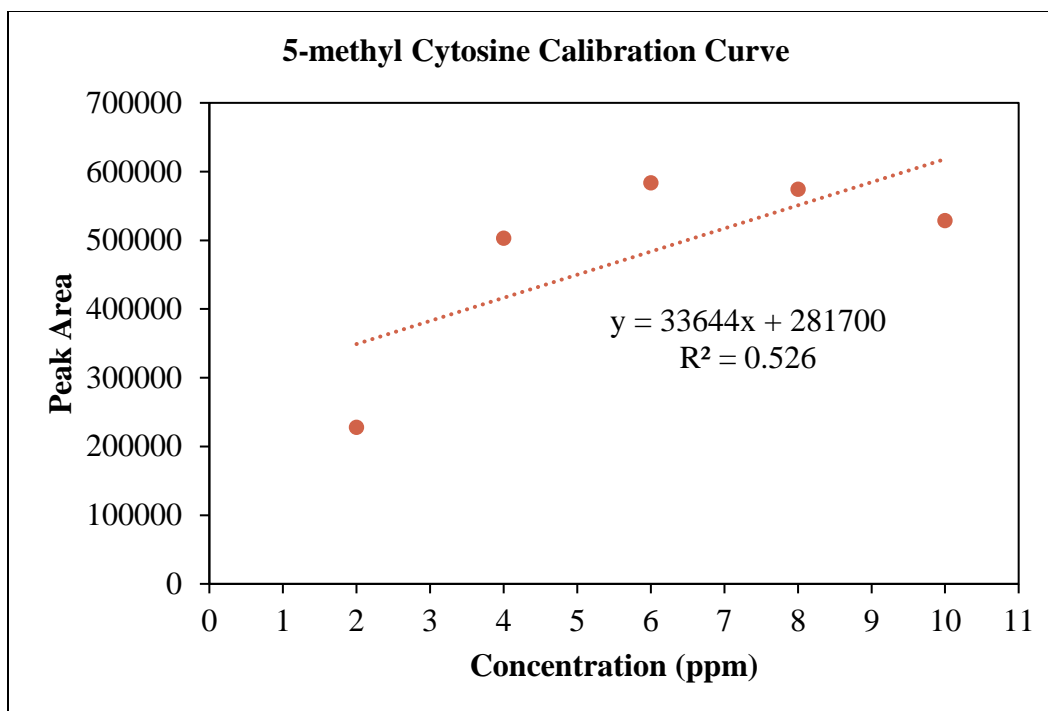


Figure 2-11. Calibration curve of Acetonitrile solutions of 5-methyl Cytosine from 2 ppm to 10 ppm

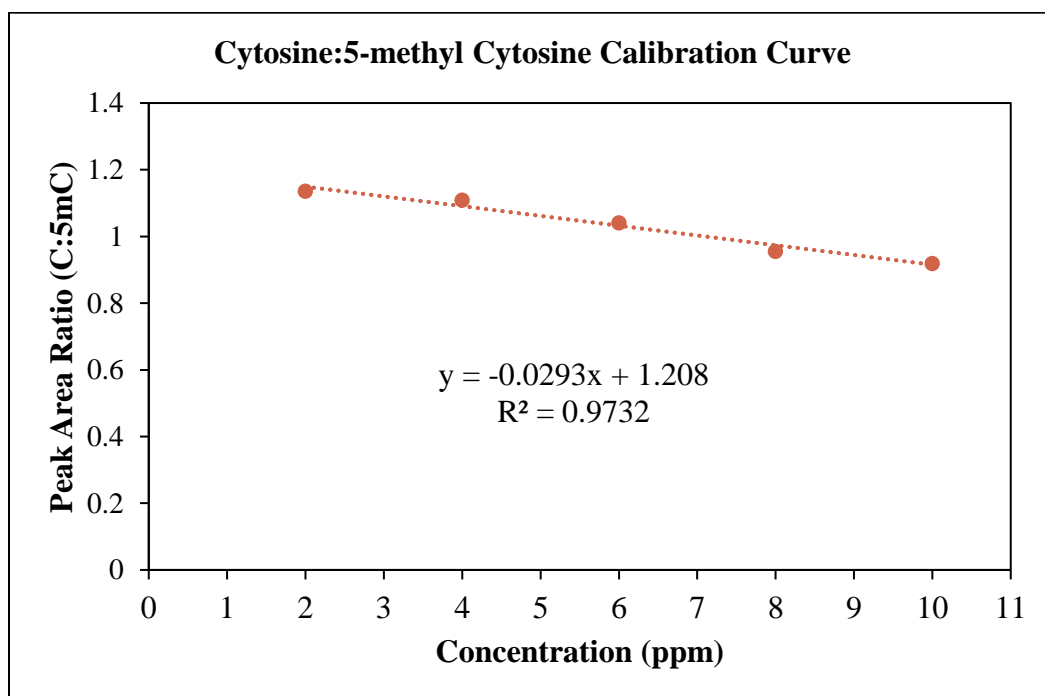


Figure 2-12. Calibration curve of Acetonitrile solutions of Cytosine to 5-methyl Cytosine from 2 ppm to 10 ppm

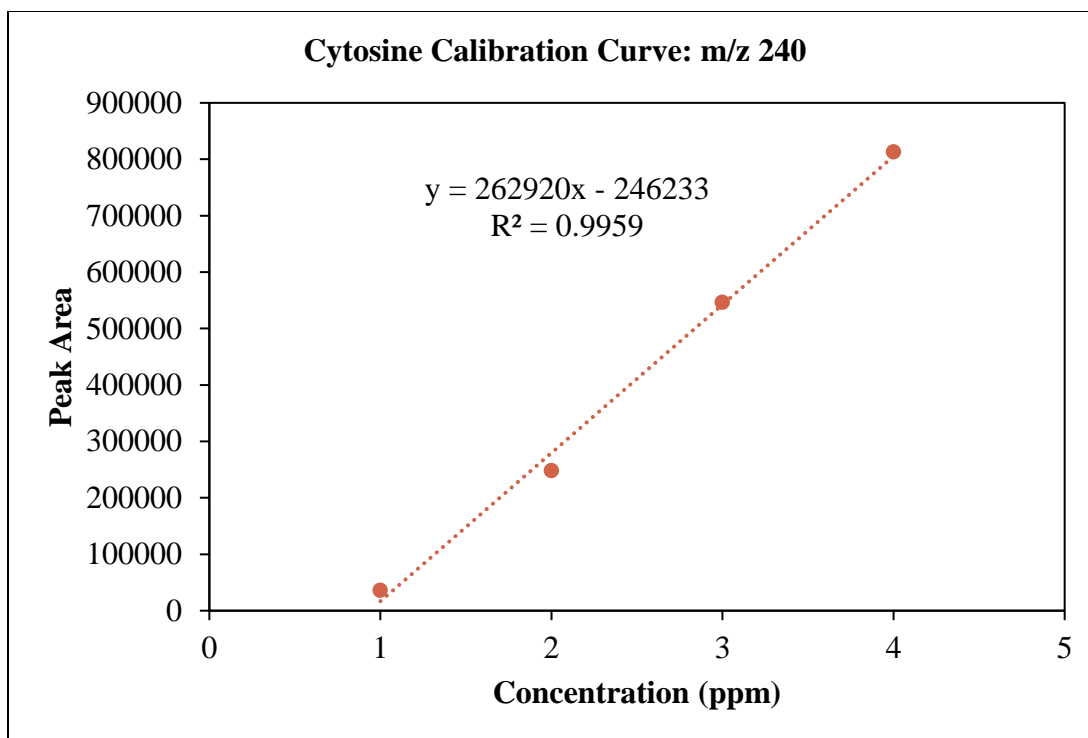


Figure 2-13. Calibration curve of Acetonitrile solutions of Cytosine from 1 ppm to 4 ppm, using the ion m/z 240

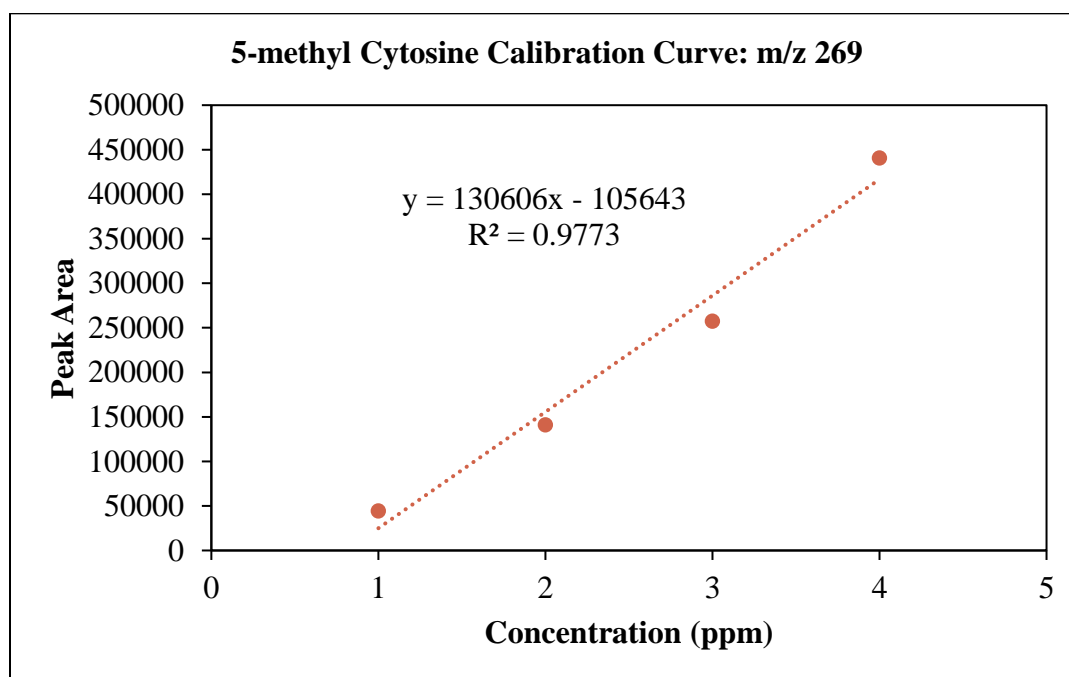


Figure 2-14. Calibration curve of Acetonitrile solutions of 5-methyl Cytosine from 1 ppm to 4 ppm, using the ion m/z 269

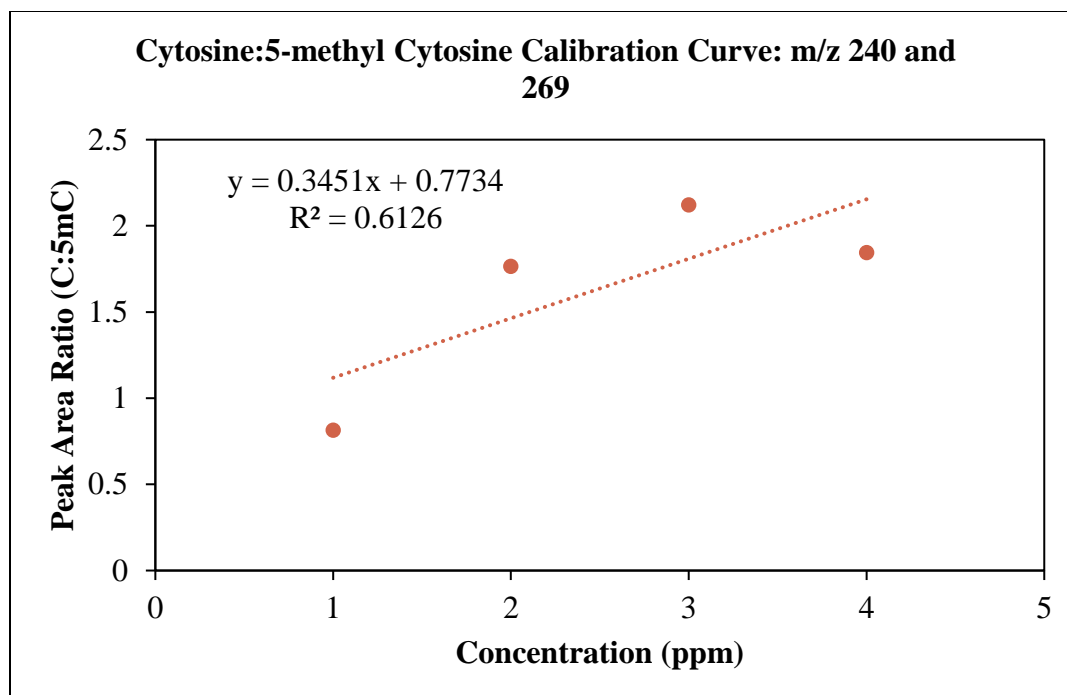


Figure 2-15. Calibration curve of Acetonitrile solutions of Cytosine to 5-methyl Cytosine from 1 ppm to 4 ppm, using the ions m/z 240 and m/z 269, respectively

Nucleosides

The nucleoside test mix contained the following: Pseudouridine, Cytidine, Uridine, 3-methyl Cytidine Methosulfate, 2-thio Cytidine, 1-methyl Adenosine, 2'-0-methyl Cytidine, 7-methyl Guanosine, Inosine, Guanosine, Ribothymidine, and 5-methyl Cytidine. Upon tautomerization, the nucleosides converted to their respective nucleobases (Table 2-3) before derivatization with BSTFA. Since the nucleoside 2'-0-methyl Cytidine was likely converted to the nucleobase Cytosine, the nucleosides Cytidine and 2'-0-methyl Cytidine likely combined to form the single peak detected for Cytosine (Figure 2-18). Of the nucleoside test mix derivatized compounds, 7-methyl Guanine, 2-thio Cytosine, Pseudouracil, and 3-methyl Cytosine Methosulfate were not detected using the method presented here. These compounds may require a higher final oven temperature. However, Pseudouracil and 3-methyl Cytosine Methosulfate may have contributed to the Uracil and 5-methyl Cytosine peaks, respectively, due to their similar structures. All other peaks present in the following chromatograms were siloxanes or potential contaminants within the test mix solution, including n-alkanes, decanoates, and benzoates. Upon observing the targeted analytes via extracted ion chromatograms (Figures 2-16, 2-17, 2-18, 2-19,

and 2-20), selected ion monitoring (SIM) mode was determined to be more suitable than scan mode for such samples (Figure 2-21).

Table 2-3. Nucleosides in the Nucleoside Test Mix and their Respective Nucleobases

Nucleoside	Nucleobase
Pseudouridine	Pseudouracil*
Cytidine	Cytosine
Uridine	Uracil
3-methyl Cytidine Methosulfate	3-methyl Cytosine Methosulfate
2-thio Cytidine	2-thio Cytosine
1-methyl Adenosine	1-methyl Adenine
2'-0-methyl Cytidine	Cytosine
7-methyl Guanosine	7-methyl Guanine
Inosine	Hypoxanthine
Guanosine	Guanine
Ribothymidine	Thymine
5-methyl Cytidine	5-methyl Cytosine

*Pseudouridine is a structural isomer of Uridine, such that a C-C glycosyl bond is present rather than the C-N glycosyl bond present in Uridine.²⁷

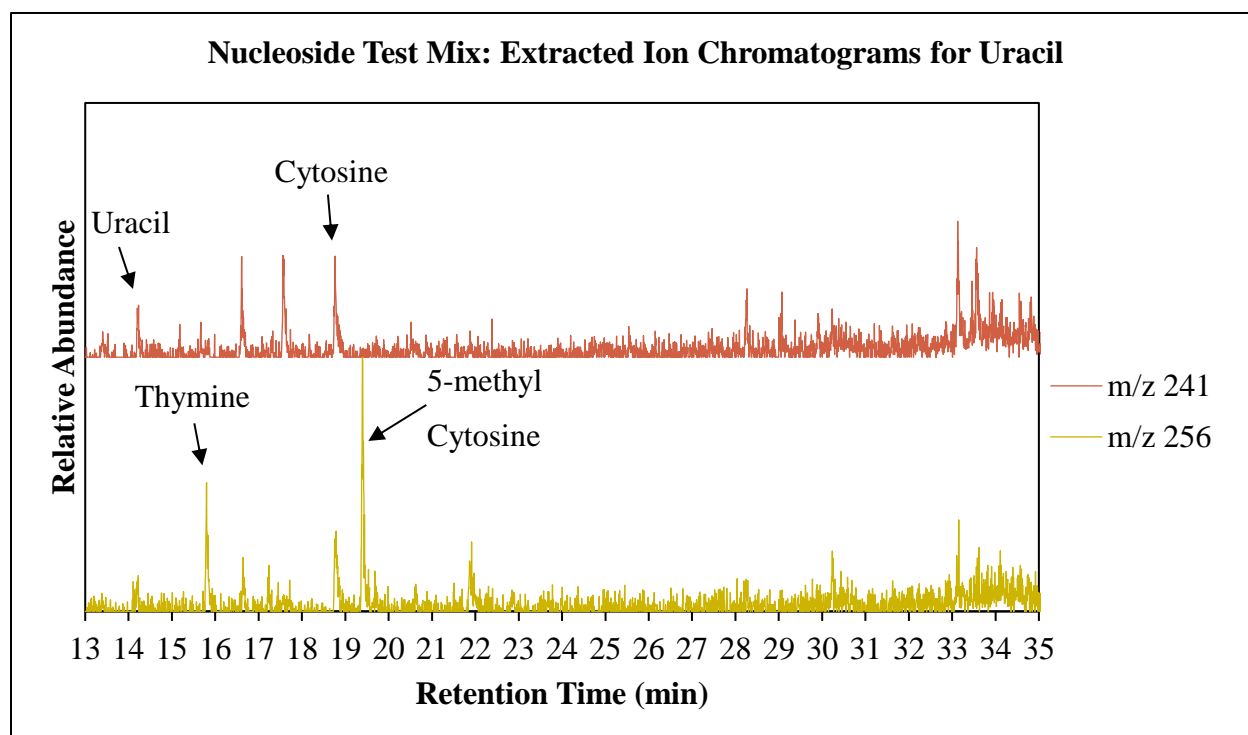


Figure 2-16. Uracil Extracted Ion Chromatograms of an Acetonitrile solution of BSTFA Derivatized Nucleoside Test Mix, containing Pseudouridine (25 ppm), Cytidine (50 ppm), Uridine (25 ppm), 3-methyl Cytidine Methosulfate (100 ppm), 2-thio Cytidine (10 ppm), 1-methyl Adenosine (25.5 ppm), 2'-O-methyl Cytidine (20 ppm), 7- methyl Guanosine (25 ppm), Inosine (25 ppm), Guanosine (25 ppm), Ribothymidine (50 ppm), and 5-methyl Cytidine (100 ppm)

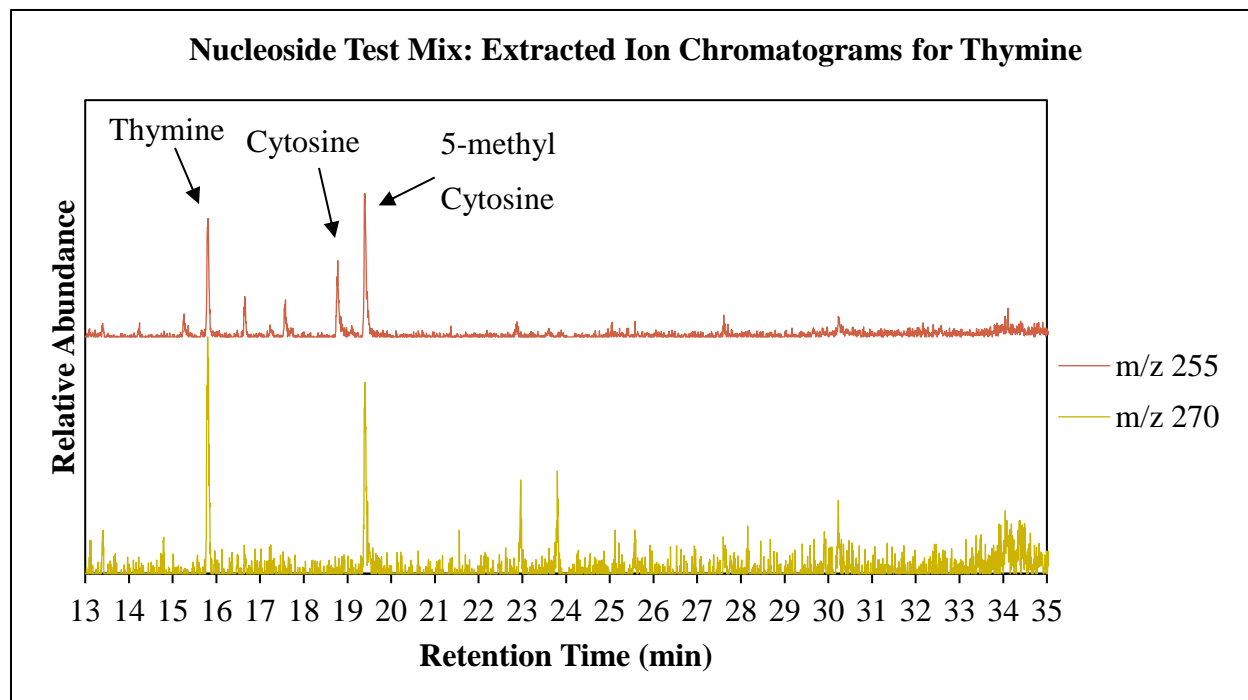


Figure 2-17. Thymine Extracted Ion Chromatograms of an Acetonitrile solution of BSTFA Derivatized Nucleoside Test Mix, containing Pseudouridine (25 ppm), Cytidine (50 ppm), Uridine (25 ppm), 3-methyl Cytidine Methosulfate (100 ppm), 2-thio Cytidine (10 ppm), 1-methyl Adenosine (25.5 ppm), 2'-0-methyl Cytidine (20 ppm), 7- methyl Guanosine (25 ppm), Inosine (25 ppm), Guanosine (25 ppm), Ribothymidine (50 ppm), and 5-methyl Cytidine (100 ppm)

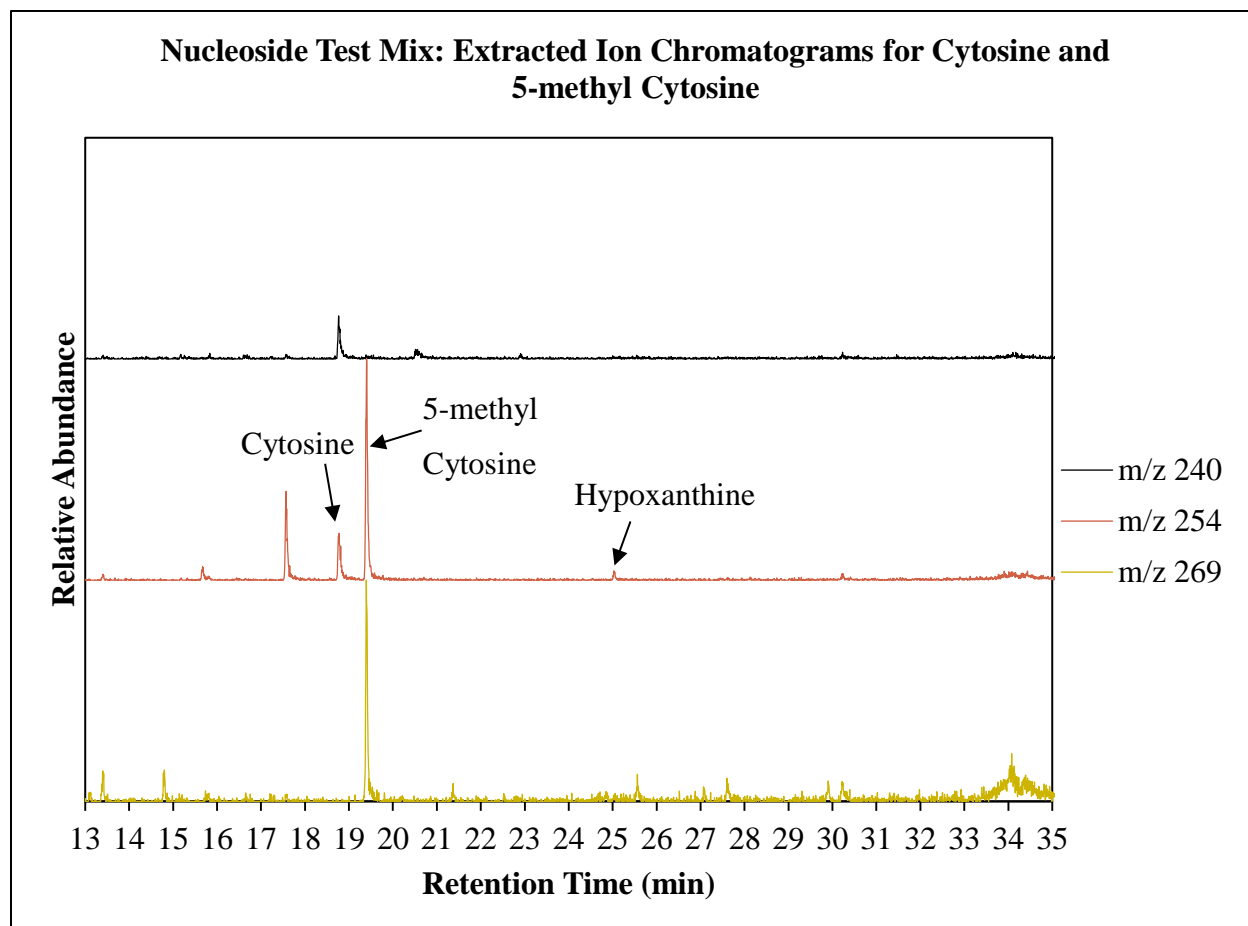


Figure 2-18. Cytosine and 5-methyl Cytosine Extracted Ion Chromatograms of an Acetonitrile solution of BSTFA Derivatized Nucleoside Test Mix, containing Pseudouridine (25 ppm), Cytidine (50 ppm), Uridine (25 ppm), 3-methyl Cytidine Methosulfate (100 ppm), 2-thio Cytidine (10 ppm), 1-methyl Adenosine (25.5 ppm), 2'-0-methyl Cytidine (20 ppm), 7- methyl Guanosine (25 ppm), Inosine (25 ppm), Guanosine (25 ppm), Ribothymidine (50 ppm), and 5-methyl Cytidine (100 ppm)

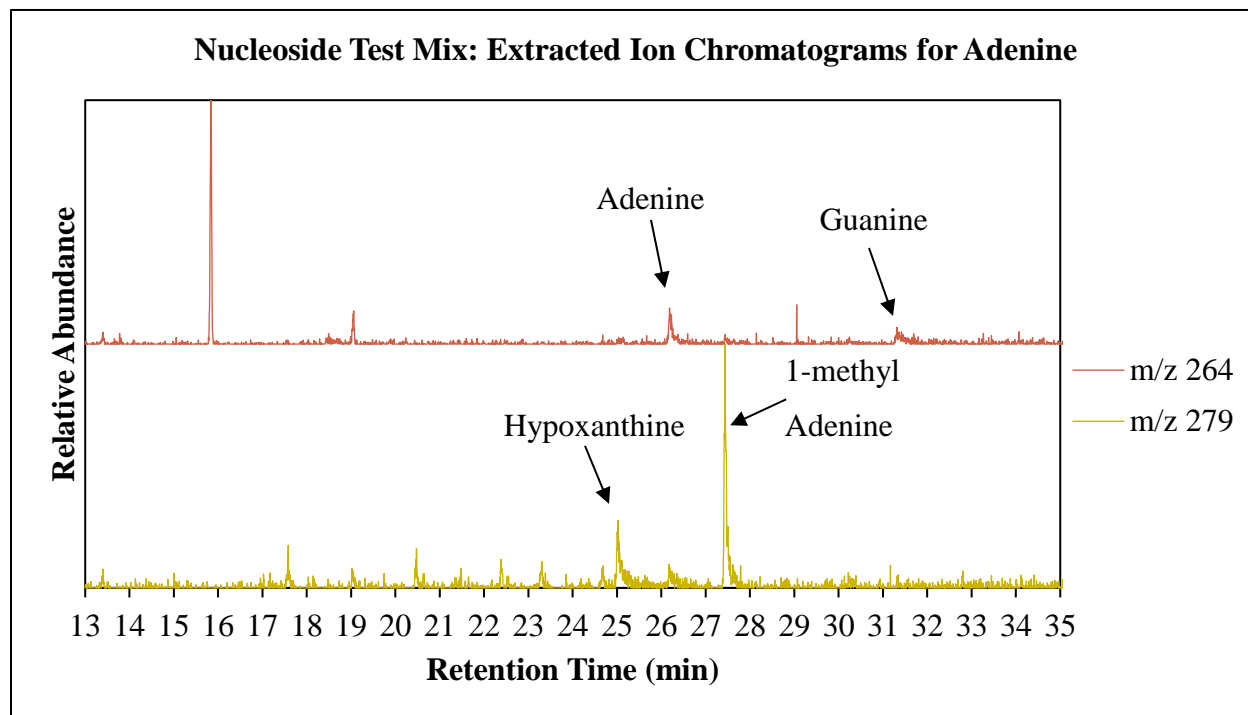


Figure 2-19. Adenine Extracted Ion Chromatograms of an Acetonitrile solution of BSTFA Derivatized Nucleoside Test Mix, containing Pseudouridine (25 ppm), Cytidine (50 ppm), Uridine (25 ppm), 3-methyl Cytidine Methosulfate (100 ppm), 2-thio Cytidine (10 ppm), 1-methyl Adenosine (25.5 ppm), 2'-0-methyl Cytidine (20 ppm), 7- methyl Guanosine (25 ppm), Inosine (25 ppm), Guanosine (25 ppm), Ribothymidine (50 ppm), and 5-methyl Cytidine (100 ppm)

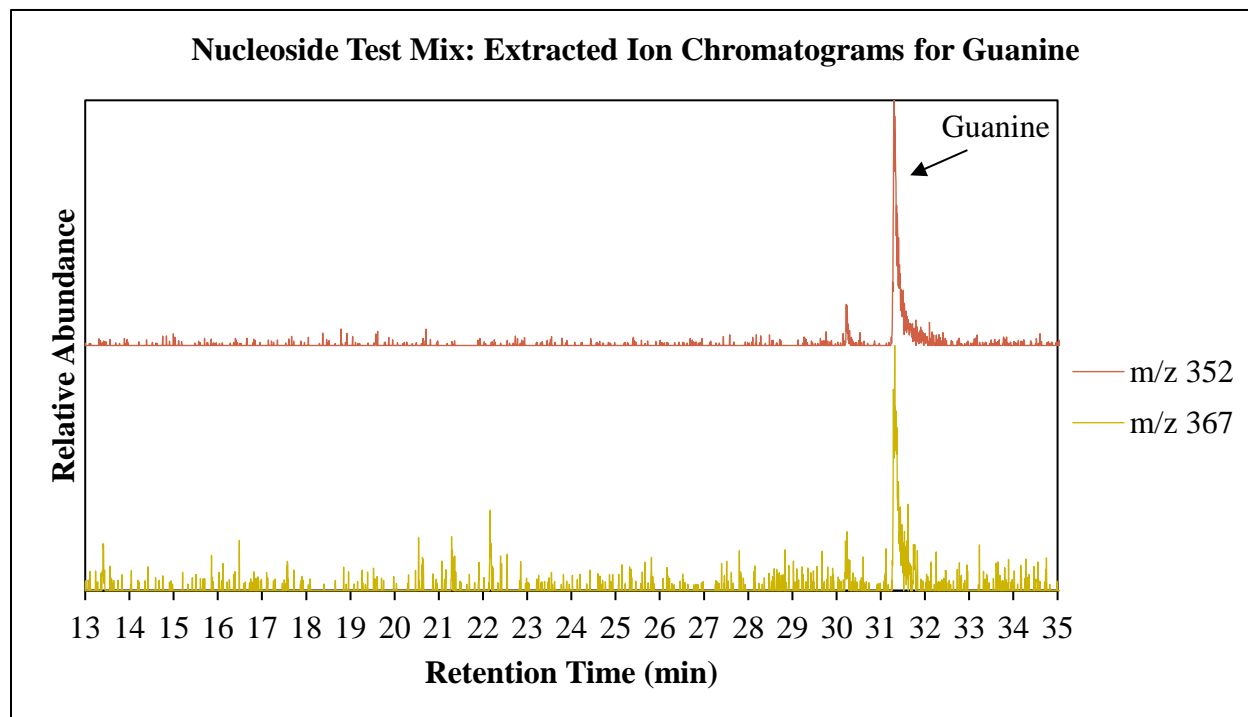


Figure 2-20. Guanine Extracted Ion Chromatograms of an Acetonitrile solution of BSTFA Derivatized Nucleoside Test Mix, containing Pseudouridine (25 ppm), Cytidine (50 ppm), Uridine (25 ppm), 3-methyl Cytidine Methosulfate (100 ppm), 2-thio Cytidine (10 ppm), 1-methyl Adenosine (25.5 ppm), 2'-0-methyl Cytidine (20 ppm), 7- methyl Guanosine (25 ppm), Inosine (25 ppm), Guanosine (25 ppm), Ribothymidine (50 ppm), and 5-methyl Cytidine (100 ppm)

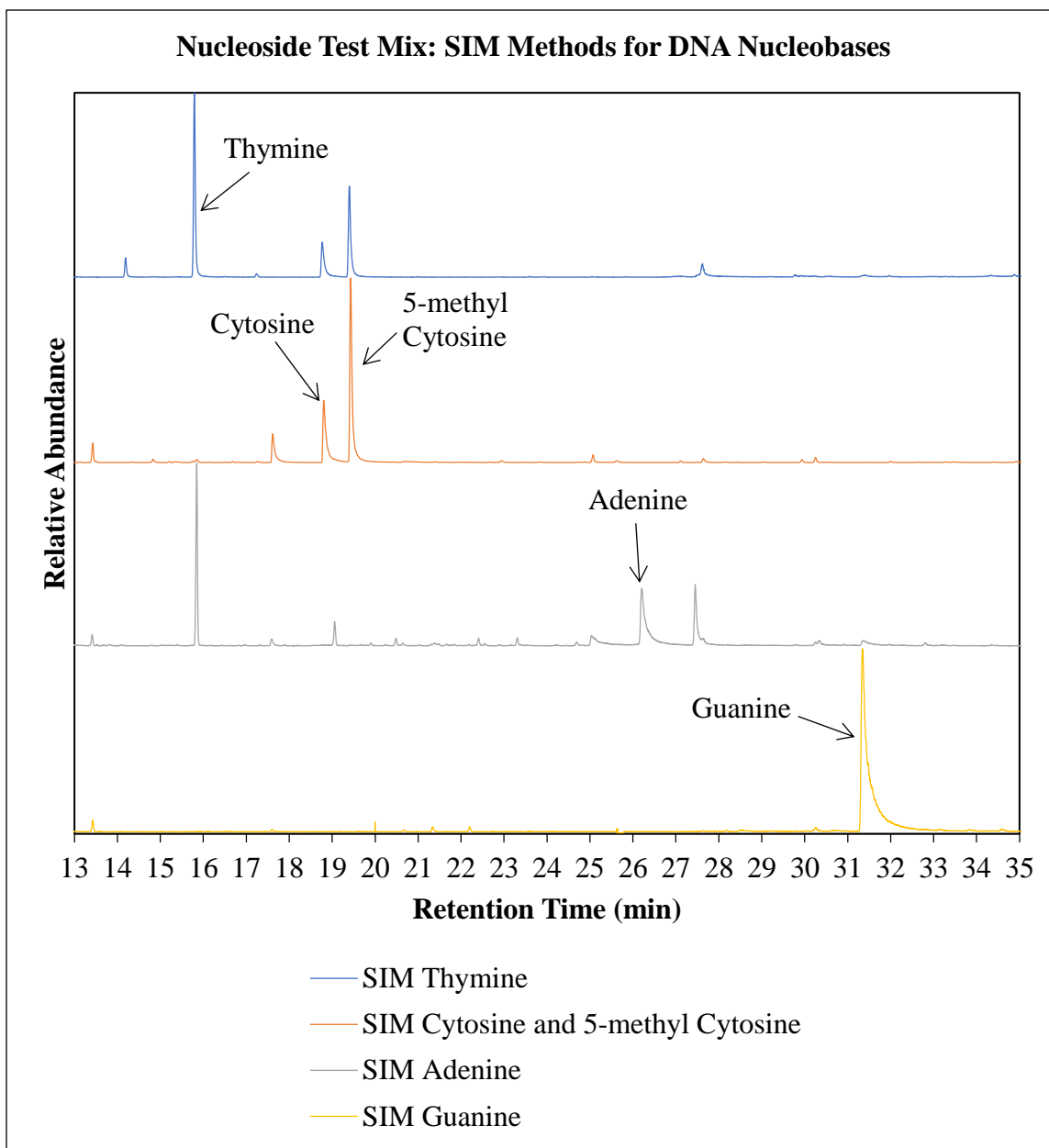


Figure 2-21. Total ion chromatograms (SIM mode) of an Acetonitrile solution of BSTFA Derivatized Nucleoside Test Mix, containing Pseudouridine (25 ppm), Cytidine (50 ppm), Uridine (25 ppm), 3-methyl Cytidine Methosulfate (100 ppm), 2-thio Cytidine (10 ppm), 1-methyl Adenosine (25.5 ppm), 2'-0-methyl Cytidine (20 ppm), 7- methyl Guanosine (25 ppm), Inosine (25 ppm), Guanosine (25 ppm), Ribothymidine (50 ppm), and 5-methyl Cytidine (100 ppm)

Fly DNA

A 25 μL solution of unamplified *Phormia Regina* fly DNA (90 $\text{ng}/\mu\text{L}$) was prepared, resulting in a final DNA concentration of 2.25 ppm. The total ion chromatogram only shows minimal detection of 2 nucleobases, neither being Cytosine nor 5-methyl Cytosine (Figure 2-22). As expected, Uracil and Thymine were the first two nucleobases detected (Figures 2-22, 2-23, and 2-24). Since only a portion of the DNA provided would be associated with each nucleobase, the concentrations of the other four nucleobases were likely below the 1 ppm limit of detection.

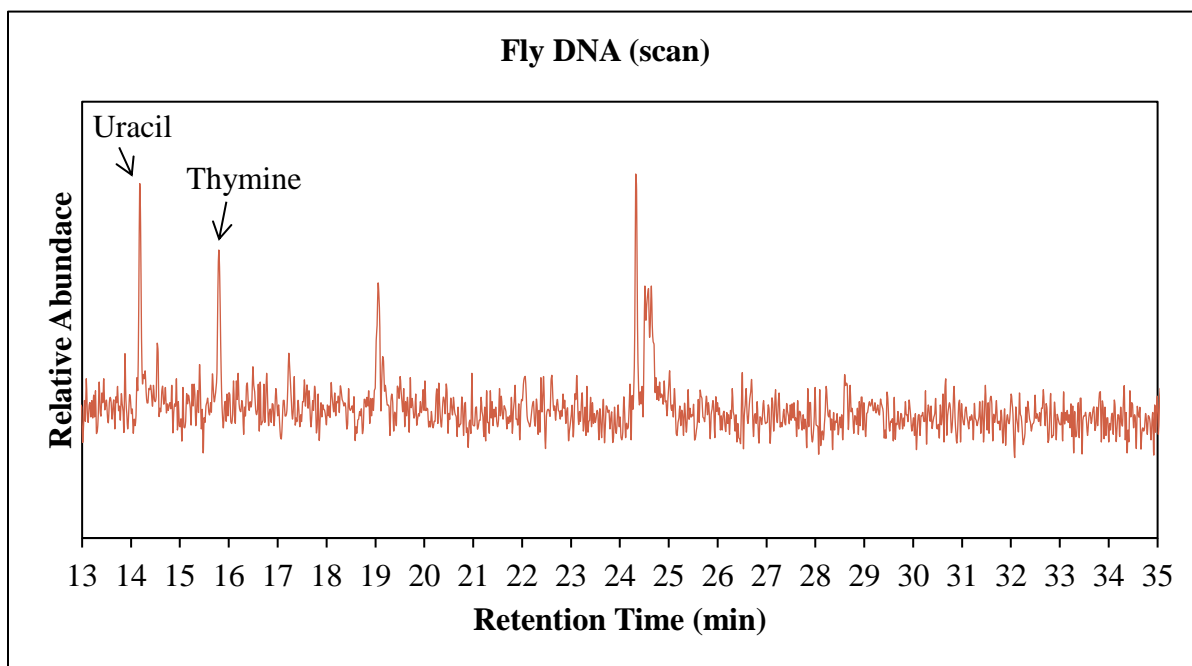


Figure 2-22. Total Ion Chromatogram (Scan) of an Acetonitrile solution of Fly DNA (2.25 ppm) Derivatized with BSTFA

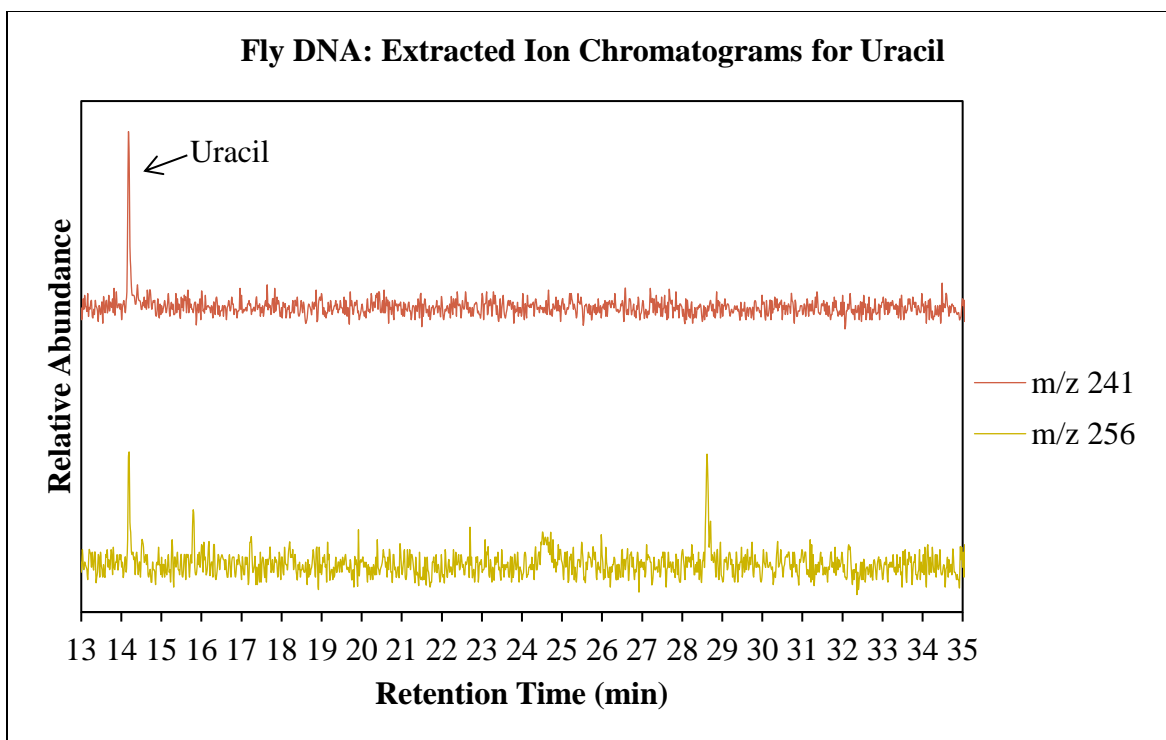


Figure 2-23. Uracil Extracted Ion Chromatograms of Fly DNA (2.25 ppm) Derivatized with BSTFA

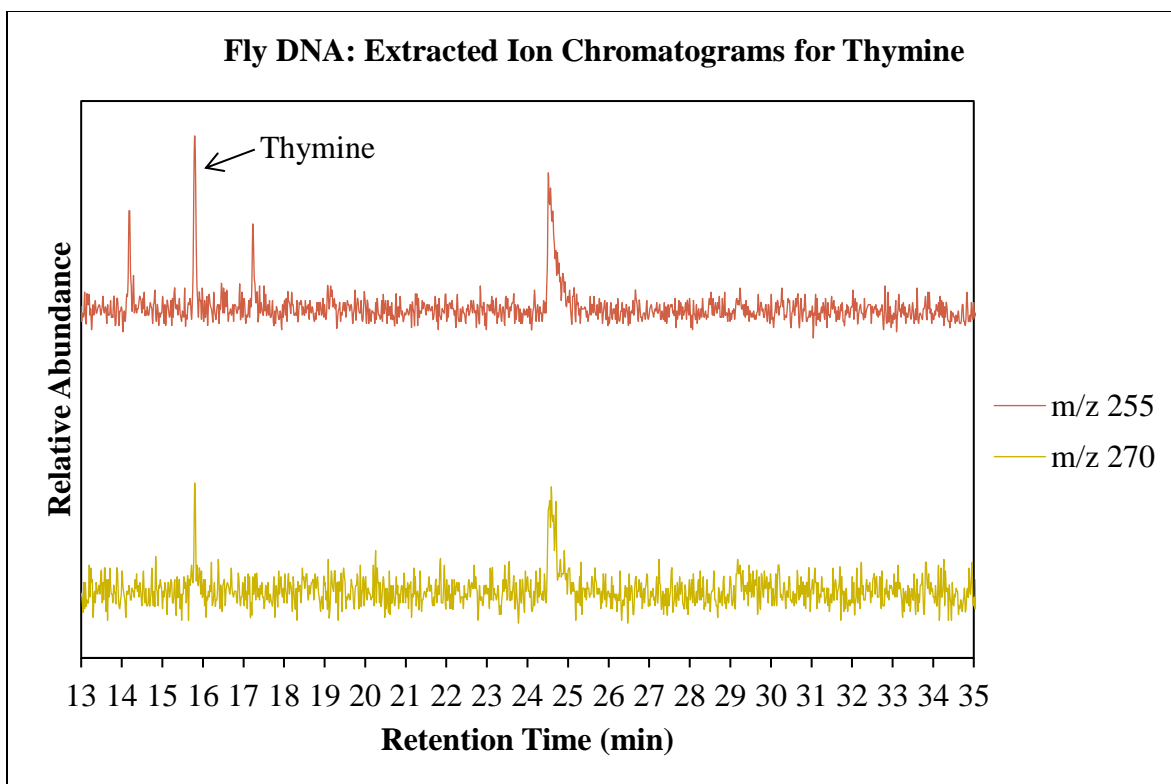


Figure 2-24. Thymine Extracted Ion Chromatograms of Fly DNA (2.25 ppm) Derivatized with BSTFA

2.4 Conclusion

Methods for analyzing DNA were explored. Derivatized samples of DNA nucleobase and nucleoside standards were analyzed to provide a basis for analyzing samples extracted from flies. Two derivatization reagents (MTBSTFA, and BSTFA) were explored. The nucleobases greatly favored derivatization via the BSTFA derivatization reagent over the MTBSTFA derivatization reagent. The targeted nucleobases derivatized with BSTFA were successfully detected (Figure 2-3).

Upon analysis of the fly DNA samples, there was little to no detection of the targeted nucleobases (Figures 2-23). Since the limit of detection was 1000 ng/mL, then 25 μ L of 243 ng/ μ L is needed if the final sample volume is 500 μ L or 25 μ L of 486 ng/ μ L if the final sample volume is 1 mL. If reversely applying the same scenario to a 25 μ L solution of 100 ng/ μ L, the sample concentration reaches 411.11 ng/mL if using a final sample volume of 500 μ L or 205.55 ng/mL if using a final sample volume of 1 mL. Therefore, to detect DNA methylation, the quantity of DNA

provided from a fly sample will need to increase for detection of both cytosine and 5-methyl cytosine.

However, the degree of methylation still would not be able to be accurately quantified with the methods presented in this chapter since the linearity relies on obtaining greater sensitivity. If GC-MS is to be used for the analysis of fly DNA, optimization must be performed with various DNA extractions and SPME and/or TV-SPME to determine the potential for detection of the fly DNA via GC-MS. Another technique that may be further explored for analysis of fly DNA would be LC-MS. These possibilities will be discussed further in “Chapter 4: Future Work.”

CHAPTER 3. ANALYSIS OF HAIR PIGMENTATION

3.1 Introduction

Hair is a common type of evidence that could be found at almost any crime scene. Obtaining hair samples from individuals for comparison to the hair evidence found at a scene can be valuable for forensic investigations. For example, the microscopic characteristics can provide associations based on the origin species, ethnicity, somatic origin, chemical modifications, and whether the hair shed naturally or was forcibly removed.²⁸ Since these are class characteristics, microscopic analysis cannot conclusively identify the source. Furthermore, the absence of a population distribution for human hair phenotypes has been a major contribution to some erroneous court testimonies.

The 1982 murder of Debbie Carter focused on two suspects Ron Williamson and Dennis Fritz. However, the hair samples presented as evidence were later shown to be unreliable. In *Williamson v. Reynolds*, defendant Williamson was exonerated by DNA testing after being convicted and sentenced to death based on an erroneous hair comparison. The hair comparison results were deemed scientifically unreliable and thus inadmissible under the *Daubert* standard. The expert testimony did not provide specific consistencies between hair samples nor any statistical data to support the conclusions. In fact, the prosecution's primary witness was the true murderer. Eventually hair comparisons were placed under further scrutiny, especially as the Innocence Project assisted in multiple cases of DNA exonerations.²⁹

Like *Williamson v. Reynolds*, Jimmy Ray Bromgard was also later exonerated by DNA evidence with the help of the Innocence Project. Bromgard had been convicted of rape based on a profile sketch, an uncertain pick from a lineup, and a hair comparison examination.³⁰ The expert witness provided a probability based on two factors: an incorrect assumption that the samples would be considered independent events and another study already considered erroneous by other experts in the field. As a result of this case and others like it, 269 case testimonies involving microscopic hair analysis were placed under review. By April 2015, ninety-six percent of them were found to include testimonial error.³¹

Hair comparisons rely on the following factors: a representative known hair sample, variations amongst the known hairs, condition of the unknown hair, expert's experience, and

relevant methods. Such observations, however, do not allow for a conclusive identification. Although the intensity of natural hair color has been represented by a numerical scale, there is no population-based statistical database for hair like there is for DNA and firearms.^{28,32} Unfortunately, the root of the hair is not always present to allow for nucleated DNA analysis. In addition, analysis of mitochondrial DNA is only a viable option if provided a sufficient amount of DNA and suspects that are not maternally related.³³ Hence, alternative analytical methods must be explored to improve the association between the hair and its source.

To form a population-based statistical database for hair color, the variation of natural hair pigmentation must be explored. Natural hair pigmentation is based on varying combinations of two melanins: eumelanin and pheomelanin. Melanin is synthesized in the hair bulb prior to being distributed throughout the hair shaft. Along the shaft, the majority of the melanin is found in the cortex, or the central layer of the hair (Figure 3-1).³⁴ While eumelanin produces the brown and black pigments, pheomelanin produces the reddish-yellow pigments. Pigmentation can also show various patterns under a microscope, such as uniformity or sparsity.³⁵ Quantitative analysis of the overall chemical composition of human hair melanin can provide quantitative identification for human hair pigmentation.

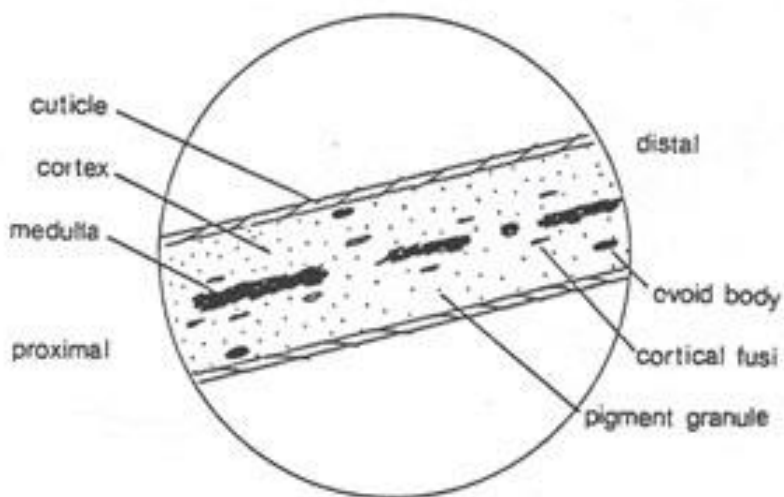


Figure 3-1. Structure of Hair³⁶

With the ability to separate and identify trace levels of volatile organic compounds, GC-MS could be the solution. Through the quantitative analysis of human hair melanin via GC-MS, a

human hair database could be formed to further determine an individual's visual phenotype. Prior to analyzing hair samples via GC-MS, a method for quantitatively analyzing eumelanin and pheomelanin must be developed. As major degradation products of eumelanin and pheomelanin, pyrrole-2,3,5-tricarboxylic Acid (2,3,5-PTCA) and L-3-aminotyrosine (3-AT), respectively, were studied (Figures 3-2, 3-3, 3-4, and 3-5).³⁷ Thus, a method for analyzing 2,3,5-PTCA and 3-AT in acetonitrile was developed. Due to the low volatility of 2,3,5-PTCA and 3-AT, a derivatization reagent was used to increase the volatility and improve the detection of each compound via GC-MS.

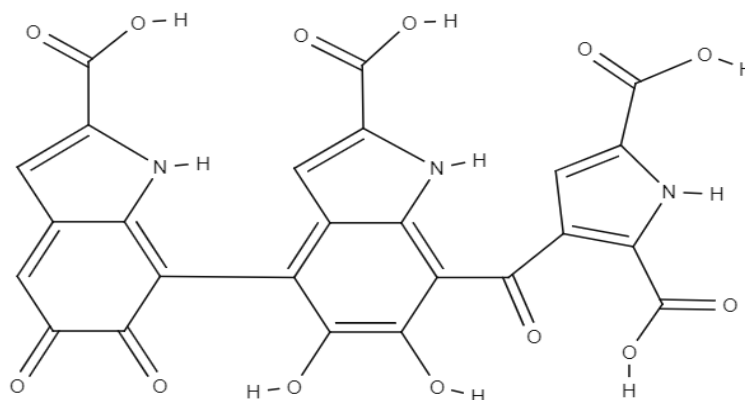


Figure 3-2. Structure of Eumelanin Monomer

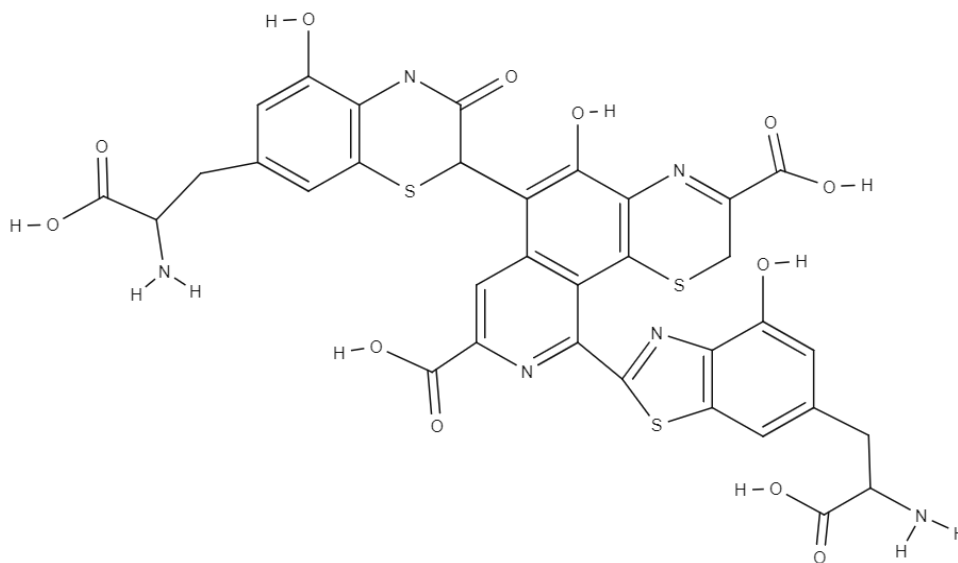


Figure 3-3. Structure of Pheomelanin Monomer

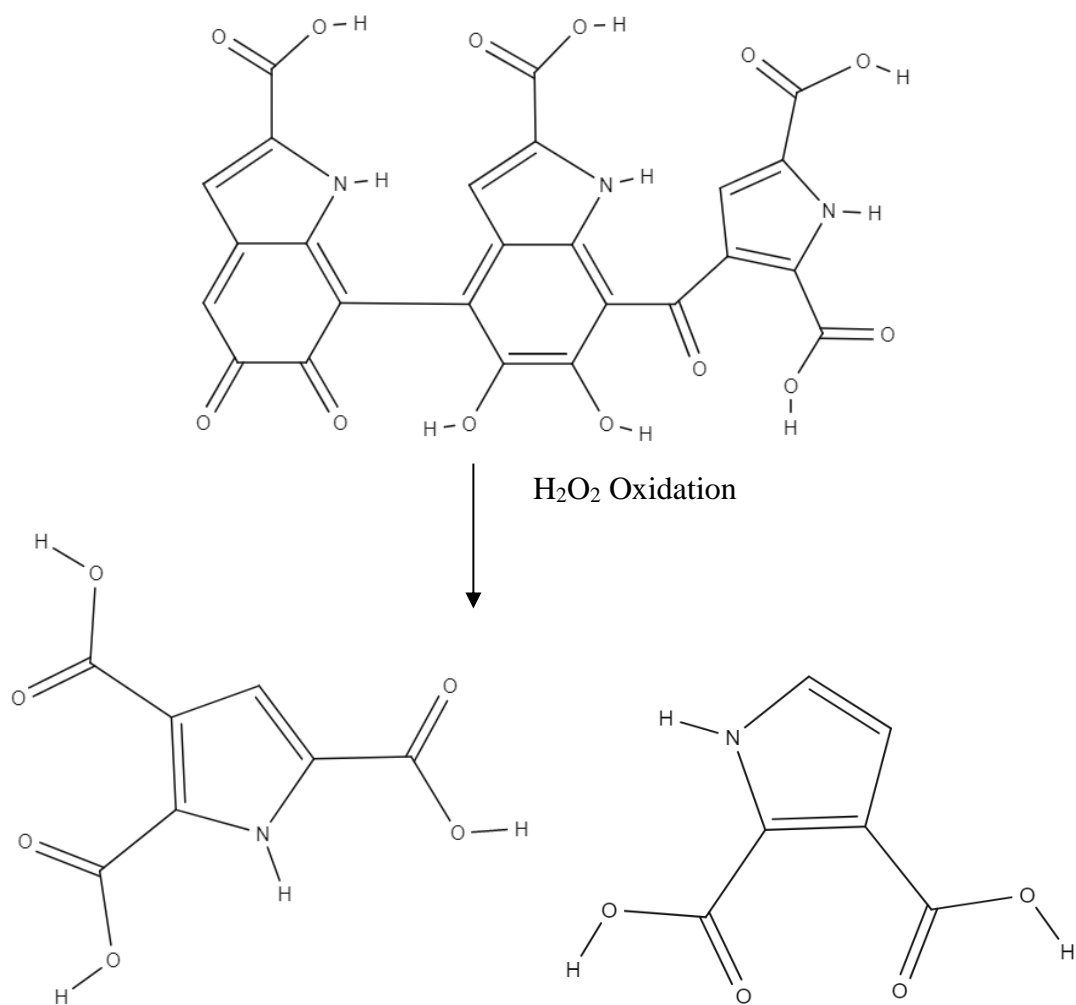


Figure 3-4. Production of 2,3,5-PTCA (bottom left) and 2,3-PDCA (bottom right) from Eumelanin Monomer (top) via Hydrogen Peroxide Oxidation

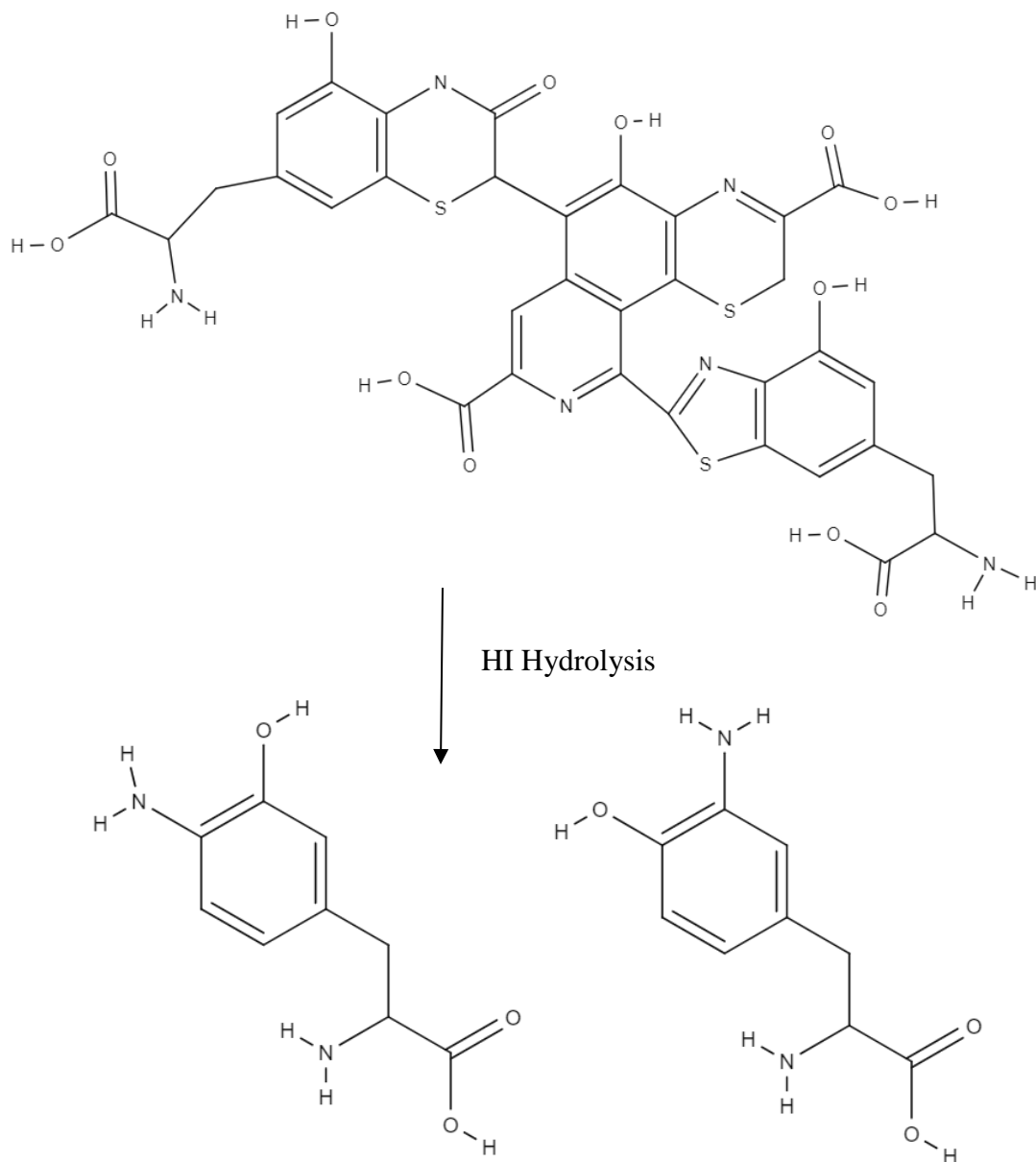


Figure 3-5. Production of 4-AT (bottom left) and 3-AT (bottom right) from Pheomelanin Monomer (top) via Hydroiodic Acid Hydrolysis

Established in their applications for fiber analyses, spectroscopic techniques such as FTIR and MSP could also be further explored for analyzing hair pigmentation.³⁸ Used for spectral identification of trace compounds, FTIR can identify hair as a protein fiber. With the ability to detect small variations in wavelength and intensity, MSP can objectively identify the sample's color.³⁹ Unlike GC-MS, these techniques require little to no sample preparation. Whereas analyzing hair pigmentation via GC-MS requires a destructive technique, analyzing the

pigmentation via FTIR and MSP would be nondestructive to the sample. With the FTIR and MSP data combined, chemometrics could be used to improve the understanding of the melanin composition in hairs and correlate the phenotypes to analytical instrument data.

Another technique established in its applications for fiber analyses, Raman spectroscopy could also be further explored for analyzing hair pigmentation. Raman spectroscopy is used for spectral identification of trace compounds. Thus, Raman spectroscopy can be used to identify some of the compounds within hair. Unlike GC-MS, this technique would require no sample preparation. Whereas analyzing hair pigmentation via GC-MS requires a destructive technique, analyzing the pigmentation via Raman spectroscopy would be semi- or non-destructive to the hair. Although chemometrics applied to FTIR and MSP spectra could provide a statistical database for hair pigmentation, the ratio for eumelanin to pheomelanin would be best obtained via Raman spectroscopy. Raman has been previously used to analyze eumelanin and pheomelanin in both feathers and hairs. In the study, the hair samples were analyzed with a 780 nm laser at 20 mW.⁴⁰

3.2 Experimental

Materials

L-3-Aminotyrosine and Pyrrole-2,3,5-tricarboxylic Acid were purchased from Santa Cruz Biotechnology, Inc. N, N-Dimethylformamide DI and Sodium Bisulfate (92%) were purchased from Acros Organics. Melanin from *Sepia Officinalis* was purchased from Sigma Aldrich. Hydrogen Peroxide (3%) was purchased from Cumberland Swan. BSTFA with 1% TMCS was purchased from CovaChem. Sodium Chloride was purchased from Fluka Analytical. Acetonitrile (HPLC Grade), Hydrogen Peroxide (30%), Potassium Permanganate, liquid injection caps and vials, and a Touch Mixer Model 232 vortex were purchased from Fisher Scientific. Several hairs of varying colors were collected. Aluminum foil was purchased from Reynolds Wrap. A 500 μ L eVol dispensing syringe, Nicolet iN10 Infrared Microscope, and Attenuated Total Reflectance (ATR) germanium crystal were purchased from Thermo Scientific. A Reacti-Therm Heating/Stirring Module was purchased from Pierce Chemical Company. A 6890N GC and a 5975 inert MSD were purchased from Agilent Technologies. A Raman Spectrometer was purchased from CRAIC Technologies.

Methods

Derivatization of Pyrrole-2,3,5-tricarboxylic Acid (2,3,5-PTCA) and L-3-Aminotyrosine (3-AT)

BSTFA + 1% TMCS or DMF-DMA was added to solutions of 2,3,5-PTCA or 3-AT in acetonitrile, such that Acetonitrile:BSTFA was 10:2. Then the solutions were heated at 60°C for 15-30 minutes.²⁴

Extractions for 2,3,5-PTCA from Sepia Officinalis Melanin

Trial Extraction 1

3 mL of 1 M Potassium Carbonate was added to 10 mg of Melanin from *Sepia Officinalis*. 200 µL of 3% Hydrogen Peroxide was added to the melanin solution and then stirred at room temperature for 3 hours. 500 µL of 5% Sodium Bisulfate was added to the melanin solution. Then the melanin solution was acidified with 500 µL of concentrated HCl. 2,3,5-PTCA was extracted from the melanin solution with 1 mL of ethyl acetate 4 times.⁴¹ The ethyl acetate extract was blown down with nitrogen and reconstituted in a 10:2 solution of acetonitrile:BSTFA. The final solution was heated at 60°C for 15-30 minutes.

Trial Extraction 2

600 µL of 1 M Potassium Carbonate was added to 2 mg of Melanin from *Sepia Officinalis*. 4 µL of 30% Hydrogen Peroxide was added to the melanin solution and then stirred at room temperature for 3 hours. 100 µL of 5% Sodium Bisulfate was added to the melanin solution. Then the melanin solution was acidified with 1M HCl to pH 2. 2,3,5-PTCA was extracted from the melanin solution with 1 mL of ethyl acetate 4 times.⁴¹ The ethyl acetate extract was blown down with nitrogen and reconstituted in a 10:2 solution of acetonitrile:BSTFA. The final solution was heated at 60°C for 15-30 minutes.

Trial Extraction 3

500 µL of 30% Hydrogen Peroxide was added to 2 mg of Melanin from *Sepia Officinalis*. 500 µL of 2M Ammonium Hydroxide was added to the melanin solution. Then the melanin solution was vortexed for 1 minute and incubated at room temperature for 8 hours. 200 µL of 10% Sodium Bisulfate was added to the melanin solution and vortexed for 5 seconds.⁴² Then the

melanin solution was blown down with nitrogen and reconstituted in a 10:2 solution of acetonitrile:BSTFA. The final solution was heated at 60°C for 15-30 minutes.

Trial Extraction 4

1 mL of 1M Sulfuric Acid was added to 5 mg of Melanin from *Sepia Officinalis*. 60 µL of 3% Potassium Permanganate was added to the melanin solution gradually until the purple color vanished for at least 10 minutes. 100 µL of 5% Sodium Bisulfate was added to the melanin solution and vortexed thoroughly. Then 2,3,5-PTCA was extracted from the melanin solution with a total of 14 mL of diethyl ether.⁴³ BSTFA was added to the ethyl acetate extract, such that diethyl ether:BSTFA was 10:2. The final solution was heated at 60°C for 15-30 minutes.

Trial Extraction 5

1 mL of 1M Sulfuric Acid was added to 10 mg of Melanin from *Sepia Officinalis*. 60 µL of 3% Potassium Permanganate was added to the melanin solution gradually until the purple color was retained for at least 10 minutes. 100 µL of 5% Sodium Bisulfite was added to the melanin solution and vortexed thoroughly. Then 2,3,5-PTCA was extracted from the melanin solution with a total of 14 mL of diethyl ether.⁴³ BSTFA was added to the ethyl acetate extract, such that diethyl ether:BSTFA was 10:2. The final solution was heated at 60°C for 15-30 minutes.

Liquid Injection

The derivatized solutions of 3-AT and 2,3,5-PTCA were analyzed using a 30 m Agilent technologies DB-5MS column with a 250 µm inner diameter and a 0.25 µm film thickness.

FTIR Sample Preparation

For transmission FTIR, individual hair strands were sandwiched between self-adhesive reinforcement labels and flattened with a roller. For ATR FTIR, multiple hair strands from the same sample were placed on a glass slide. This was done for blonde, brown, and black hair samples.

MSP Sample Preparation

Individual hair strands were mounted on quartz slides with glycerin mounting media and quartz coverslips to observe spectral features in the UV region of the scan range.³²

Raman Sample Preparation

Individual hair strands were placed on aluminum foil and adhered to the stage with magnets. The 20X objective lens was used to focus on the sample.

Instrumental

GC-MS

An Agilent 6890N Network GC coupled to an Agilent 5975 Inert MSD was used for analyses, along with a Gerstel MultiPurpose Sampler. The column used was a DB5-MS with dimensions of 30 m x 0.25 mm x 0.25 μ m. Hydrogen carrier gas was utilized at a flow rate of 2.0 mL/min. The oven temperature program started at 50°C for 1 minute and was then ramped at 10°C/min to 250°C and held there for 3 minutes. The mass transfer line into the MS was set to 250°C and the source temperature was set to 230°C. The MS was in negative ionization mode. Selected ion monitoring was used and set at m/z 218 ([3-AT, 2 TMS – C₇H₉NO]⁺) and m/z 266 ([3-AT, 2 TMS – 1TMS]⁺) for detection of 3-AT. The total scan time was 24 minutes, scanning from 40 amu to 550 amu.

FTIR

A Thermo Scientific Nicolet iN10 Infrared Microscope was used for analyses, along with an ATR germanium crystal. The scan range was between 700 cm⁻¹ and 4000 cm⁻¹.

MSP

A CRAIC Microspectrophotometer was used for analysis. The power source used was transmittance with a pure xenon short-arc (XBO) lamp set at 75 W. The scan range was between 200 nm and 900 nm.

Raman Spectroscopy

A CRAIC Raman Spectrometer was used for analysis. The laser excitation wavelength was set at 780 nm. The power was set to its maximum at 2.5 mW. The average count was 100.

3.3 Results and Discussion

GC-MS

Detection of derivatized 2,3,5-PTCA and 3-AT

Due to the variety of degradation products related to hair, a separation technique prior to detection using a Mass Spectrometer (MS) is needed.

DMF-DMA

N,N-Dimethylformamide dimethyl acetal (DMF-DMA) was chosen for its methyl esterification of carboxylic acid functional groups since these are found in both of the targeted compounds.²⁴ The derivatized sample was placed in an autosampler vial and analyzed over three consecutive days. However, GC-MS identified two derivatized peaks for 3-AT, a kinetic product and a thermodynamic product (Figure 3-6). While kinetic products form faster, thermodynamic products have greater stability due to greater substitution. As expected, only the thermodynamic product peak remained on the third day. The only other peaks detected were siloxanes.

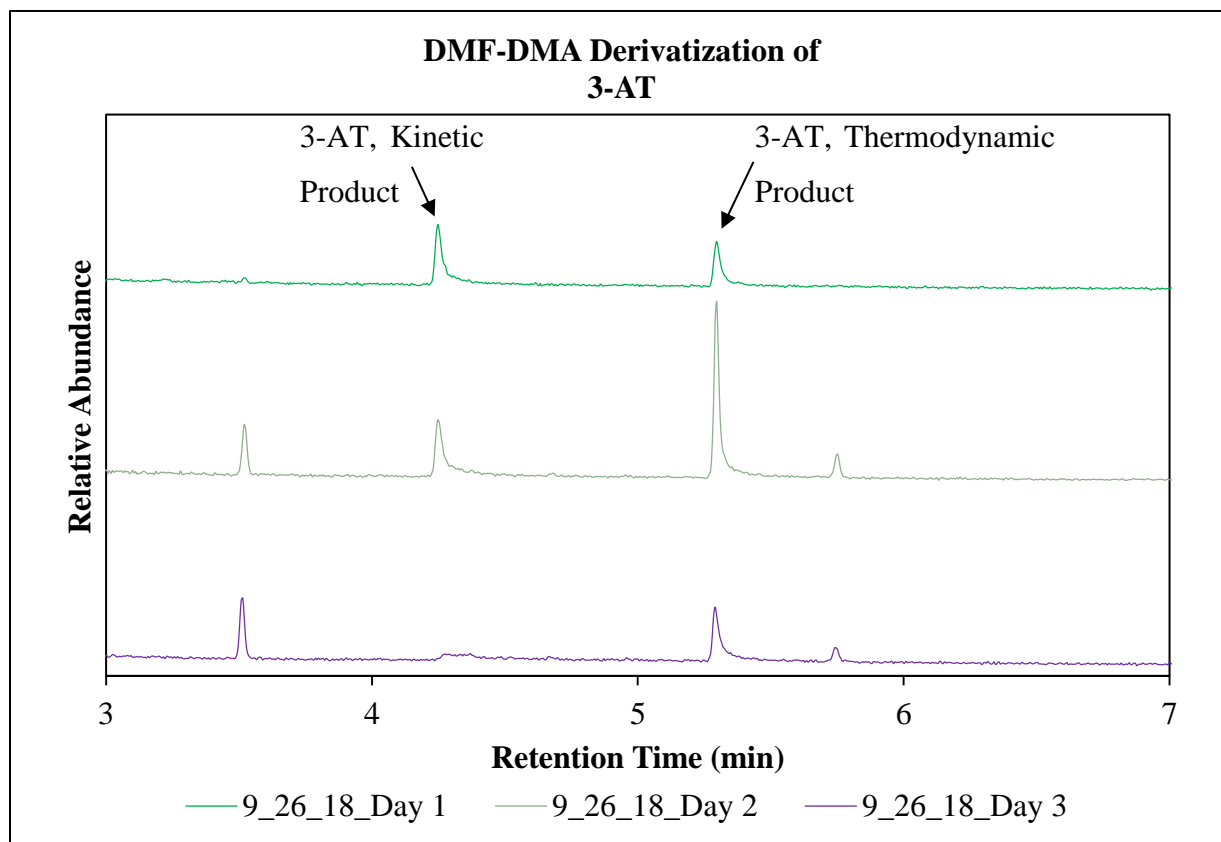


Figure 3-6. Total ion chromatograms of an Acetonitrile solution of DMF-DMA derivatized 3-AT over 3 days

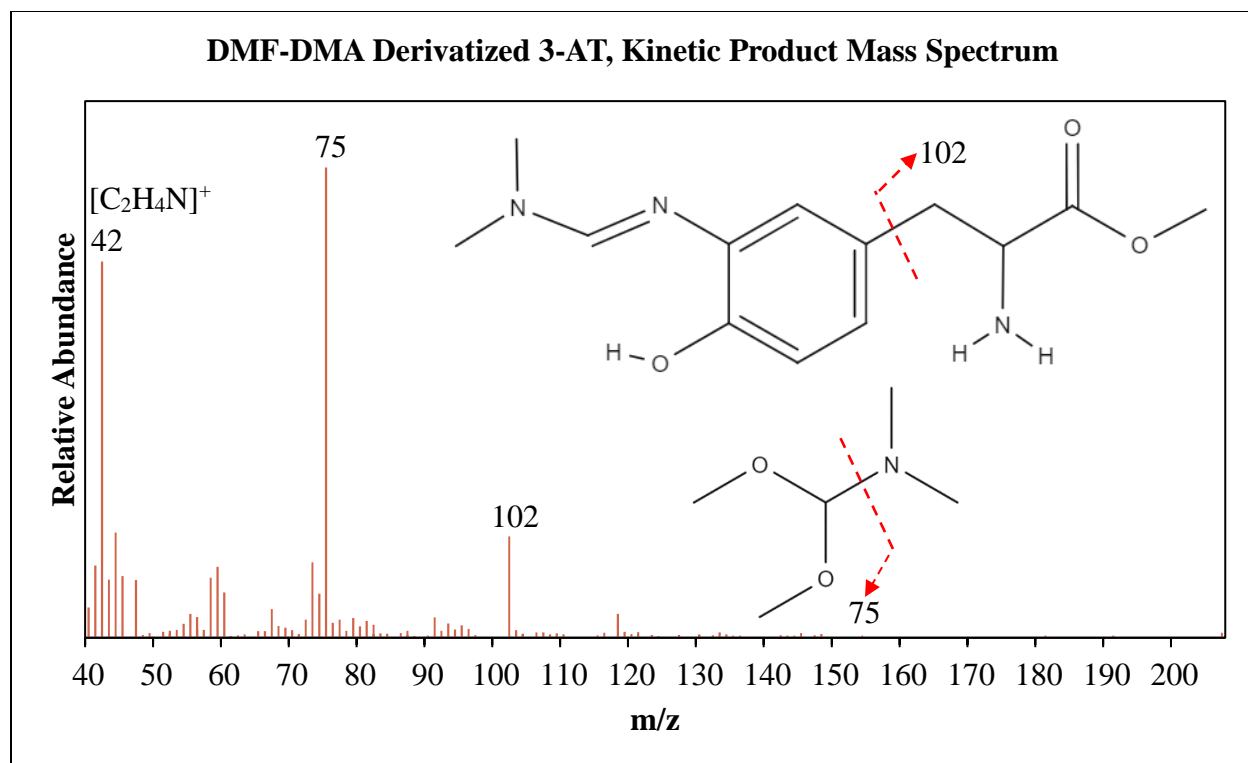


Figure 3-7. Structure and Significant Fragmentation of DMF-DMA derivatized 3-AT, Kinetic Product

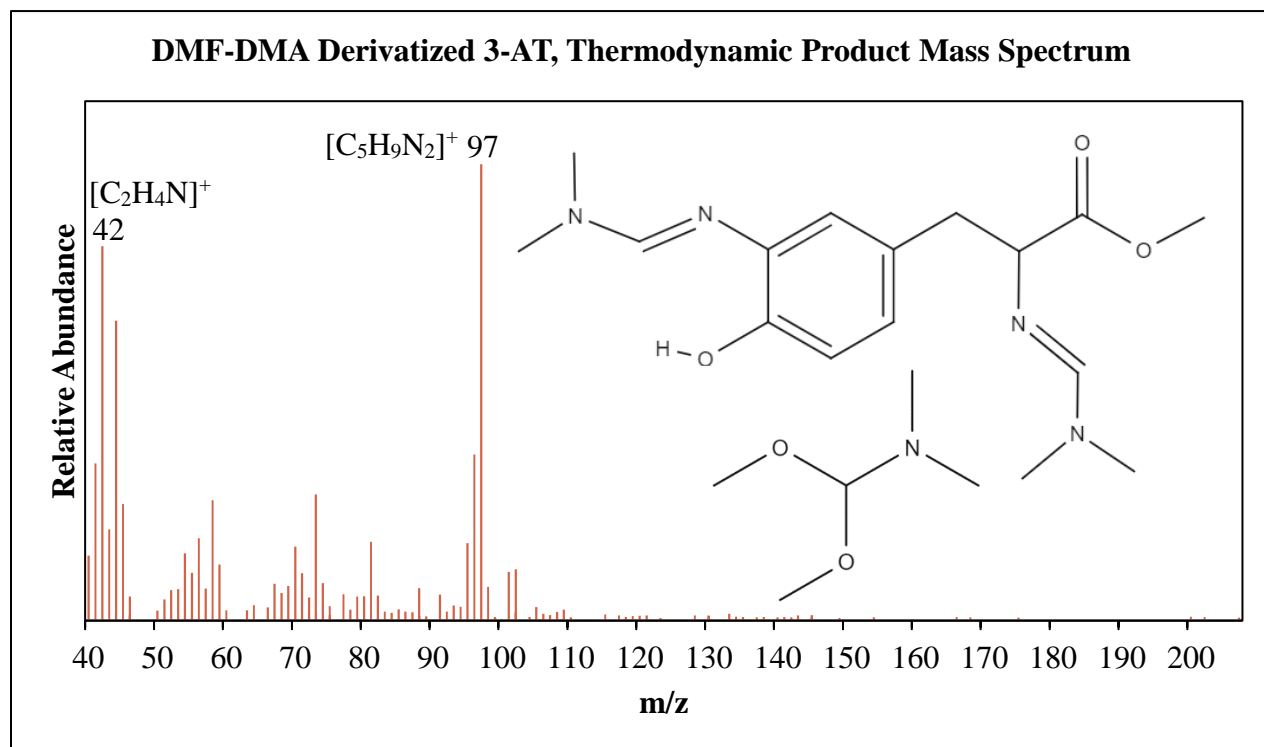


Figure 3-8. Structure and Significant Fragmentation of DMF-DMA derivatized 3-AT, Thermodynamic Product

BSTFA

N,O-bis(trimethylsilyl)trifluoroacetamide (BSTFA) was chosen for its moderate reactivity with carboxylic acid functional groups since these are found in both of the targeted compounds.²⁴ Both 2,3,5-PTCA and 3-AT were able to be fully derivatized by BSTFA. GC-MS sufficiently separated and identified BSTFA-derivatized 2,3,5-PTCA from 3-AT, our degradation products of interest (Figure 3-9). However, scan mode was insufficient for concentrations below 200 ppm (Figure 3-12).

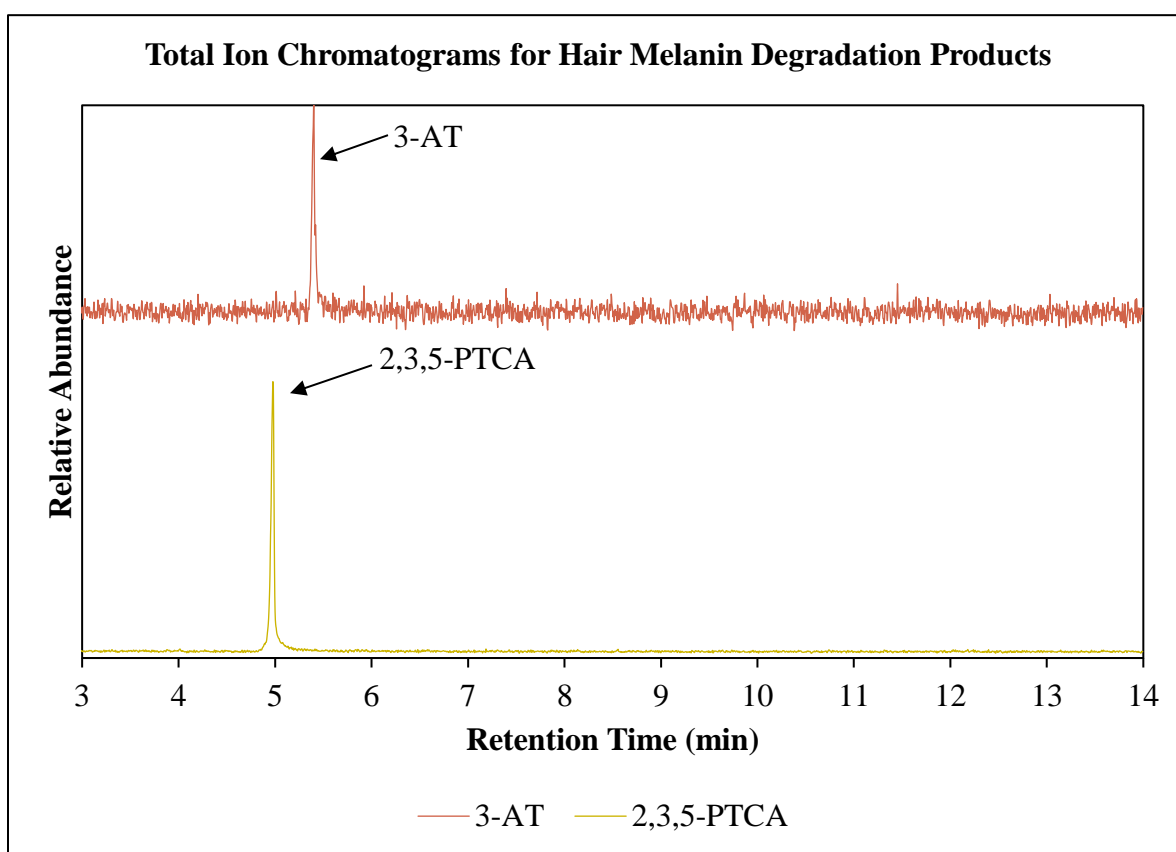


Figure 3-9. Total ion chromatograms of Acetonitrile solutions of BSTFA derivatized 3-AT (200 ppm) (blue) and 2,3,5-PTCA (7500 ppm) (orange)

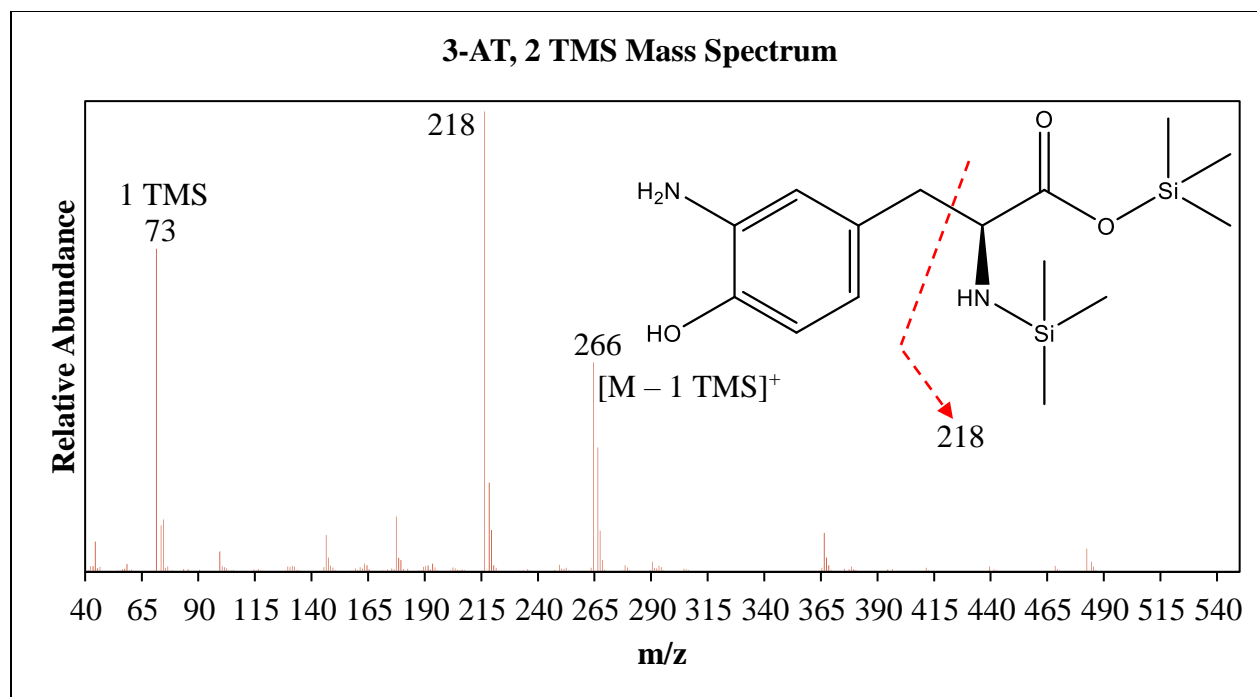


Figure 3-10. Structure and Significant Fragmentation of BSTFA derivatized 3-AT overlaid on its Mass Spectrum

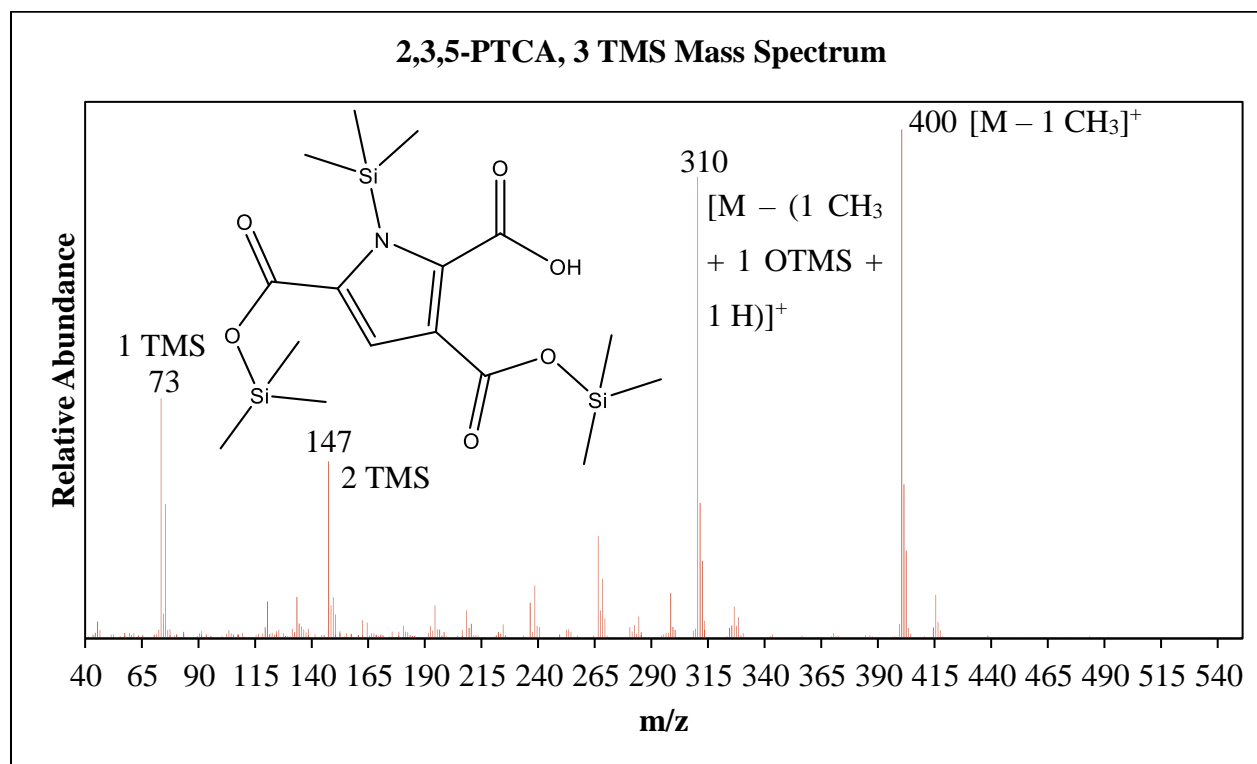


Figure 3-11. Structure and Significant Fragmentation of BSTFA derivatized 2,3,5-PTCA overlaid on its Mass Spectrum

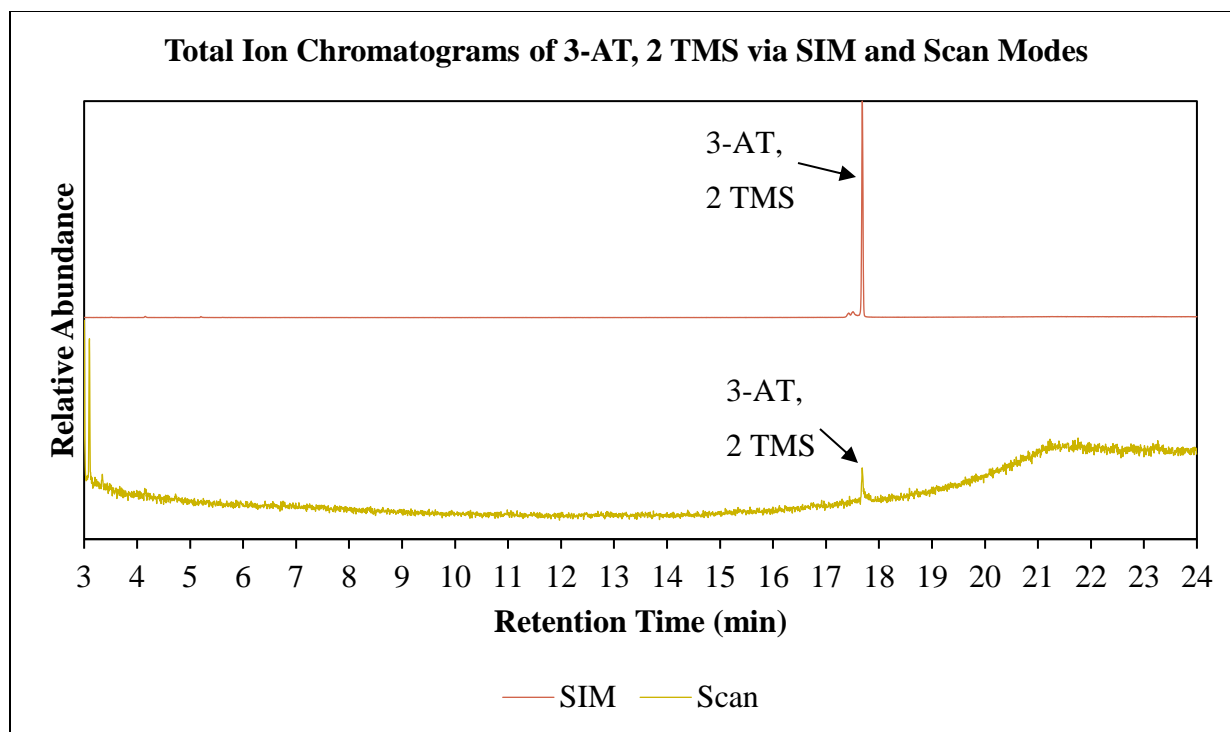


Figure 3-12. Total Ion Chromatograms of an Acetonitrile solution of 200 ppm 3-AT, 2 TMS via SIM mode (blue) and scan mode (orange)

Extractions for 2,3,5-PTCA from Sepia Officinalis Melanin

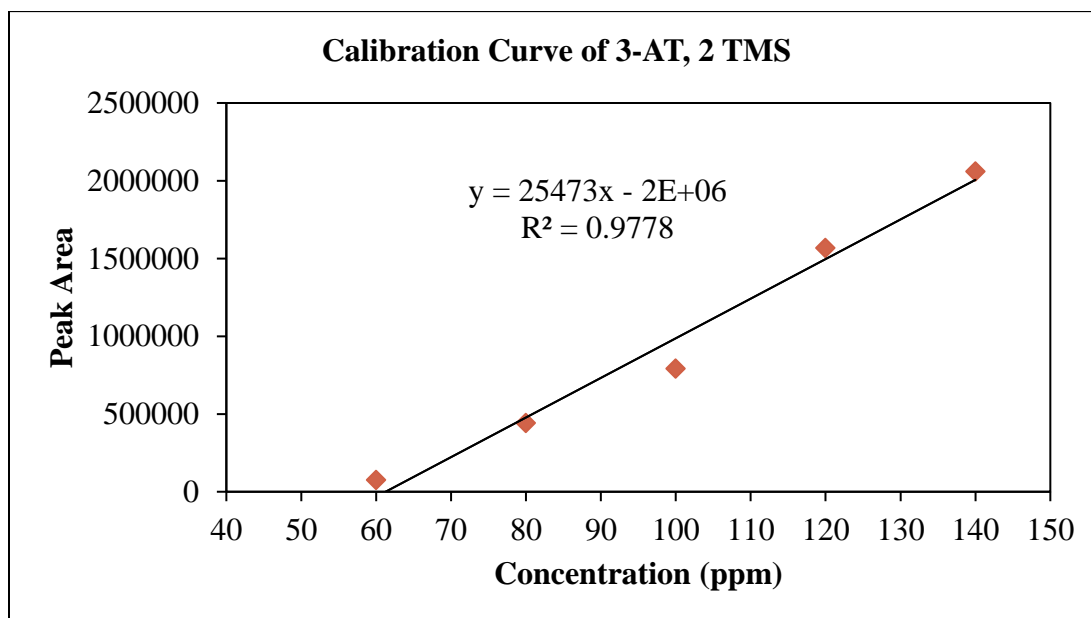


Figure 3-13. Calibration curve for Acetonitrile solutions of BSTFA derivatized 3-AT via Liquid Injection

The trial extractions were based on either hydrogen peroxide oxidation or potassium permanganate oxidation. However, none of these approaches showed success extracting 2,3,5-PTCA from *Sepia Officinalis* melanin. Furthermore, to extract 2,3,5-PTCA from hair would require prior extraction of the melanin from the hair. Multiple studies of extractions of 2,3,5-PTCA from melanin have provided approximately 1-10% yields.⁴³⁻⁴⁵ Hence, the melanin degradation products would likely require detection levels in the ppb range. As seen with 3-AT, the limit of detection only reached 60 ppm. Therefore, these extractions coupled with GC-MS are not currently viable options.

FTIR

Both transmission and ATR modes were applied to the given hair samples to determine which is better suited for the structural identification of hair.

Transmission

A single hair strand analyzed via transmission on FTIR resulted in a saturated spectrum rather than one with clearly defined peaks.

ATR

ATR was used to reduce the saturated absorption observed in the transmission spectra.⁷ Multiple strands of hair side-by-side analyzed via ATR on FTIR showed typical protein fiber characteristics (Figure 3-14).⁴⁶ Multiple resolutions and scans were also explored. To minimize noise and elucidate fine structure, a minimum of 2 scans and a resolution between 2 cm^{-1} and 6 cm^{-1} should be used for FTIR examinations of hair samples (Figures 3-15 and 3-16).

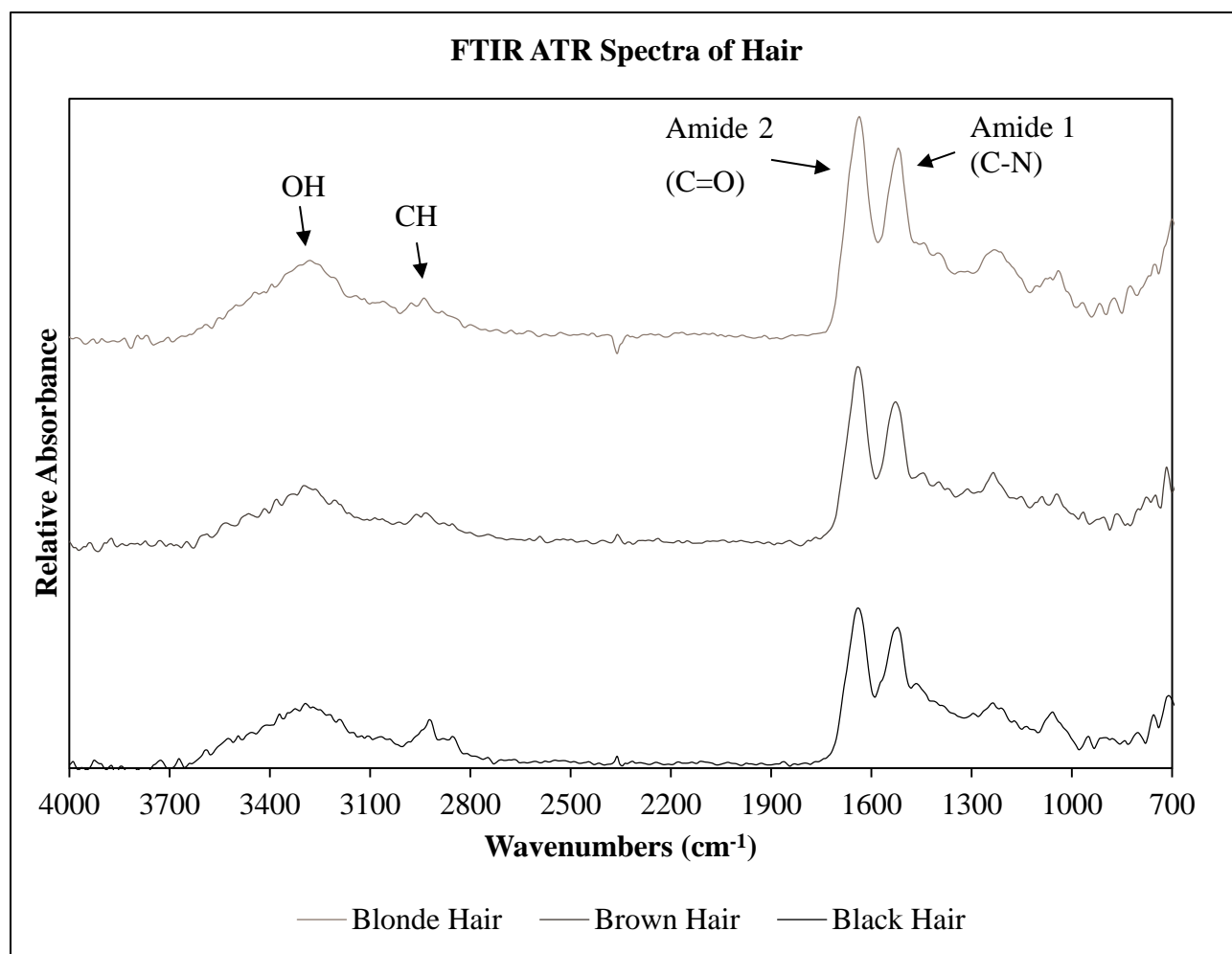


Figure 3-14. Stacked FTIR ATR Spectra of blonde (top) and brown (bottom) hair

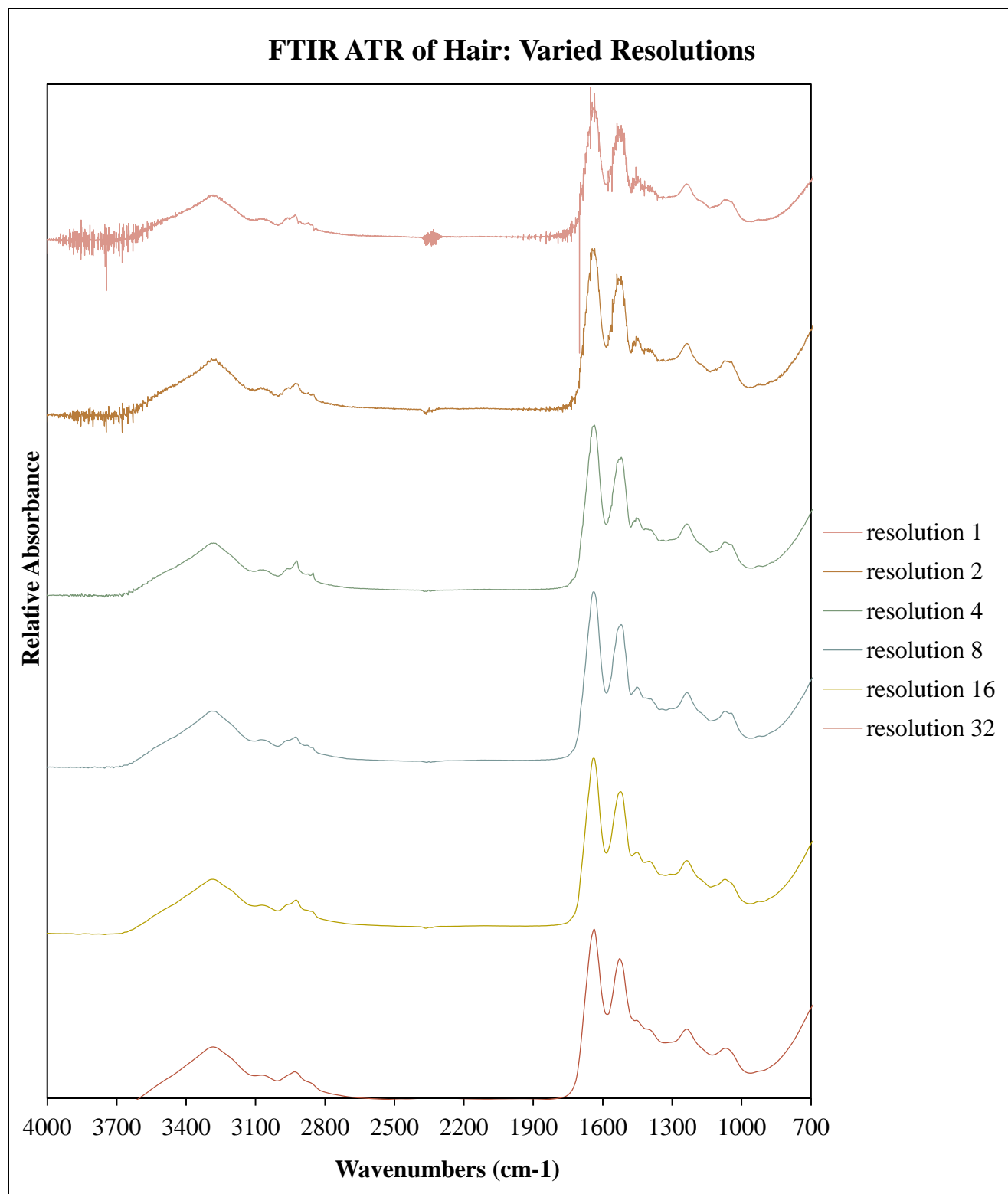


Figure 3-15. Stacked FTIR ATR Spectra of brown hair with varying resolution at 16 scans

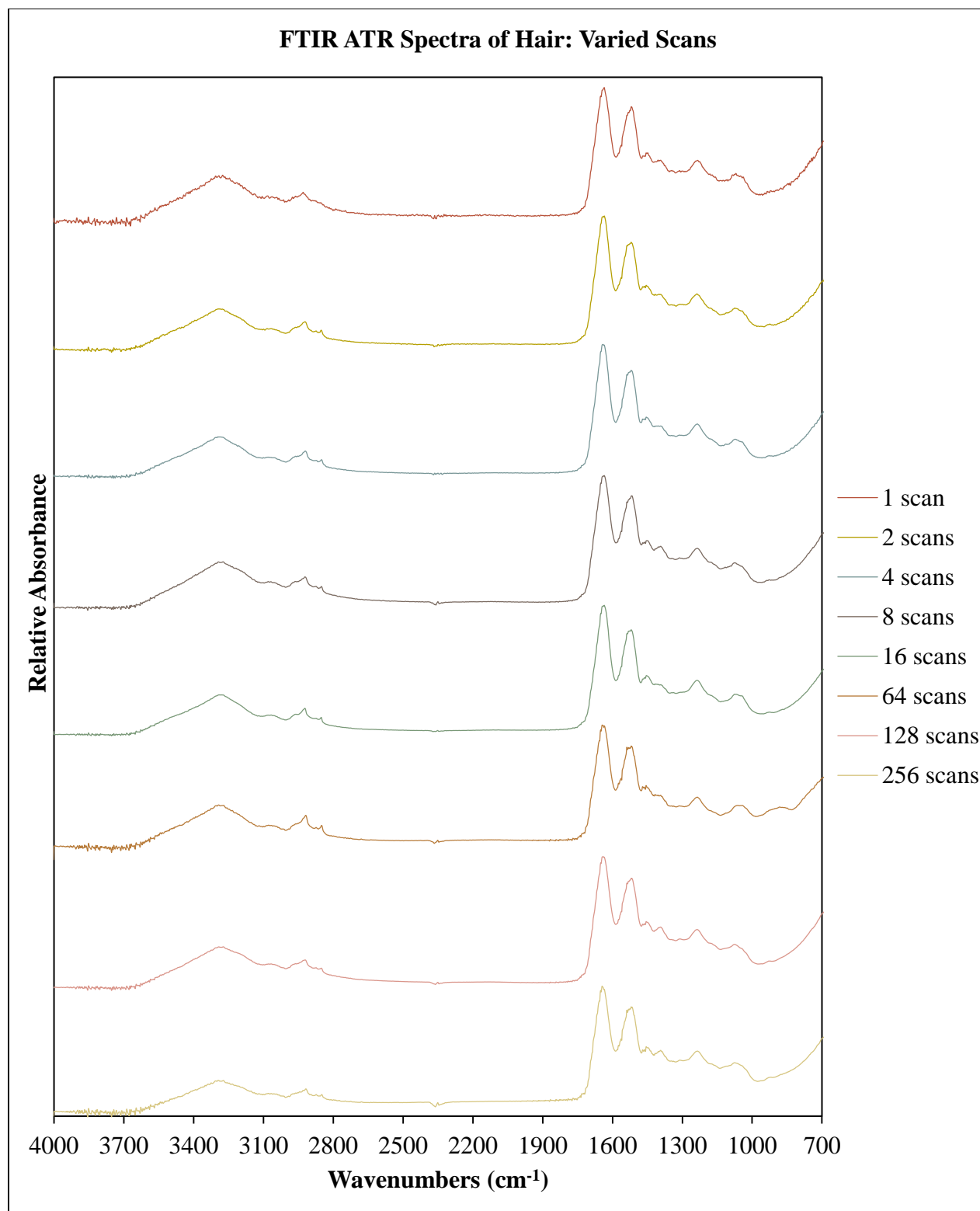


Figure 3-16. Stacked FTIR ATR Spectra of brown hair with varying number of scans at a resolution of 4 cm⁻¹

MSP

Although MSP showed similar wavelengths for brown and blonde hair, there was a higher absorbance for darker hairs. There was also an apparent redshift from light-colored to dark-colored hair (Figure 3-17).

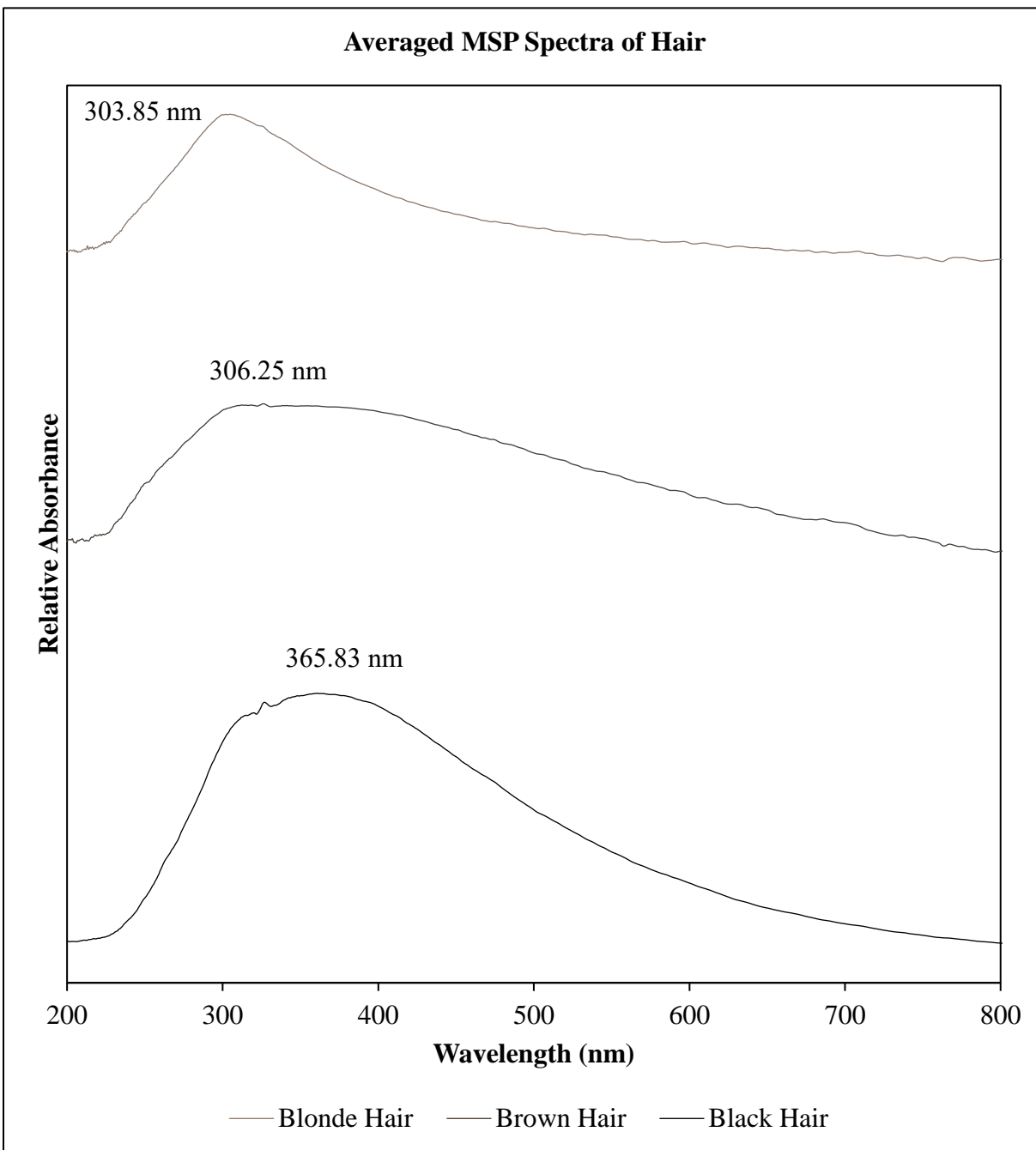


Figure 3-17. Stacked MSP Spectra of blonde hair (blue), brown hair (orange), and black hair (grey)

Raman Spectroscopy

Melanin Degradation Products

Since 2,3,5-PTCA is a major degradation product of eumelanin and 3-AT is a major degradation product of pheomelanin, the spectra obtained are partially representative of eumelanin and pheomelanin, respectively. Although potential peaks around 1420 and 1430 cm^{-1} could be attributed to C-H bending, there is low signal-to-noise (Figure 3-18). Therefore, analyzing the degradation products via Raman spectroscopy does not provide a reliable way of determining the amount of eumelanin relative to pheomelanin.

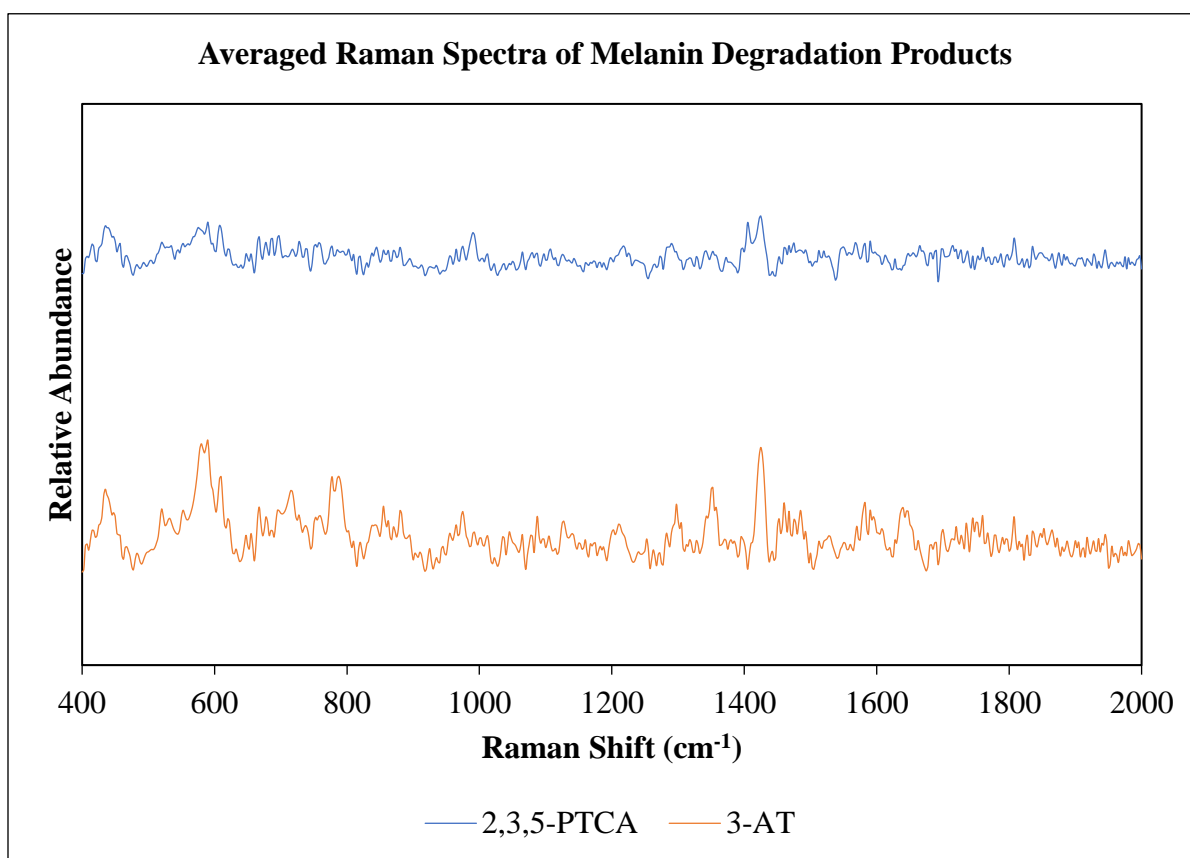


Figure 3-18. Stacked Raman Spectra of the Melanin Degradation Products 2,3,5-PTCA and 3-AT

Sepia Officinalis Melanin and Hair Samples

Since *Sepia Officinalis* melanin is pure eumelanin found in nature, the spectrum obtained is representative of eumelanin. Single hair strands were also analyzed via Raman spectroscopy. Significant peaks were noted around 1350, 1430, and 1580 cm^{-1} . The black hair spectrum

resembled the *Sepia Officinalis* melanin spectrum. For example, as in the *Sepia Officinalis* melanin spectrum, the peaks at 1350 cm^{-1} and 1580 cm^{-1} in the hair spectra could be attributed to aromatic C-C stretching and aromatic C=C stretching, respectively. The peak at 910 cm^{-1} could be attributed to C-C-C deformation (Figure 3-19).⁴⁷

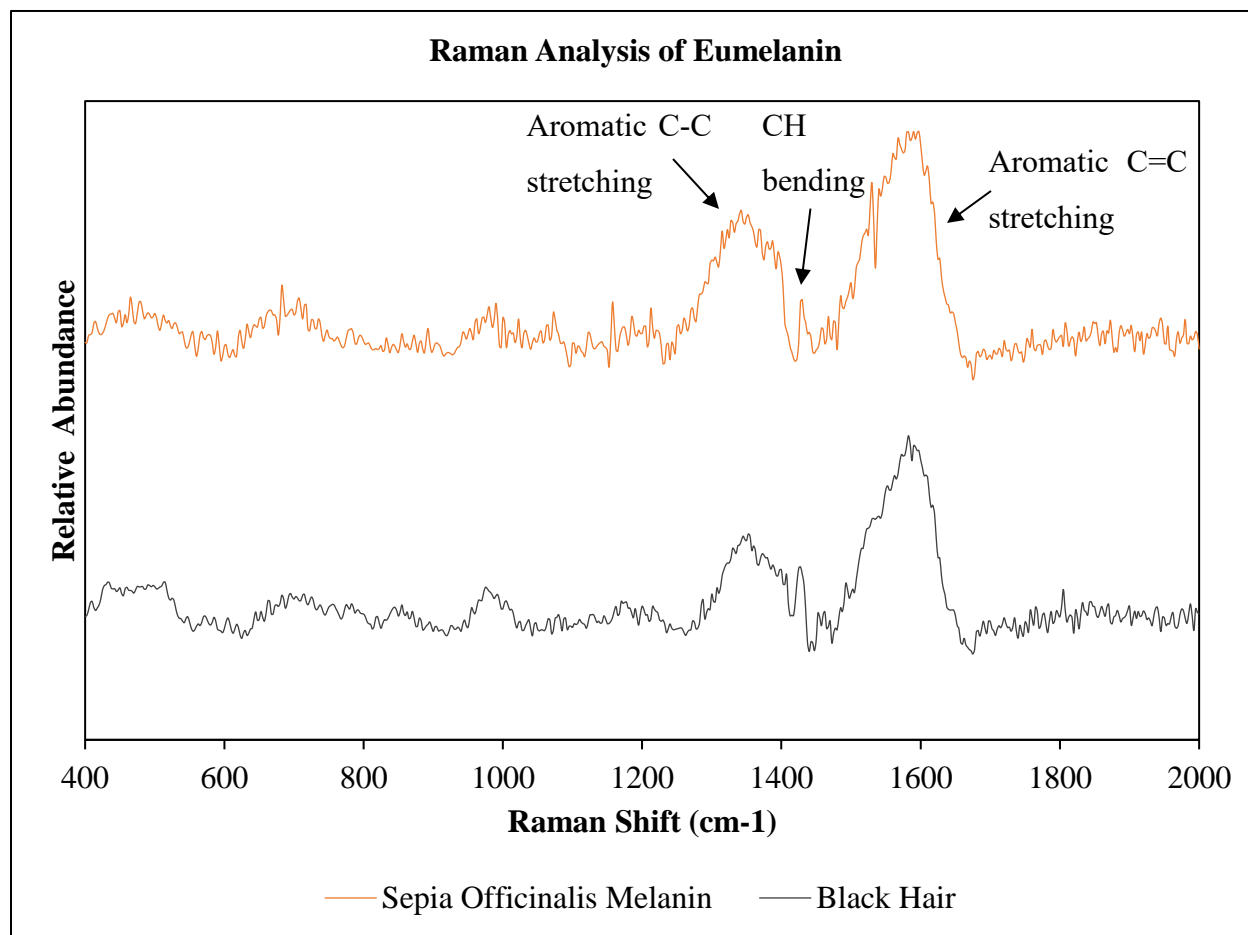


Figure 3-19. Stacked Raman Spectra for Analysis of Eumelanin: 2,3,5-PTCA (blue), *Sepia Officinalis* Melanin (orange), and Black Hair (grey)

3.4 Conclusion

Methods for analyzing eumelanin and pheomelanin in hair were explored. Derivatized samples of 2,3,5-PTCA and 3-AT in acetonitrile were analyzed via GC-MS to provide a basis for analyzing samples extracted from hair melanin. Two derivatization reagents (DMF-DMA and BSTFA) were explored. Overall, the two degradation products greatly favored BSTFA for full

derivatization. Multiple methods for extracting 2,3,5-PTCA from *Sepia Officinalis* melanin were explored. Upon analysis of the extractions, there was no detection of 2,3,5-PTCA. Hence, variation in hair pigmentation would be better analyzed via FTIR and MSP if coupled with chemometrics. Whereas these two techniques do not provide the desired quantitation of the two types of melanin in hair, eumelanin is readily identifiable by Raman spectroscopy. Therefore, analysis of melanin via Raman spectroscopy should be further explored. These possibilities will be discussed further in “Chapter 4: Future Work.”

CHAPTER 4. FUTURE DIRECTIONS

4.1 M-Vac Collection Efficiency of TNT Project

In this work, the efficiency of the M-Vac collection of explosives was inconclusive. Hence, other parameters must be further explored. This includes exploring other types of explosives, materials for containing explosive devices, and M-Vac buffers. Upon determining the optimal materials, the method could be applied to field investigations with the combined use of the M-Vac and a portable GC-MS.

Inorganic Explosives

In this work, only an organic explosive was analyzed. Although the recovery of TNT with the current M-Vac buffer was low, the recovery of inorganic explosives could be much greater. However, to analyze inorganic explosives, desorption electro-flow focusing ionization-mass spectrometry (DEFFI-MS) with collision induced dissociation (CID), surface-enhanced Raman spectroscopy (SERS), or infrared spectroscopy (IR) would need to be used in replacement of GC-MS. As commonly used inorganic explosives, black powder, ammonium nitrate, and potassium chlorate would be good choices to test.⁴⁸

Various Surfaces

In this work, TNT showed limited ability to bind to the polyester/polypropylene blend backpack. Hence, other materials to conceal the explosive device could be explored. Other items often used to conceal an explosive device include bags and boxes.⁴⁹ These new items along with backpacks made from different material should be further explored.

Various Buffers

Provided the M-Vac buffer utilized remains nuclease- and DNA-free for the collection of DNA, various buffer solutions could be explored for the collection of organic explosives like TNT. The buffer provided with the M-Vac System, Butterfield's Buffer, is a phosphate buffer solution. The use of the surfactant sodium dodecyl sulfate was previously studied but showed an interference with the collection of DNA.⁵⁰⁻⁵¹

Portable GC-MS

Upon optimization of the M-Vac System for collection of explosives, a portable GC-MS could be explored for this application in field operation. The Combating Terrorism Technical Support Office has worked with Torion Technologies and Smiths Detection to produce two viable instruments, the Torion T-9 (Figures 4-2 and 4-3) and the Guardian (Figure 4-1), respectively. These portable instruments have been used primarily for the detection of chemical warfare agents (CWAs) and toxic industrial chemicals (TICs) in various environments. Weighing approximately 30 pounds, a portable GC-MS would allow investigators on the scene to obtain fast results. With step-by-step instructions provided on the instrument's screen, the instrument would be easy for non-experts to use. The portable instrument's available sample injection technique allows for the analysis of samples in the gas, liquid, or solid phases. SPME also remains a viable technique with this portable instrument. Currently these portable instruments take less than 10 minutes for qualitative screening and quantitative analysis. Although the portability of this instrument comes with a wireless lifetime limitation of a few hours, its Lithium-ion battery is replaceable and rechargeable.⁵²⁻⁵⁴ As performed for the study in Chapter 1, post-blast debris would need to be collected. Following collection, the M-Vac would be used to extract explosive residue from the debris. After sample preparation, the solution would then be run on the portable GC-MS.



Figure 4-1. A Smiths Detection Guardian portable GC-MS⁵²



Figure 4-2. Diagram of a Torion T-9 portable GC-MS⁵⁵



Figure 4-3. Top view diagram of a Torion T-9 portable GC-MS⁵⁵

4.2 Analysis of DNA Methylation in Blowflies

In this work, the analysis of DNA in flies was inconclusive. Hence, other parameters must be further explored. This includes exploring other derivatization reagents and instrumentation. Upon optimization of the sample preparation and analysis methods, the procedure could be applied to determining the age of individual blowflies based on variation in cytosine methylation.

Other Derivatization Reagents

Exploring other derivatization reagents may improve the sensitivity for DNA analysis. However, this may also require exploration of other techniques, such as LC-MS, due to the chemical properties of each reagent and the subsequent derivatized nucleobases.

2-Acetylaminofluorene

2-Acetylaminofluorene (AAF) has been previously used to analyze DNA via LC-MS in the positive ion mode. One study showed that N-acetoxy-2-acetylaminofluorene (AAAF) experienced greater DNA binding in comparison to N-Hydroxy-2-acetylaminofluorene.⁵⁶ During the formation of the nucleobase-AAF adduct, the acetoxy group in AAAF is lost. Upon modification of such adducts to form the hexamethyleneimine derivatives, more organic solutions were used to improve the volatility of the mobile phase. The signal-to-noise, peak shape, and sensitivity of the derivatized adducts are significantly greater than to those of the underivatized adducts. Unlike reagents which require enzymatic digestion, the hexamethyleneimine reagent further allows for the analysis of backbone DNA phosphate adducts rather than only the nucleobase adducts.⁵⁷ However, if the nucleobase-AAF adduct is to be analyzed via GC-MS, then derivatization with mono- or di-tBDMS may be preferred. This will result in the characteristic fragment ion $[M-57]^+$ and high mass ions for quantitative analysis.⁵⁸

2-Bromoacetophenone

The derivatization reagent 2-bromoacetophenone has also been used to analyze DNA. 2-bromoacetophenone is known to form phenacyl derivatives upon reacting with carboxylic acids.⁵⁹⁻⁶⁰ In one study, DNA methylation was detected via High Performance Liquid Chromatography with Spectrofluorimetric Detection (HPLC-FLD) in submicrogram nucleoside samples with high selectivity for derivatized cytosine moieties. Nucleosides and nucleotides were derivatized with 2-

bromoacetophenone, producing fluorescent derivatives. Due to stability, the derivatized compounds could be analyzed over the course of approximately 3 days.⁶¹

Isobutyl Chloroformate

Isobutyl chloroformate (IBCF) has been used to derivatize nucleobases for analysis via a Gas Chromatography-Flame Ionization Detector (GC-FID) technique. Prior to derivatization, the DNA must undergo acid hydrolysis. IBCF reacts with primary and secondary low-molecular mass aliphatic amines, dicarboxylic acids, amino acids, and 4-(5-)methylimidazole. Upon derivatization, IBCF loses its Chlorine atom. In one study, the IBCF derivatized nucleobases were successfully detected in both blood and plant samples.⁶²

Degree of Methylation Quantitation

Once sensitivity is improved for this experiment, then the degree of methylation must be quantitated. To perform the calibration curves, an internal standard should be held at a constant concentration while analyzing multiple concentrations of Cytosine. This would be repeated for 5-methyl Cytosine. After linearity is achieved for the calibration curves of Cytosine and 5-methyl Cytosine, X-Y plots could be made for the peak area ratios of 5-methyl Cytosine:Cytosine against the degree of methylation, or concentration ratios, examined. Furthermore, either Cytosine or 5-methyl Cytosine should be held at a constant concentration while varying the other's concentration for the X-Y plots.

Blowfly Aging Study

Upon optimizing the analysis for DNA methylation, the next logical step would be to perform a fly aging study. Reproducible changes would be expected in the relative amount of DNA methylation as the flies age. However, multiple parameters must be examined to confirm this. These parameters include the type of blowfly, ambient temperature, relative humidity, light exposure, age of the blowfly, and sex of the blowfly (Table 4-1). The various ages are necessary to establish a range for which age could be accurately determined. The remaining parameters are necessary to understand any differences that may occur due to various environments.

Table 4-1. Parameters of Blowfly DNA Aging Study

Species	Temperature	Relative Humidity	Light:Dark (L:D)	Ages (days)	Samples (3 flies per treatment X 2 sexes) X 3 replicates
<i>Phormia regina</i>	15C	60%	6:18	1, 2, 5, 7,	180
			12:12	10, 14,	180
			18:6	21, 28,	180
			24:0	35, 42	180
	20C	60%	X 4	X 10	720 (180)
	25C	60%	X 4	X 10	720
	30C	60%	X 4	X 10	720 (180)
<i>Cochliomyia macellaria</i>	X 4	60%	X 4	X 10	2,880
<i>Lucilia sericata</i>	X 4	60%	X 4	X 10	2,880
TOTAL					8,640

4.3 Analysis of Hair Pigmentation

In this work, the analysis of hair pigmentation was inconclusive. However, spectroscopic techniques were explored and showed potential. Hence, further exploration of this techniques is essential. Upon applying chemometrics to combined data obtained from FTIR and MSP, a statistical database could be formed for hair pigmentation. On the other hand, further analysis using Raman spectroscopy could provide a database for hair pigmentation based on the ratio of eumelanin to pheomelanin within each hair sample.

Chemometrics with FTIR and MSP

Preliminary results of hair were gathered via FTIR and MSP techniques in Chapter 3. However, the MSP data could be further supplemented with molar absorptivity calculations based on the hair diameters obtained via a Polarized Light Microscope's calibrated reticule. Here the data of both FTIR and MSP techniques were combined. As seen in Figure 4-4, there are distinct spectroscopic differences between blonde, brown, and black hair. Hence, the use of chemometrics could provide pattern recognition and data discrimination to support forensic evidence in court cases.⁶³ Chemometrics provides a way to analyze complex data sets for class evidence in an objective, statistical manner. Agglomerative hierarchical clustering (AHC), principal component analysis (PCA), and discriminant analysis (DA) have been used previously to study MSP data of red-dyed hair samples.⁶⁴ Here the spectral data was preprocessed via mean centering and then

normalization. To perform mean centering on the data, the average absorbance of each peak (A_{λ}) was determined and subtracted from each point of its respective peak ($A_{i,\lambda}$) (Figure 4-5). Then the data was normalized by dividing the mean centered absorbance data by the standard deviations of the respective peaks (Figure 4-6). To better observe the data, a logarithmic scale was used for the x-axis.

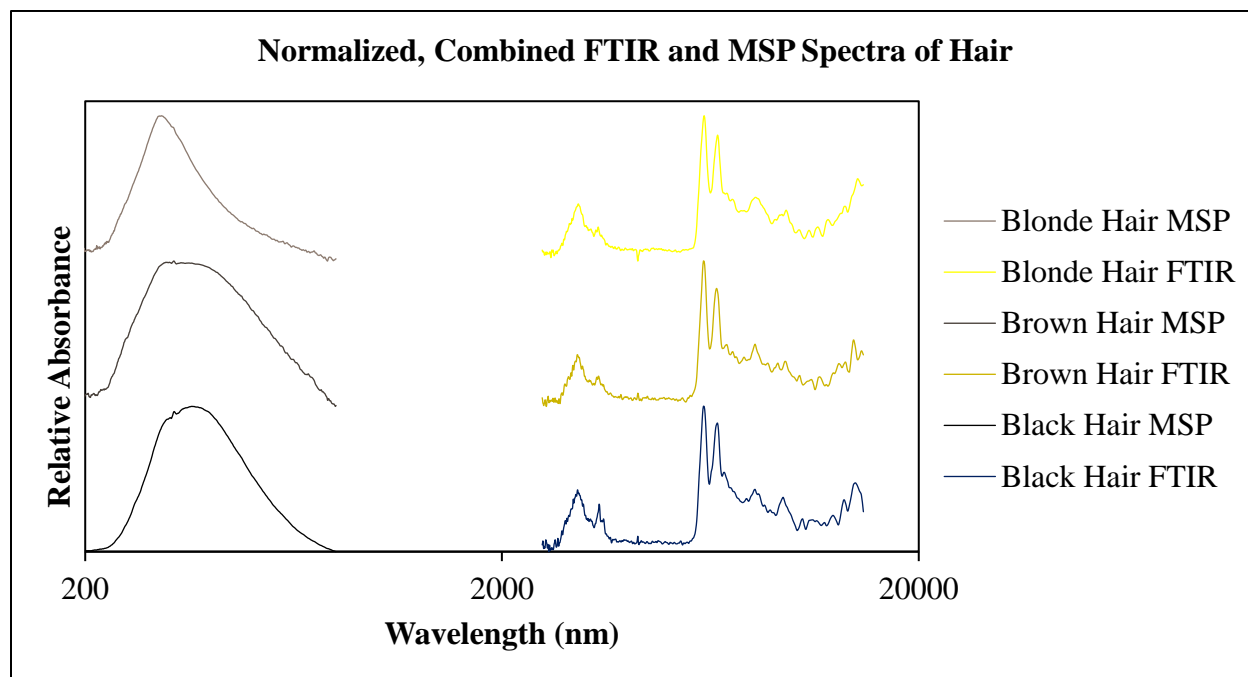


Figure 4-4. Normalized Combined FTIR and MSP Spectra of Blonde Hair, Brown Hair, and Black Hair

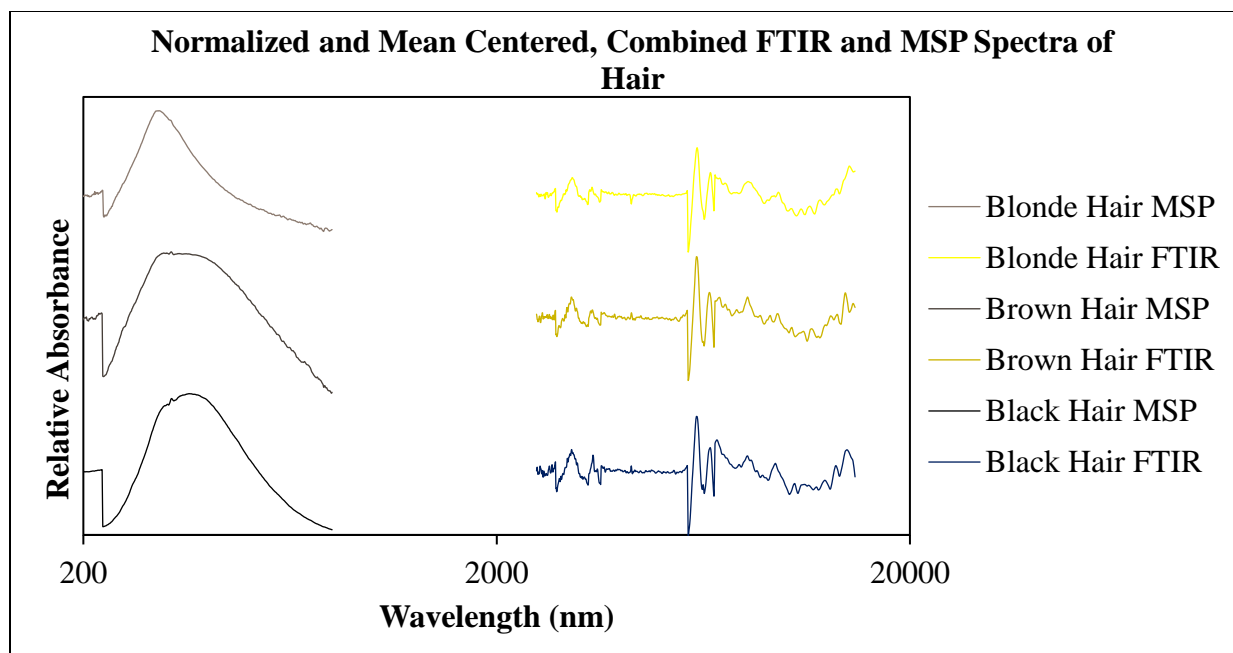


Figure 4-5 Normalized and Mean Centered, Combined FTIR and MSP Spectra of Blonde Hair, Brown Hair, and Black Hair

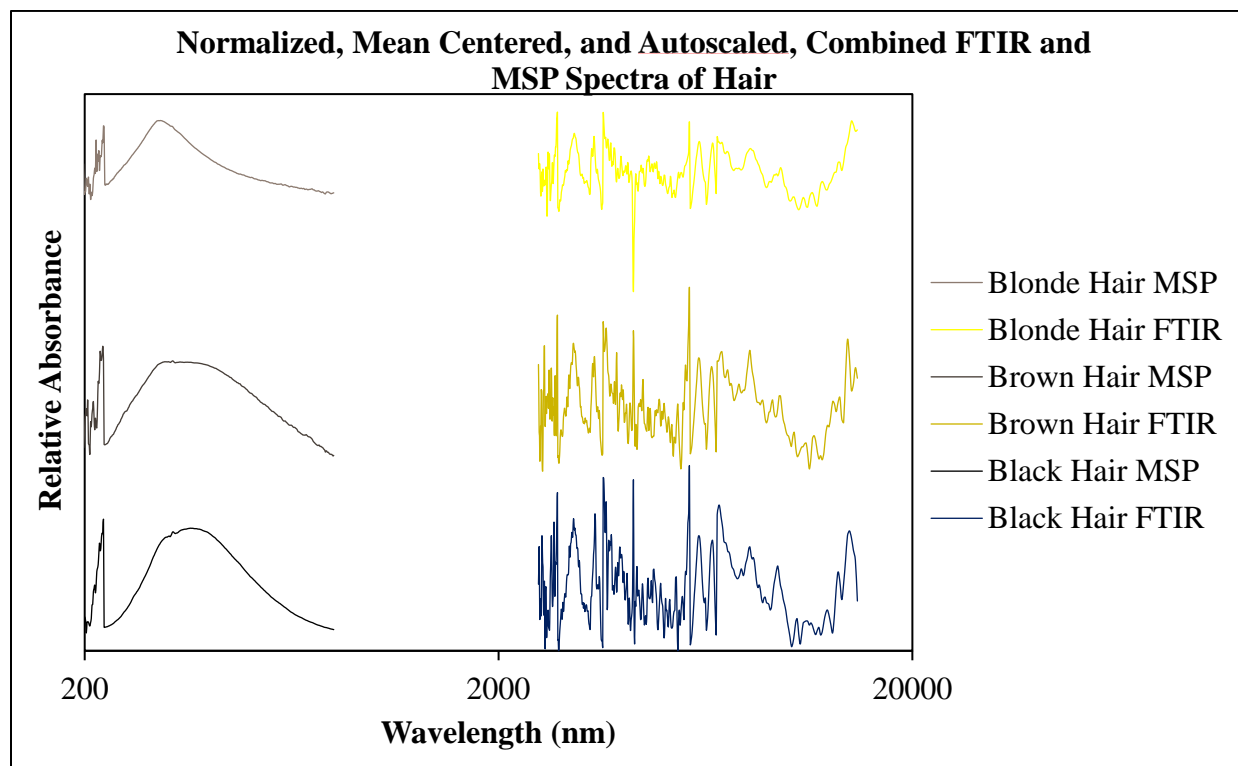


Figure 4-6. Normalized, Mean Centered, and Autoscaled, Combined FTIR and MSP Spectra of Blonde Hair, Brown Hair, and Black Hair

Raman Spectroscopy

The Raman signal was weak in most of the hair melanin analyses. Therefore, the laser excitation wavelength and power of the Raman instrument must be optimized further. For example, longer wavelengths between should be further examined. The longer laser excitation wavelengths would allow a greater observation of Raman bands.⁴⁰ Upon optimization of the Raman instrument, more hair should be collected and analyzed. After analyzing the naturally colored hairs (blonde, brown, black, red, white, and grey), dyed hairs should also be analyzed to determine how the natural pigmentation is affected.

REFERENCES

1. Rowlands, J., IED Awareness. Ruchti, J., Ed. 2017.
2. United States Bomb Data Center. *2017 Explosives Incident Report* Bureau of Alcohol, Tobacco, Firearms and Explosives: 2017.
3. Gingras, B.; Grinberg, E.; McLaughlin, E. Suspect in attempted 'terrorist attack' pledged allegiance to ISIS, officials say. <https://www.cnn.com/2017/12/11/us/new-york-possible-explosion-port-authority-subway/index.html> (accessed February 1, 2018).
4. Havens, E. Southern Utah student accused of bringing bomb to school charged with attempted murder, use of WMD. <https://www.thespectrum.com/story/news/2018/03/27/utah-student-accused-bringing-bomb-school-promoting-isis-gets-felony-charges/462184002/> (accessed April 1, 2018).
5. Dathan, J.; Kearney, J., Monitoring Explosive Violence in 2017. *Action of Armed Violence* **2018**.
6. Burke, J. Mogadishu truck bomb: 500 casualties in Somalia's worst terrorist attack. <https://www.theguardian.com/world/2017/oct/15/truck-bomb-mogadishu-kills-people-somalia>.
7. Grdadolnik, J., Saturation effects in FTIR spectroscopy: Intensity of Amide I and Amide II bands in protein spectra. *Acta Chim Slov* **2003**, *50* (4), 777-788.
8. Forensic Chemistry: Fundamentals and Applications. *Forensic Sci Foc* **2016**, 1-523.
9. Ash, J. R.; Purdue University. Chemistry., *Design and implementation of Gas Chromatography/Mass Spectrometry (GC/MS) methodologies for the analysis of thermally labile drugs and explosives*. p 1 electronic resource (100 pages).
10. Hickey, L., Towards Simultaneous Extraction of TNT and DNA from Blood on Cotton. Indiana University Purdue University Indianapolis: 2018.
11. M-Vac Systems. Why M-Vac. <https://www.m-vac.com/> (accessed October 1, 2017).
12. Shrey, A.; Coon, C. *Phenol-Chloroform Isoamyl Alcohol (PCI) DNA Extraction*; University of South Florida.
13. Zhao, Z.; Yinon, J., Characterization and origin identification of 2,4,6-trinitrotoluene through its by-product isomers by liquid chromatography–atmospheric pressure chemical ionization mass spectrometry. *Journal of Chromatography A* **2002**, *946* (1-2).
14. Bhal, S. *LogP—Making Sense of the Value*; Advanced Chemistry Development, Inc. .
15. Marzulli, F.; Maibach, H., *Dermatotoxicology*. 4th ed.; Hemisphere Publishing Corporation: 1991.
16. Sharma, M. B. a. A., Review of some recent techniques of age determination of blow flies having forensic implications. *Egyptian Journal of Forensic Sciences* **2016**, *6* (3).
17. Lehane, M. J., Determining the age of an insect. *Parasitol Today* **1985**, *1* (3), 81-5.
18. Zakhari, S., Alcohol metabolism and epigenetics changes. *Alcohol Res* **2013**, *35* (1), 6-16.
19. Chwialkowska, K.; Korotko, U.; Kosinska, J.; Szarejko, I.; Kwasniewski, M., Methylation Sensitive Amplification Polymorphism Sequencing (MSAP-Seq)-A Method for High-Throughput Analysis of Differentially Methylated CCGG Sites in Plants with Large Genomes. *Front Plant Sci* **2017**, *8*, 2056.

20. Tang, Y.; Gao, X. D.; Wang, Y.; Yuan, B. F.; Feng, Y. Q., Widespread existence of cytosine methylation in yeast DNA measured by gas chromatography/mass spectrometry. *Anal Chem* **2012**, *84* (16), 7249-55.
21. Hu, C. W.; Chen, J. L.; Hsu, Y. W.; Yen, C. C.; Chao, M. R., Trace analysis of methylated and hydroxymethylated cytosines in DNA by isotope-dilution LC-MS/MS: first evidence of DNA methylation in *Caenorhabditis elegans*. *Biochem J* **2015**, *465* (1), 39-47.
22. Delaney, C.; Garg, S. K.; Yung, R., Analysis of DNA Methylation by Pyrosequencing. *Methods Mol Biol* **2015**, *1343*, 249-64.
23. Sinden, R. R., *DNA Structure and Function*. Elsevier: 2012.
24. Knapp, D., *Handbook of Analytical Derivatization Reactions*. John Wiley & Sons, New York: 1980.
25. Forsdyke, D. R.; Mortimer, J. R., Chargaff's legacy. *Gene* **2000**, *261* (1), 127-137.
26. DNeasy Blood & Tissue Handbook. Qiagen, Ed. 2006; p 62.
27. Charette, M.; Gray, M. W., Pseudouridine in RNA: What, where, how, and why. *Iubmb Life* **2000**, *49* (5), 341-351.
28. Scientific Working Group on Materials Analysis., Forensic Human Hair Examination Guidelines *Forensic Science Communications* **2005**, *7* (2).
29. Giannelli, P., Forensic Science: *Daubert's Failure*. *Faculty Publications* **2017**.
30. Neufeld, P., The (Near) Irrelevance of *Daubert* to Criminal Justice and Some Suggestions for Reform. *American Journal of Public Health* **2004**, *95* (S1).
31. Norton, J.; Anderson, W.; Divine, G., Flawed forensics: Statistical failings of microscopic hair analysis. *Significance Magazine* 2016, pp 26-29.
32. Barrett, J. A.; Siegel, J. A.; Goodpaster, J. V., Forensic Discrimination of Dyed Hair Color: I. UV-Visible Microspectrophotometry. *Journal of Forensic Sciences* **2010**, *55* (2), 323-333.
33. Siegel, J.; Mirakovits, K., *Forensic Science: The Basics*. 3 ed.; CRC Press: 2015.
34. Harkey, M. R., Anatomy and Physiology of Hair. *Forensic Sci Int* **1993**, *63* (1-3), 9-18.
35. Smith, S. L.; Linch, C. A., A review of major factors contributing to errors in human hair association by microscopy. *Am J Foren Med Path* **1999**, *20* (3), 269-273.
36. Deedrick, D.; Koch, S., Microscopy of Hair Part II: A Practical Guide and Manual for Animal Hairs. *Forensic Science Communications* **2004**, *6* (3).
37. Ito, S.; Wakamatsu, K., Diversity of human hair pigmentation as studied by chemical analysis of eumelanin and pheomelanin. *J Eur Acad Dermatol* **2011**, *25* (12), 1369-1380.
38. Houck, M., *Identification of Textile Fibers*. Woodhead Publishing in Textiles: 2009; Vol. 84, p 1-375.
39. Martin, P. C.; Eyring, M. B., Microspectrophotometry. *Exptl Meth Phys Sci* **2014**, *46*, 489-517.
40. Galvan, I.; Jorge, A.; Ito, K.; Tabuchi, K.; Solano, F.; Wakamatsu, K., Raman spectroscopy as a non-invasive technique for the quantification of melanins in feathers and hairs. *Pigm Cell Melanoma R* **2013**, *26* (6).
41. Napolitano, A.; Pezzella, A.; dIschia, M.; Prota, G., New pyrrole acids by oxidative degradation of eumelanins with hydrogen peroxide. Further hints to the mechanism of pigment breakdown. *Tetrahedron* **1996**, *52* (26), 8775-8780.

42. Szekely-Klepser, G.; Wade, K.; Woolson, D.; Brown, R.; Fountain, S.; Kindt, E., A validated LC/MS/MS method for the quantification of pyrrole-2,3,5-tricarboxylic acid (PTCA), a eumelanin specific biomarker, in human skin punch biopsies. *J Chromatogr B* **2005**, 826 (1-2), 31-40.
43. Ito, S.; Fujita, K., Microanalysis of eumelanin and pheomelanin in hair and melanomas by chemical degradation and liquid chromatography. *Anal Biochem* **1985**, 144 (2), 527-36.
44. Wakamatsu, K.; Ito, S., Advanced chemical methods in melanin determination. *Pigment Cell Res* **2002**, 15 (3), 174-83.
45. Ito, S.; Wakamatsu, K., Quantitative analysis of eumelanin and pheomelanin in humans, mice, and other animals: a comparative review. *Pigment Cell Res* **2003**, 16 (5), 523-31.
46. Gallagher, W., FTIR Analysis of Protein Structure. *Biochemistry* **1997**.
47. Thomas, D. B.; McGoverin, C. M.; McGraw, K. J.; James, H. F.; Madden, O., Vibrational spectroscopic analyses of unique yellow feather pigments (spheniscins) in penguins. *J R Soc Interface* **2013**, 10 (83).
48. Choi, Y.; Remmler, D.; Ries, M.; Rösicke, F.; Sarhan, R.; Stete, F.; Zhang, Z., Forensic Analysis of Explosives. Deutsche Forschungsgemeinschaft.
49. Hoffmann, S. G.; Stallworth, S. E.; Foran, D. R., Investigative Studies into the Recovery of DNA from Improvised Explosive Device Containers. *Journal of Forensic Sciences* **2012**, 57 (3), 602-609.
50. Gunn, L. Validation of the M-Vac cell collection system for forensic purposes. Thesis (M.S.), Boston University, 2013, Boston.
51. Johnson, G. Concentration of large volume biological samples for effective and efficient forensic DNA analysis. M.S., Boston University, 2012.
52. Detection, S., Guardion. 2012.
53. PerkinElmer, I., Product Note: Gas Chromatography/Mass Spectrometry. 2016.
54. Combating Terrorism Technical Support Office. Person Portable GC-MS. <https://cttso.gov/CBRNE/PersonPortableGC-MS.html>.
55. PerkinElmer, I., Torion T-9 User's Guide. Inc., T. T., Ed. 2017.
56. Vu, V. T.; Grantham, P. H.; Roller, P. P.; Hankins, W. D.; Wirth, P. J.; Thorgeirsson, S. S., Formation of DNA adducts from N-acetoxy-2-acetylaminofluorene and N-hydroxy-2-acetylaminofluorene in rat hemopoietic tissues in vivo. *Cancer Res* **1986**, 46 (1), 233-8.
57. Flarakos, J.; Xiong, W.; Glick, J.; Vouros, P., A deoxynucleotide derivatization methodology for improving LC-ESI-MS detection. *Analytical Chemistry* **2005**, 77 (8), 2373-2380.
58. Ibanez, M. A. D.; Chessebeufpadieu, M.; Nordmann, P.; Padieu, P., Gas Chromatography-Mass Spectrometry Analysis of Tert-Butyldimethylsilyl Derivatives of 2-Acetylaminofluorene and Metabolites in Isolated Rat Hepatocytes. *Cell Biol Toxicol* **1987**, 3 (3), 327-340.
59. Sigma-Aldrich, I., 2-Bromoacetophenone, 98%. 2018.
60. Longmuir, K. J.; Rossi, M. E.; Resele-Tiden, C., Determination of monoenoic fatty acid double bond position by permanganate-periodate oxidation followed by high-performance liquid chromatography of carboxylic acid phenacyl esters. *Anal Biochem* **1987**, 167 (2), 213-21.

61. Torres, A. L.; Barrientos, E. Y.; Wrobel, K.; Wrobel, K., Selective Derivatization of Cytosine and Methylcytosine Moieties with 2-Bromoacetophenone for Submicrogram DNA Methylation Analysis by Reversed Phase HPLC with Spectrofluorimetric Detection. *Analytical Chemistry* **2011**, 83 (20), 7999-8005.
62. Brohi, R.; Khuhawar, M.; Khuhawar, T., GC-FID determination of nucleobases guanine, adenine, cytosine, and thymine from DNA by precolumn derivatization with isobutyl chloroformate. *J Anal Sci Technol* **2016**, 7.
63. Blackledge, R., Forensic analysis on the cutting edge new methods for trace evidence analysis. J. Wiley & Sons, Hoboken, NJ, 2007; p. 1 online resource (490 p.).
64. Barrett, J. A.; Siegel, J. A.; Goodpaster, J. V., Forensic Discrimination of Dyed Hair Color: II. Multivariate Statistical Analysis. *Journal of Forensic Sciences* **2011**, 56 (1), 95-101.

VITA

Jacqueline Ruchti graduated from Wheeler High School (Valparaiso, IN) as a valedictorian in 2013. She went on to pursue a B.S. in Natural Sciences with a chemistry concentration, B.A. in Administration of Justice with a forensics concentration, and a minor in Mathematics from the University of Pittsburgh (Pittsburgh, PA). After graduating cum laude from the University of Pittsburgh in 2017, she began graduate school at Indiana University – Purdue University Indianapolis (Indianapolis, IN), performing research in gas chromatography – mass spectrometry under Dr. John Goodpaster. In 2019, she obtained her M.S. in Forensic and Investigative Sciences with a forensic chemistry concentration.